Modulation of Cell Differentiation and Epigenetic Landscape by Methionine Metabolism

by

Yudong Sun

Department of Biochemistry
Duke University

Defense Date: March 21, 2024

Approved:

Meta Kuehn, Supervisor

Michael Boyce

Christopher Nicchitta

Xiao-Fan Wang

Dissertation submitted in partial fulfillment of the requirements for the degree of
Doctor of Philosophy in the Department of Biochemistry
in the Graduate School of Duke University
2024

ABSTRACT

Modulation of Cell Differentiation and Epigenetic Landscape by Methionine Metabolism

by

Yudong Sun

Department of Biochemistry
Duke University

Defense Date: March 21, 2024

Approved:

Meta Kuehn, Supervisor

Michael Boyce

Christopher Nicchitta

Xiao-Fan Wang

An abstract of a dissertation submitted in partial fulfillment of the requirements
for
the degree of Doctor of Philosophy in the Department of Biochemistry
in the Graduate School of Duke University
2024

Copyright © 2024 by Yudong Sun
All rights reserved except the rights granted by the
Creative Commons Attribution-Noncommercial Licence

Abstract

Histone modifications are an integral component of epigenetic mechanisms, crucially influencing DNA accessibility and gene expression. These modifications are increasingly recognized as being deeply intertwined with cellular metabolism, particularly through the use of metabolic intermediates as substrates or catalytic cofactors for histone modifiers. This is especially evident in the metabolism of methionine, which significantly affects histone methylation by modulating the availability of substrates for histone methyltransferases. The activities of these enzymes are highly sensitive to substrate concentration due to their unique kinetic properties. Despite some degree of observation and study, the direct impact of methionine availability on specific histone modifications, like H3K36me3, and their ensuing effects on cellular functions have not been extensively explored.

To address this knowledge gap, I employed a combination of genetic, biochemical, and pharmacological approaches to examine the consequences of methionine restriction on H3K36me3 and its impact on cellular differentiation. This involved characterizing the dynamics, and reversibility of these processes, and identifying the mediating factors between methionine and cellular differentiation. Our findings highlight a significant dependency of myogenic differentiation on methionine and establish the methionine-SAM-SETD2 pathway as a critical component in this process.

This work provides compelling evidence of a connection between nutrient sta-

tus and cell-fate determination, potentially mediated by histone status. These insights offer new perspectives on the complex interplay between metabolism and epigenetics, laying the foundation for a more profound understanding of how these processes interconnect to influence cellular fate decisions.

Dedication

To all those who kindled the spark of curiosity within me.

Contents

Abstract **iv**

List of Tables **x**

List of Figures **xi**

List of Abbreviations and Symbols **xiv**

Acknowledgements **xvi**

1 Introduction **1**

1.1 Histone and epigenetic regulation 1

1.2 The metabolic aspect of epigenetic regulation 3

1.3 Methionine metabolism and histone methylation 5

1.4 Trimethylation of histone H3K36 (H3K36me3) 7

1.5 Histone methyltransferase SETD2 8

1.6 Mouse myoblast cell, C2C12 10

1.7 Scope of this thesis 11

2 The bioavailability and cellular transport properties of S-adenosylmethionine **14**

2.1 Summary 14

2.2 Introduction 15

2.3 Transport properties of SAM 16

2.4 Chemical stability of SAM under physiological conditions 17

2.5 Cellular permeability of 5′-methylthioadenosine (MTA) and the methionine salvage pathway 18

2.6 Implications of the indirect SAM transport schematic 20

2.7 Conclusions 21

3 Methionine-dependent H3K36me3 and myogenic differentiation 22

3.1 Summary 22

3.2 Introduction 23

3.3 Results 24

3.3.1 Myogenic differentiation and H3K36me3 are methionine-dependent processes 24

3.3.2 Methionine dynamically controls H3K36me3 and myogenic differentiation 30

3.3.3 H3K36me3 and methionine metabolism rapidly respond to methionine restriction 32

3.3.4 Early stage methionine availability is critical for myogenic differentiation 35

3.3.5 Myogenic differentiation and H3K36me3 are SAM-dependent 35

3.3.6 SETD2 expression is linked to to methionine restriction . . . 39

3.3.7 Methionine-dependent differentiation acts through SETD2 . 41

3.3.8 Methionine restriction preferentially reduces H3K36me3 levels at differentiation related genes 42

3.3.9 Methionine restriction and Setd2 knockout preferentially reduce chromatin accessibility at differentiation related genes 48

3.4 Discussions 51

3.5 Methods 58

3.5.1 Cell culture 58

3.5.2 Microscopy 58

3.5.3 Differentiation Quantification 59

3.5.4 Histone extraction 59
3.5.5 Total protein extraction 60
3.5.6 Immunoblot 60
3.5.7 Metabolites extraction 61
3.5.8 Liquid chromatography 61
3.5.9 Mass spectrometry 62
3.5.10 Peak extraction and metabolomics data analysis 62
3.5.11 Quantitative PCR 62
3.5.12 Lentiviral transduction 63
3.5.13 CRISPR Knockout of Setd2 64
3.5.14 ChIP-Seq and data analysis 64
3.5.15 ATAC-Seq and data analysis 65
3.5.16 Statistical analysis 66
3.5.17 Generative AI 66

4 Conclusions **68**

4.1 Summary 68
4.2 Future directions 70

Bibliography **72**

Biography **86**

List of Tables

1.1 Kinetic properties of representative histone methyltransferase. . . . 5

List of Figures

1.1 Structural representation of the nucleosome core particle. 2

1.2 The link between metabolism and epigenetics. 4

1.3 Comparative sensitivity of HMTs and kinases to substrate availability 5

1.4 Schematic representation of the methionine cycle with key intermediates. 7

1.5 Domain architecture of Setd2. 9

1.6 Comparative visualization of SET domains across species. 10

1.7 Close-up view of the SET domain substrate binding site. 11

1.8 Morphological changes in C2C12 cells at different stages. 12

2.1 The chemical structures of S-adenosylmethionine (SAM) and 5′-methylthioadenosine (MTA). 17

2.2 Schematic of an indirect SAM transport mechanism. 19

3.1 Schematic representation of the experimental design for exploring dependency on methionine in myogenic differentiation. 25

3.2 Schematic of training and prediction process of DiffQuant. 26

3.3 Myogenic differentiation is methionine-dependent. 27

3.4 Methionine cycle metabolites reduced in response to methionine restriction. 27

3.5 H3K36me3 is methionine-dependent. 28

3.6 Methionine restriction has minimal impact on C2C12 cell proliferation. 28

3.7 Dose-dependent relationship between methionine concentration, relative differentiation score, MyHC expression, and H3K36me3. . . . 29

3.8 Schematic representation of the experimental design for investigating the reversibility of the effects of methionine restriction on H3K36me3 and myogenic differentiation. 31

3.9 Methionine-dependent myogenic differentiation is reversible. . . . 31

3.10 Methionine-dependent H3K36me3 is reversible. 32

3.11 H3K36me3 levels rapidly respond to methionine availability. 33

3.12 Methionine cycle metabolites levels rapidly respond to methionine availability. 34

3.13 Schematic outline of the experimental design for the methionine cut-off study for determining the critical stage for methionine in differentiation. 36

3.14 Early stage methionine availability is critical for myogenic differentiation. 36

3.15 Schematic representation of SAM synthesis highlighting the SAM synthetase, MAT2A, and its inhibition by cycloleucine (cLEU). . . . 37

3.16 cycloleucine (cLEU) reduces levels of SAM, SAH and HCY. 38

3.17 Myogenic differentiation and H3K36me3 are SAM-dependent. . . . 38

3.18 Inhibition of MAT2A through AG-270 results in a disruption of differentiation comparable to that observed with cLEU. 39

3.19 SETD2 levels are potentially responsive to methionine availability. 40

3.20 Schematic of the experimental design to evaluate the response of SETD2 to MR. 41

3.21 Methionine restriction leads to increased level of SETD2 expression. 42

3.22 Ectopic expression of Setd2 increases H3K36me3 levels under MR. 43

3.23 Ectopic expression of Setd2 improves differentiation under MR. . . 43

3.24 Setd2 knockout leads to the loss of H3K36me3. 44

3.25 Setd2 knockout leads to disruptions in differentiation. 44

3.26 H3K36me3 abundance increases at differentiation-related genes during normal course of differentiation. 45

3.27 Gene-specific H3K36me3 profiles under CTL and MR conditions at representative genes. 45

3.28 Schematic representation of the workflow for differential ChIP peak analysis of H3K36me3 under different methionine conditions. . . . 46

3.29 Methionine restriction preferentially diminishes H3K36me3 levels at differentiation-related genes. 47

3.30 Schematic representation of the workflow for differential ChIP peak analysis of H3K36me3 under different methionine conditions. . . . 48

3.31 Methionine restriction and Setd2 knockout preferentially reduce chromatin accessibility at differential related genes. 49

3.32 ATAC-seq profiles and heatmaps of peaks that are diminished in response to MR compared to CTL. 50

3.33 Top results from Over-Representation Analysis (ORA). 53

3.34 Aggregated levels of H3K36me3 at all genes or at myogenic-related genes. 54

3.35 Effect of K_{eff} on reaction rate based on Michaelis-Menten Kinetics. . 56

List of Abbreviations and Symbols

DNA	Deoxyribonucleic Acid
LECA	Last Eukaryotic Common Ancestor
SAM	S-adenosylmethionine
TCA	Tricarboxylic Acid Cycle
MAT2A	Methionine Adenosyltransferase 2a
MTs	Methyltransferases
SAH	S-adenosylhomocysteine
AHCY	Adenosylhomocysteinase
MS	Methionine Synthase
HMTs	Histone Methyltransferases
HP1	Heterochromatin Protein 1
NURF	Nucleosome Remodeling Factor
PTB	Polypyrimidine Tract-Binding Protein
IDH	Isocitrate Dehydrogenase
2-HG	2-Hydroxyglutarate
α-KG	α-ketoglutaric Acid
C2C12	Mouse Myoblast Cell Line
MyHC	Myosin Heavy Chain
MTA	5′-Methylthioadenosine
ATP	Adenosine Triphosphate

GM	Growth Media
DM	Differentiation Media
MR	Methionine Restriction
MD	Methionine Depletion
ChIP-Seq	Chromatin Immunoprecipitation Sequencing
SETD2	SET Domain Containing 2, Histone Lysine Methyltransferase
cLEU	Cycloleucine
ATAC-Seq	Assay for Transposase-Accessible Chromatin using Sequencing
GREAT	Genomic Regions Enrichment of Annotations Tool
RNAPII	RNA Polymerase II
SRI	Set2-Rbp1 Interaction Domain
CTD	C-terminal Domain
STAT1	Signal Transducer and Activator of Transcription 1
IFNa	Interferon Alpha
GO	Gene Ontology
CRISPR	Clustered Regularly Interspaced Short Palindromic Repeats
WT	Wild Type
KO	Knockout
CTL	Control
GREAT	Genomic Regions Enrichment of Annotations Tool

Acknowledgements

The completion of this thesis marks a milestone that was made possible only through the collective encouragement, wisdom, and unwavering belief of many. I am profoundly fortunate for my position and remain eternally grateful to everyone who has been part of my journey.

First and foremost, I want to thank my parents for their unwavering support and, more importantly, their trust in me. They trusted my judgments, my decisions, and embraced my independence. Their trust gave me the freedom to make my own choices, and they stood fully behind me with encouragement and unconditional support. In many ways, they are the textbook definition of angel investors, investing not for any returns but out of belief and a genuine wish to see me succeed in whatever path I choose. It is this trust and freedom that taught me the lesson of agency and to be responsible for myself, propelling me to choose things that I am deeply passionate about and to live my life confidently.

My gratitude extends to my friends, especially my core support group—Aili, Xuyi, Runsheng, Yunhe, and Wenting—affectionately known as the touching fish group. Their presence in my life has been a source of immense joy and learning. They have taught me crucial lessons about optimism and love, both of which have been instrumental in navigating my way to where I stand today.

I am immensely thankful for my teachers and mentors, who introduced me to the wonders of the world, the joy of learning, and kindled my curiosity. This curiosity has made learning an everlasting joy. I would like to extend special thanks to Miss Huan Liu, Prof. Seth Blair, Prof. Antony Stretton, Prof. Michael Cox, Prof. Alessandro Senes, Dr. Elizabeth Caselle and Prof. Caitlin Pepperell, who were all pivotal in my academic journey.

I also want to thank my thesis committee for their support over the years, being flexible and supportive, stepping in to make things work, and keeping me on track, even on the day of my dissertation, accommodating all situations.

My appreciation also goes out to the members of the Locasale Lab, especially Luis Vergara, Annamarie Allen, Vijyendra Ramesh, Juan Liu, Zhengtao Xiao, Ziwei Dai, Michael Reid, Shiyu Liu and Fangchao Wei. Your collective intellect, technical expertise, and emotional support have provided a nurturing environment that helped me grow as a scientist.

The final word is reserved for my mentor, Jason Locasale, without whom this Ph.D. would have been impossible. He welcomed me into his lab under extraordinary circumstances, and over the years, he has provided me with countless opportunities, virtually unlimited resources, and unwavering encouragement and support along the way. Jason has not only imparted concrete skills and knowledge but has also taught me the philosophical aspects of science and how to think critically. I am truly grateful for everything he has done for me.

1

Introduction

1.1 Histone and epigenetic regulation

Cells in multicellular organisms possess near-identical genomic DNA. Yet, through the differential expression of this singular genome, cells acquire distinct identities, giving rise to the specific functions and characteristics that define various cell types [53]. Crucially, these alterations in gene expression are preserved through subsequent rounds of cell division [75]. This phenomenon is termed as epigenetics [39, 6], and it is primarily realized through the modifications of DNA [117, 119] and DNA-associated proteins [67, 18].

When fully extended, the DNA in human cells spans 2 meters [91]. This length poses significant challenges in terms of cellular packaging. Approximately 2 billion years ago, during the time of the Last Eukaryotic Common Ancestor (LECA), histone proteins evolved to address the challenges presented by an expanding genome [30, 11]. These challenges not only included packaging but also ensuring accessibility [11]. In contemporary eukaryotic cells, there are various histone proteins that collectively form the histone complex. DNA wraps around this hi-

stone complex every 147 base pairs, forming the fundamental unit known as the nucleosome [29] (Figure 1.1). This, in turn, gives rise to higher-order structures like chromatin.

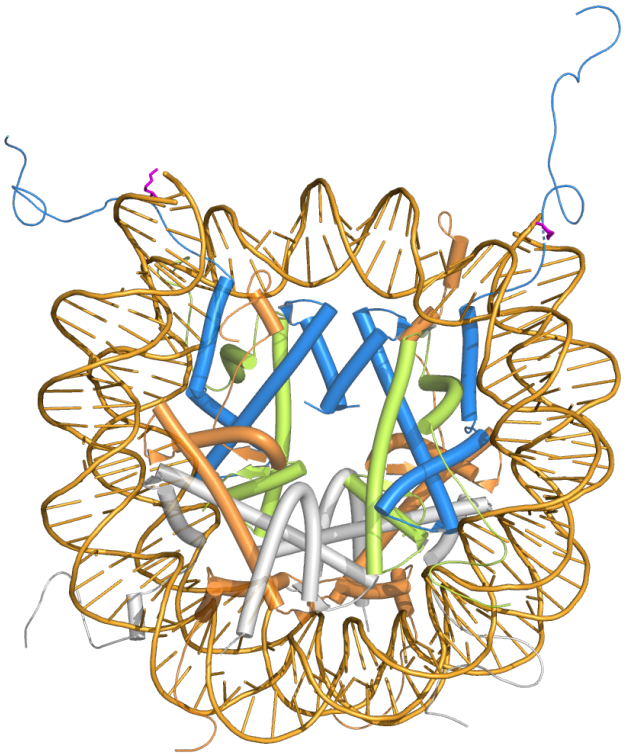

FIGURE 1.1: **Molecular model of the nucleosome core particle, derived from PDB ID: 1KX5.** It illustrates the histone octamer around which DNA is wrapped, a key component of chromatin in eukaryotic cells. Each histone sub-unit is distinctively colored for clarity: H3 in blue, H4 in green, H2B in grey, and H2A in orange. The residue H3K36, a known regulatory site for enzymatic modification, is highlighted in magenta.

The histone complex has a core globular domain rich in positively charged lysine residues, enabling them to easily bind with the negatively charged phosphate groups in DNA, ensuring tight packaging [29, 95]. The tails of histones protrude from this core and contain numerous modification sites that allow dynamic reg-

ulation of their interactions with DNA [29, 95]. These modifications, such as the methylation and acetylation of lysine residues, offer another layer of control over gene expression [55, 108].

Such modifications can either change the local electrostatic environment, as observed with lysine acetylation that neutralizes its positive charge, thereby weakening its interaction with DNA, or serve as binding sites to recruit other histone remodelers that can either relax or compact the local structure [85].

1.2 The metabolic aspect of epigenetic regulation

Cellular metabolism transforms nutrients into metabolites, utilized by cells for energy, structure, and signaling [19]. While the roles of metabolism in energy production and as a cellular building block are well-understood—thanks to extensive research on core metabolic pathways like glycolysis and the TCA cycle—the regulation of gene expression in response to metabolic changes has primarily been studied in contexts such as stress response or within certain feedback loops. Only recently has the direct link between metabolism and epigenetics come to light [98, 56]. The previously mentioned histone modifications rely on substrates produced by key metabolic pathways [67, 94, 16]. For example, Acetyl-CoA for histone acetylation originates from glycolysis, and the TCA cycle [115, 23, 84], while S-adenosylmethionine for histone methylation is sourced from the methionine cycle [126, 81, 106]. This intertwining underscores the relationship between metabolism and epigenetics (Figure 1.2)[1]. Additionally, the enzyme kinetics of histone modifiers, like histone methyltransferases, are primed to respond to metabolic changes, given that the K_m values of these enzymes closely match the standard cellular con-

[1] Adapted from Reid, M.A., Dai, Z., and Locasale, J.W. (2017). The impact of cellular metabolism on chromatin dynamics and epigenetics. *Nature Cell Biology* 19, 1298. [94]

centrations of their substrates (Table 1.1 & Figure 1.3)[2]. Hence, minor variations in substrate concentration might lead to significant changes in the reaction rate, which in turn can influence the degree of histone modifications [94].

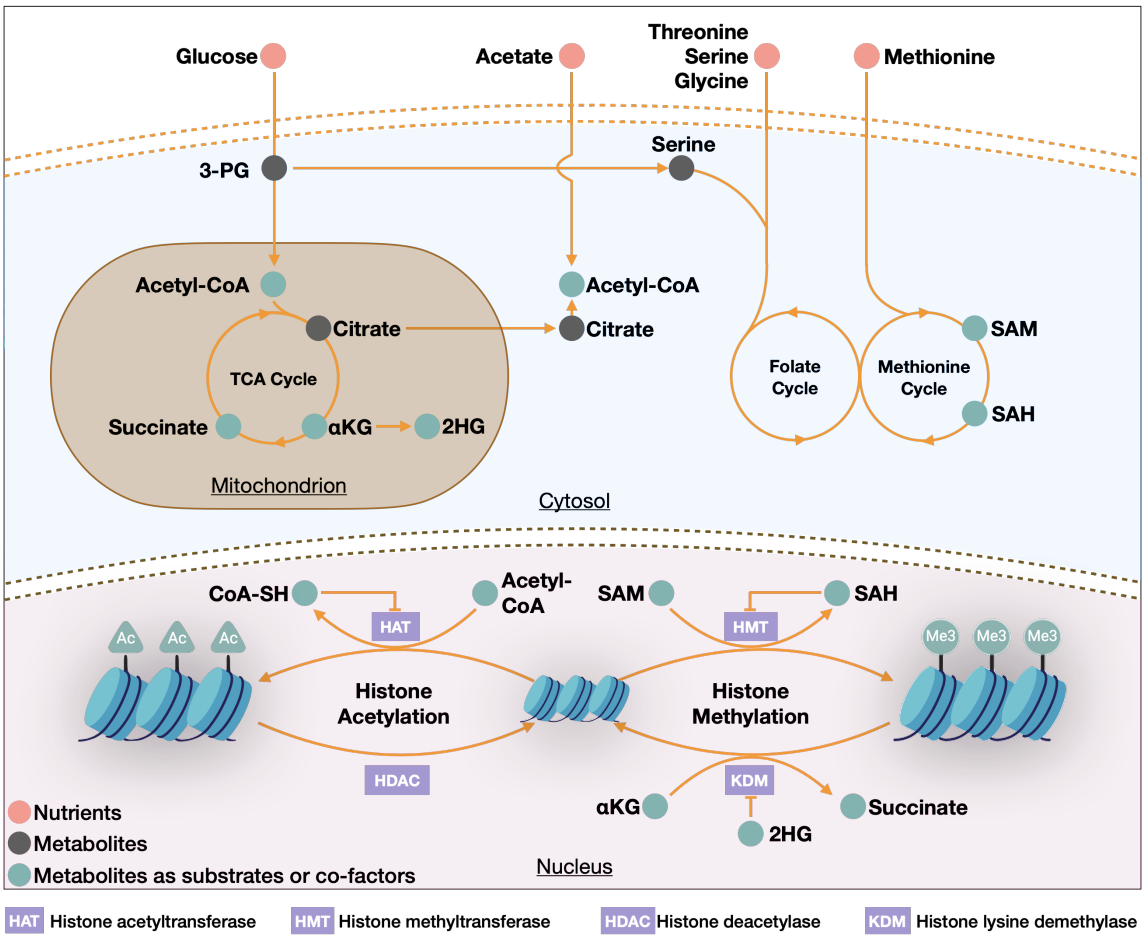

FIGURE 1.2: **Metabolism and epigenetics are interconnected.** Nutrient uptake by cells, including methionine and glucose, is converted into metabolic intermediates such as Acetyl-CoA and SAM. These intermediates serve as substrates for histone acetyltransferases (HATs) and histone methyltransferases (HMTs). In other instances, metabolic products like α-KG or 2HG act as cofactors or inhibitors for histone-modifying enzymes.

[2] Adapted from Reid, M.A., Dai, Z., and Locasale, J.W. (2017). The impact of cellular metabolism on chromatin dynamics and epigenetics. *Nature Cell Biology* 19, 1298. [94]

Table 1.1: **Kinetic properties of representative histone methyltransferase.**

Enzyme	Modification	K_m (SAM) [μM]	References
MLL1	H3K4me3	6.5-10.4	Patel et al., 2014 [90]
DIM5	H3K9me3	1.2-1.3	Rathert et al., 2008 [93]
SETD2	H3K36me3	3.3-5.5	Eram et al., 2015 [37]

1.3 Methionine metabolism and histone methylation

Due to its sulfur-containing properties and capacity for methyl donation, methionine is pivotal for various cellular processes, including protein synthesis, methylation of DNA, RNA, lipids, and proteins, polyamine synthesis, as well as redox balancing, among others [114, 127, 125, 49, 9, 99]. Notably, since mammals cannot

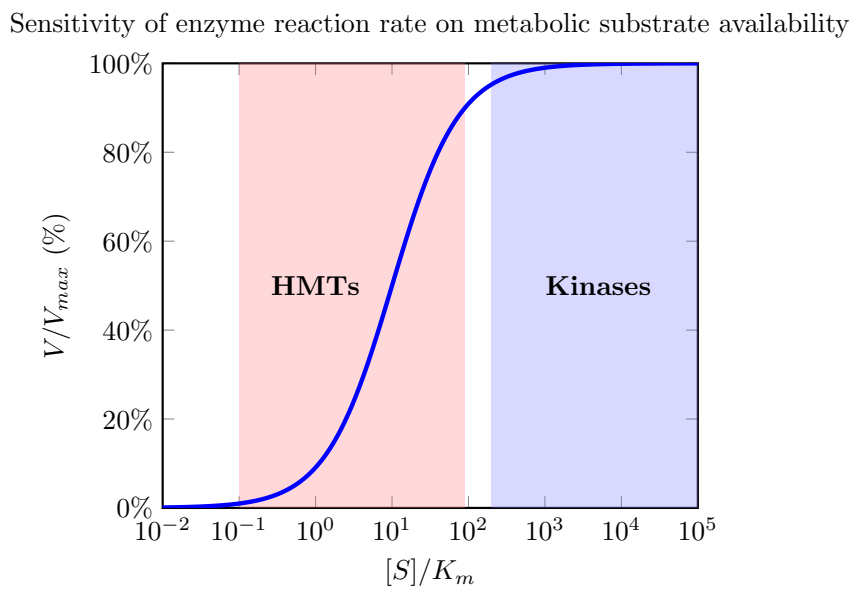

FIGURE 1.3: **An illustrative comparison of enzyme activity versus substrate concentration for two enzyme classes.** The graph shows the percentage of maximum reaction rate (V/Vmax) against substrate concentration normalized to Michaelis constant (K_m). The shaded regions represent the typical substrate sensitivity ranges for histone methyltransferases (HMTs) in red and kinases in blue.

synthesize methionine and need obtain it entirely from their diet, physiological methionine levels can be modulated through dietary means [81, 42]. This presents exciting possibilities for influencing cellular processes through dietary interventions [52], as there is significant variation in methionine content across different diets [27].

At the heart of methionine metabolism lies the methionine cycle (Figure 1.4). Methionine enters this cycle and is transformed into S-adenosylmethionine (SAM) by methionine adenosyltransferase 2a (MAT2A). SAM has a dual role: it can be channeled into polyamine synthesis pathways, or it can act as a universal methyl group donor for various methyltransferases (MTs), becoming S-adenosylhomocysteine (SAH) in the process after losing a methyl group. SAH is subsequently converted to homocysteine by adenosylhomocysteinase (AHCY). From here, homocysteine can either feed into the transsulfuration pathway for glutathione synthesis or be converted back to methionine by methionine synthase (MS) with a methyl group sourced from the folate cycle, thus completing the methionine cycle [70, 99].

Histone methylation is crucial in modulating chromatin structure [120, 26]. Methylation primarily occurs on the lysine and arginine residues on the histone tail. Lysine residues, in particular, can be found in several states: mono-, di-, and tri-methylation. Histone methyltransferases (HMTs) deposit these methyl groups, using SAM as the universal methyl donor . The resulting methylation marks typically exert their effects by recruiting specific reader proteins [10, 108]. For instance, the heterochromatin Protein 1, HP1, recruited by H3K9 methylation helps to form and maintain heterochromatin regions [87]. Another example is the nucleosome remodeling factor (NURF), which is recruited by H3K4 methylation to promote nucleosome sliding and transcription [118]. Beyond recruiting chromatin remodelers, these methylation marks also attract reader proteins that participate in various gene expression regulatory processes, such as DNA methylation and

transcription initiation [33, 44].

Crucially, the cellular availability of SAM is intrinsically tied to that of methionine. It has been established that variations in methionine availability can influence levels of H3K4me3 [81], a critical mark for gene activation. This relationship underscores how metabolism can directly affect epigenetic regulations and gene expression.

1.4 Trimethylation of histone H3K36 (H3K36me3)

As one of the major histone methylation marks, H3K36me is predominantly localized to the 3′ end of the gene body [50, 62]. This mark is predominantly associated

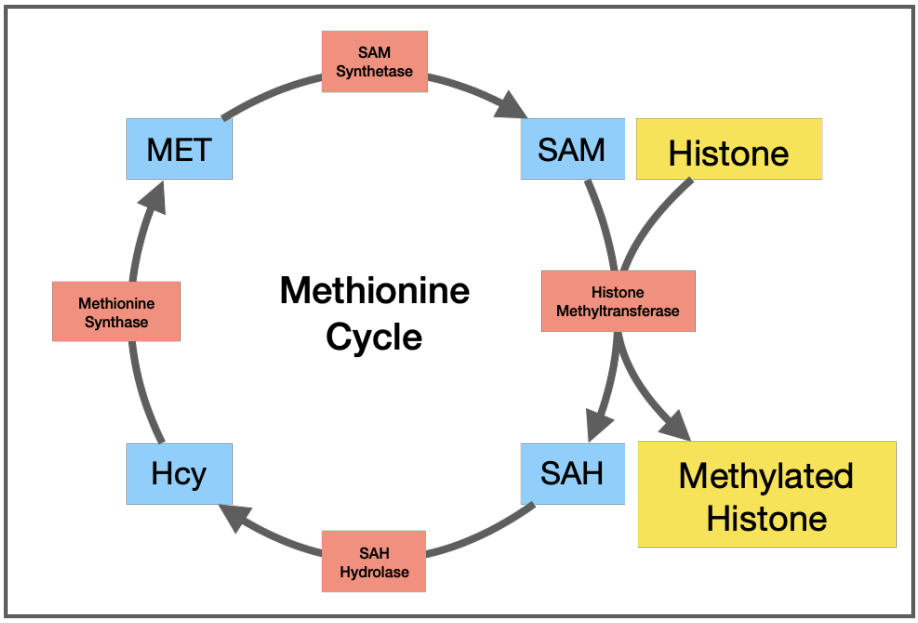

FIGURE 1.4: **Schematic representation of the methionine cycle with key intermediates.** Starting with methionine (MET), the cycle progresses to the synthesis of S-adenosylmethionine (SAM), a principal methyl donor within the cell, involved in the methylation of histones and other proteins. S-adenosylhomocysteine (SAH) is produced as a byproduct of these methylation reactions and is subsequently hydrolyzed into homocysteine (Hcy) by SAH hydrolase. Homocysteine then assimilates a carbon unit from the folate cycle and is converted back to methionine by the action of methionine synthase, thereby completing the cycle.

with transcription elongation [50, 62]. Like other histone methylation marks, its influence is mainly mediated through interactions with various effector proteins [85].

For instance, it engages with the histone deacetylase Rpd3S complex [45], which deacetylates histones, aiding in the suppression of transcription from cryptic promoters in budding yeast. It can also inhibit the H3K27 methyltransferase, the PRC2 complex [41], thus preventing the addition of H3K27me3, a marker of repression.

Apart from regulating transcription, H3K36me3 is crucial in several cellular functions. It is associated with DNA repair, notably by interacting with MutSα through its PWWP domain for mismatch repair [65] and with LEDGF to support homologous recombination during double strand breaks [28]. H3K36me3 also plays a role in alternative splicing, mainly by facilitating the recruitment of MRG15 and the polypyrimidine tract-binding protein (PTB) [74].

Furthermore, H3K36me3 is associated with DNA methylation through its interaction with DNMT3B [82], contributing its role in the suppression of cryptic transcription [86]. H3K36me3 is also associated with RNA methylation via its interaction with METTL14 [51]. Consequently, the multifaceted functions of H3K36me3 are evident in its significant roles in various cancer types and its influence on cell fate determination.

1.5 Histone methyltransferase SETD2

SETD2, as depicted in Figure 1.5, is likely the only enzyme in mammals responsible for the trimethylation of H3K36. The SET domain, central to the catalytic activity of SETD2, is shown in Figure 1.6A. This domain is a characteristic feature of many histone methyltransferases [129, 31, 77, 34, 104], as illustrated in

Figure 1.6B. Extensive research has explored the enzymatic mechanisms of SET family methyltransferases. Such studies have provided insights, including the effects of mutations on substrate binding and reaction kinetics, which are crucial for understanding proteins similar to SETD2 (Figure 1.7) [123, 46, 13, 100, 3]. For instance, it has been documented that arginine and tyrosine residues in the SAM binding pocket can influence SAM binding capabilities and catalytic activity [129]. Besides the SET domain and the associated AWS and PS domains, the C-terminal region of SETD2 contains domains vital for regulatory functions and substrate specificity[77]. The Set2-Rbp1 Interaction domain (SRI) is critical for its association with the C-terminal domain (CTD) of RNA Pol II (RNAPII) [66, 59, 124]. Additionally, domains in the C-terminal region, like the WW and CC domains, play important roles in regulation [77]. While the N-terminal is largely unstructured, it is instrumental in regulating SETD2 degradation [7, 8].

FIGURE 1.5: **Domain architecture of Setd2.**

In addition to methylating H3K36, Setd2 has shown capability in methylating non-histone substrates. For instance, SETD2 has been identified as mediating the methylation of STAT1 at K525, crucial in IFNa antiviral immunity [20]. SETD2 is also attributed to the trimethylation of lysine 40 on α-tubulin (α-TubK40me3) during mitosis, suggesting its potential involvement in chromosome segregation [88, 58]. In another context, Setd2 has been observed to methylate lysine 68 on actin (ActK68me3), a modification associated with cell migration [103]. Collectively, these findings underscore the significance of Setd2 in fundamental cellular activities.

1.6 Mouse myoblast cell, C2C12

C2C12 is a mouse myoblast cell line that is widely used in studying skeletal muscle development and differentiation. In their proliferation phase, C2C12 cells exhibit a spindle-shaped, mononucleated structure (Figure 1.8A) [122]. However, when exposed to low-serum conditions that trigger differentiation, they undergo fusion, leading to the formation of multinucleated myotubes (Figure 1.8B) [122]. This pronounced morphological transition provides a straightforward indicator for monitoring differentiation stages. Beyond the evident morphological changes, there is a meticulous orchestration of gene expression [128]. This intricate interplay makes C2C12 cells an appealing model for investigating the impact of nutrients on epigenetic processes.

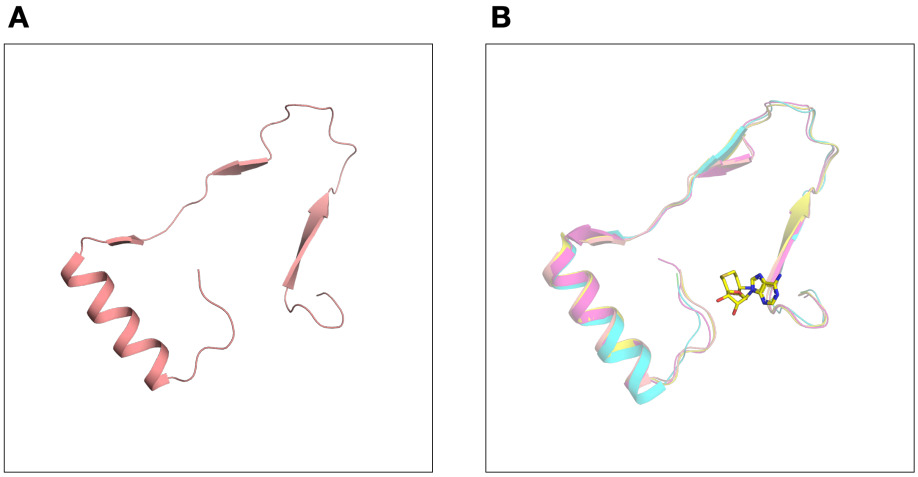

FIGURE 1.6: **Comparative visualization of SET domains across species.** (A) Structural depiction of a segment of the SET domain from mouse Setd2. (B) Superimposed structures of the SET domain across different species and sources: Neurospora DIM-5, a histone H3 lysine 9 methyltransferase (PDB: 1PEG), yeast Set2 (predicted by AlphaFold), human Setd2 (PDB: 4H12), and mouse Setd2 (predicted by AlphaFold). S-adenosylmethionine (SAM) is highlighted in stick representation.

1.7 Scope of this thesis

As previously noted, methionine serves functions beyond just histone methylation. For instance, its involvement in DNA methylation has also been linked to roles in epigenetic regulations. Additionally, various facets of methionine metabolism may have implications for both epigenetic regulation and gene expression. While there are a multitude of histone modifications beyond just methylation, even within histone methylation itself, there are a plethora of types to consider.

In this thesis, I delve into the effect of methionine on the specific histone methylation mark, H3K36me, and the implications in myogenic differentiation of C2C12

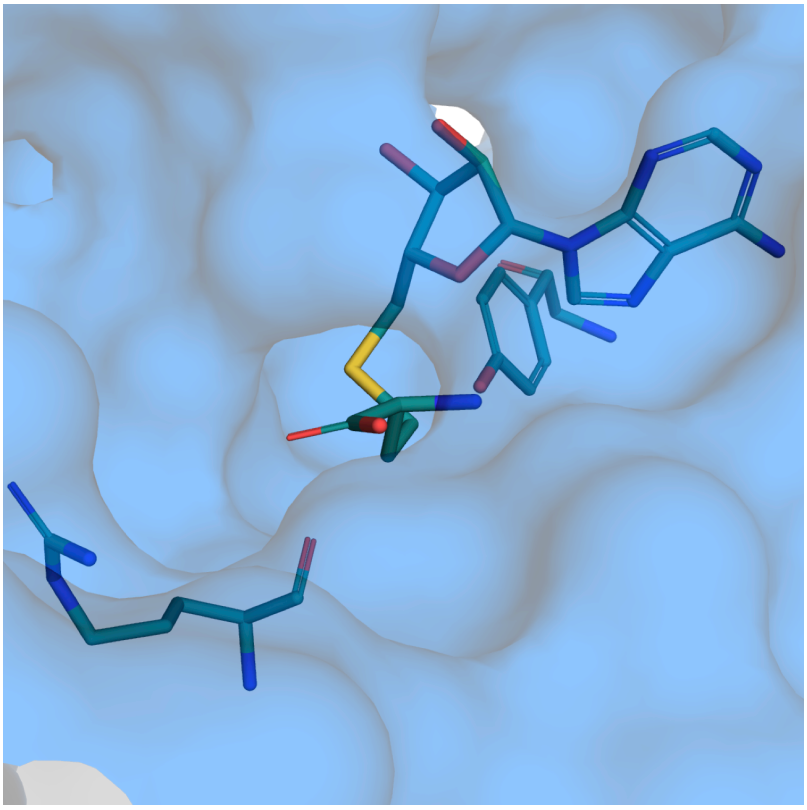

FIGURE 1.7: **Close-up view of the SET domain substrate binding site.** Shown here are S-adenosylhomocysteine (SAH) and nearby arginine and tyrosine residues, which have been implicated in S-adenosylmethionine (SAM) binding and methyltransferase activities. (PDB: 4H12)

mouse myoblast cells. I've made considerable efforts to control for potential confounding factors. While I cannot exclude the influence of other methionine-related processes on the final cellular outcomes, my objective is to ascertain the roles of methionine, SAM, Setd2, and H3K36me3 in determining these outcomes. Through this work, I hope to illuminate some of these intriguing questions regarding metabolism and epigenetics.

In the forthcoming chapter, I turn my attention to an often-overlooked facet of methionine metabolism: the bioavailability of S-adenosylmethionine (SAM). I discuss the chemical stability of SAM, delve into its cellular transport mechanisms, and discuss their implications. This consideration is not only vital for designing experiments but also for interpreting results, insights that have greatly informed my own research project.

In Chapter 3, I present the main findings from my investigation into the impact

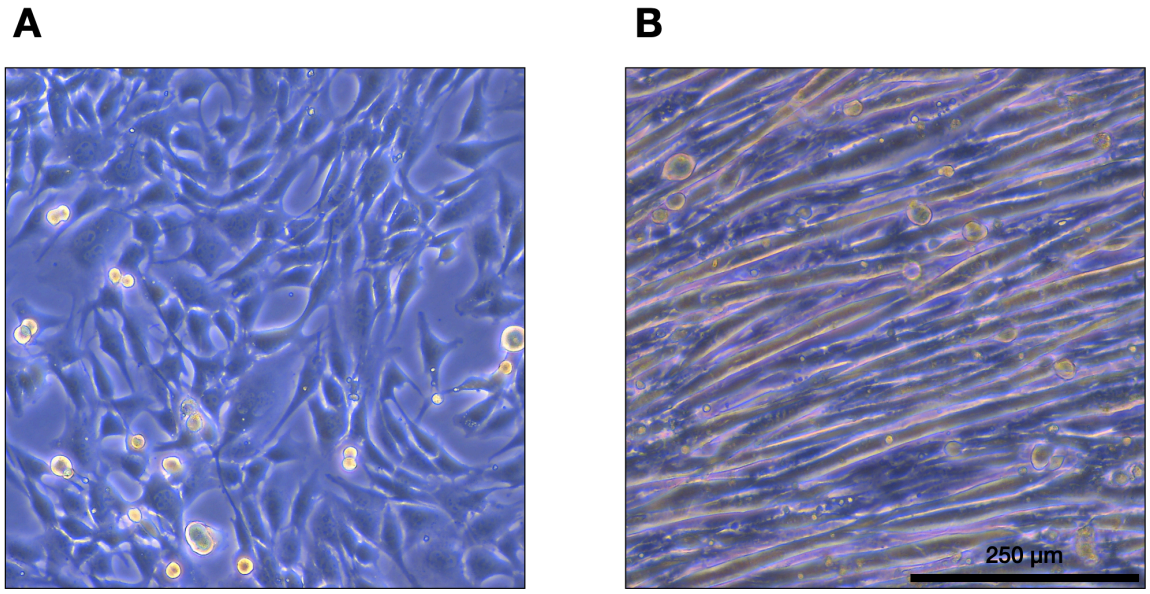

FIGURE 1.8: **Morphological changes in C2C12 cells at different stages.** (A) C2C12 cells display a mononucleated, spindle-shaped morphology. (B) Differentiated C2C12 cells demonstrate the formation of multinucleated myotubes.

of methionine on H3K36me3 and the myogenic differentiation. I begin by establishing a dependency, followed by an examination of the dynamics and reversibility of this dependency. Subsequent sections delve into the roles of SAM and Setd2 in mediating the methionine-dependent phenotype. I complement these findings with data on H3K36me3 distribution and global chromatin accessibility, underscoring the significance of H3K36me3 in the process.

2

The bioavailability and cellular transport properties of S-adenosylmethionine[1]

2.1 Summary

S-adenosylmethionine (SAM) is a versatile metabolite involved in many types of reactions, including methylation and transsulfuration. Through them, SAM can impact cellular processes such as gene expression and redox equilibrium. Its significance is underscored by its common use both as an over-the-counter nutrient supplement and as an experimental reagent in molecular biology. Yet, the bioavailability and cellular transport dynamics of SAM often remain overlooked in these scenarios. This can hinder its therapeutic potential and add complexity to experimental result interpretations. Here, we scrutinize the chemical stability and cellular permeability of SAM, suggest a model for its indirect transport across mammalian plasma membranes, and explore the consequences stemming from this proposed transport mechanism.

[1] This chapter was adapted and modified from published work: Sun Y. and Locasale JW. "Rethinking the bioavailability and cellular transport properties of S-adenosylmethionine" *Cell Stress* (2022). [109]

2.2 Introduction

The presence of an electron-deficient sulfur within SAM renders the covalent bond between the sulfur and its adjacent groups particularly prone to nucleophilic attacks. This susceptibility facilitates the transfer of these groups to other molecules, allowing SAM to engage in a plethora of chemical reactions, including methylation, transsulfuration, and aminopropylation [22]. Cells leverage these reactions for essential functions such as protein and nucleic acid methylation, sulfur amino acid metabolism, and polyamine synthesis. Therefore, SAM plays pivotal roles in regulating gene expression, maintaining redox balance, and other critical cellular processes. Altering intracellular SAM availability can profoundly influence cell biology, physiology, and even disease progression.

Given its significance, SAM is frequently employed as a reagent in tissue culture studies, particularly those centered on methionine metabolism and other SAM-mediated processes. A common thread in many of these studies is the initial identification of genes related to SAM. This is frequently followed by complementation or rescue experiments, where direct SAM supplementation is used to further validate the causal relationship between SAM availability and the observed cellular outcomes. In such experiments, SAM is typically introduced directly into the cell culture medium, spanning durations from overnight to several days, as seen in cell proliferation studies. However, the cellular uptake and utilization of such externally supplied SAM is often overlooked, posing challenges in experiment design and result interpretation.

Unlike tissue culture experiments, where the components of the culture medium can be relatively well-defined, animal experiments often involve diets with less precise chemical compositions. This is further complicated by the interactions among the microbiota, food, and the host, all of which can influence the bioavail-

ability of a supplemented nutrient in studies. For instance, the enzyme L-methioninase, which breaks down methionine, is commonly found in fungi and bacteria [36]. Since SAM is the direct metabolic product of methionine, the metabolism of methionine by the host's microbiota could also potentially affect SAM availability and metabolism. Additionally, microbiota might also influence the host's SAM metabolism through B-vitamin production and choline consumption [63]. Some complexities stemming from host-microbiota interactions can be probed by manipulating metabolic genes governing nutrient utilization. Yet, in many instances, such isolation proves difficult, leaving the broader effects of host-microbiota interactions largely uncharted. Given these considerations, this thesis will mainly focus on the transport and availability of SAM at the cellular level.

2.3 Transport properties of SAM

Synthesized from methionine and ATP, SAM is distinctly polar (Figure 2.1). This polarity poses obstacles for its passive diffusion across biological membranes. Cellular uptake studies in hepatocytes have shown that the intracellular accumulation of SAM is limited, with an equilibrium ratio of intracellular to extracellular SAM concentrations being 0.19 μM : 1 μM [80]. Further research in an intestinal epithelial model indicates that the apparent permeability coefficient of SAM (ranging from 0.6×10-6 to 0.7×10-6 cm/s) is significantly below standard values for passive diffusion [80]. This suggests that the primary mode of transport for SAM is paracellular, where molecules mainly navigate through the tight junctions.

This idea is reinforced by the likely absence of SAM-specific transporters in the plasma membranes of mammalian cells. While SAM transporters have been identified in yeast plasma membranes (SAM3) [97] and in the inner membranes of human mitochondria (SAMC) [1], the absence of a mammalian counterpart to

SAM3, combined with the mitochondrial localization of SAMC [1], implies the absence of a dedicated SAM transporter in mammalian plasma membranes. Given these findings, one might conclude that direct SAM supplementation would have minimal impact on cellular biology due to its inefficient cellular absorption. However, both clinical trials and lab experiments have reported positive outcomes from SAM supplementation. This apparent paradox may be explained if SAM is taken up by the cell not in its intact form, but rather as breakdown products, which are then reconstituted back into SAM within the cell.

2.4 Chemical stability of SAM under physiological conditions

Standard cell culture media are typically buffered to maintain a slightly basic environment. Such conditions, combined with a temperature of 37°C, have been shown to compromise the covalent stability of SAM. Liquid chromatographic analyses indicate that SAM is highly unstable at pH 7.5, undergoing rapid non-enzymatic cleavage to form 5′-methylthioadenosine (MTA) [116] [15] (Figure 2.1). Attempts to enhance SAM's stability have led to the development of more stable salts, such as the widely utilized sulfate and p-toluenesulfonate double salts of SAM. These modifications have improved its stability in the dry state, signifi-

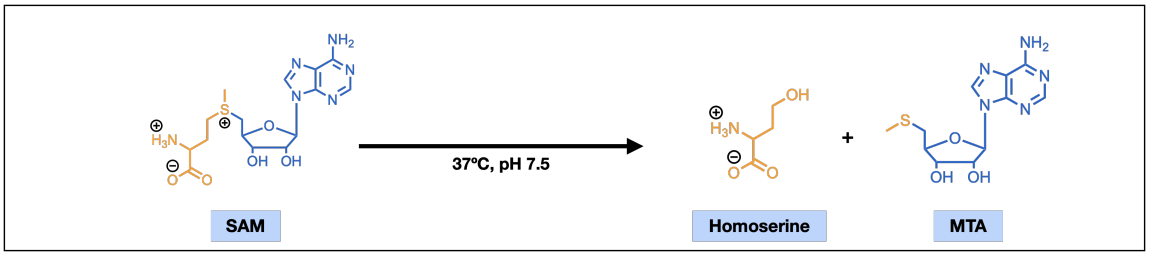

FIGURE 2.1: **SAM, featuring elements of an amino acid (highlighted in yellow) and a ribose nucleotide (highlighted in blue), is highly polar.** In physiological conditions, SAM can spontaneously cleave in a non-enzymatic reaction, leading to the formation of homoserine and MTA.

cantly extending shelf life [40]. However, concerns regarding its in-solution stability persist. The reported half-life of SAM in solution ranges between 16 to 42 hours [22]. Notably, this time frame coincides with the duration of many rescue experiments in tissue culture studies, potentially impacting the intracellular availability of SAM throughout these experiments.

2.5 Cellular permeability of 5′-methylthioadenosine (MTA) and the methionine salvage pathway

MTA, in contrast to SAM, can effectively cross the plasma membrane of mammalian cells [107]. Given its chemical resemblance to an adenosine nucleoside, MTA can permeate the cell via the general nucleoside transport system [107]. Furthermore, kinetic investigations suggest that MTA might also enter the cell through passive diffusion, which, in some scenarios, could account for more than half of its total influx [107]. This provides a potential avenue for cells to utilize extracellular MTA sourced from degraded extracellular SAM.

Typically arising as a byproduct during polyamine synthesis, MTA often undergoes recycling back into methionine via the coordinated actions of enzymes in what's known as the methionine salvage pathway. In this pathway, both the methylthio group of MTA and the carbon backbone of its ribose are conserved, eventually reassembling into methionine [2]. Methionine produced this way can then be combined with intracellular ATP to restore intracellular SAM levels. Notably, the methionine salvage pathway has been observed to ramp up in response to specific SAM-demanding processes, like polyamine synthesis in yeast [2]. This suggests that the methionine salvage pathway might play a supplementary role in maintaining SAM levels, in addition to its regular sources.

Such findings hint at an indirect transport mechanism for the sulfur and methyl group of extracellular SAM, where MTA serves as the intermediary (illustrated in

Figure 2.2). Indeed, research has shown that MTA's passive diffusion alone can support a methionine salvage capacity up to 50 μM. Moreover, MTA supplementation has been found to sustain the short-term growth of lymphoblasts even in methionine-depleted culture media [14].

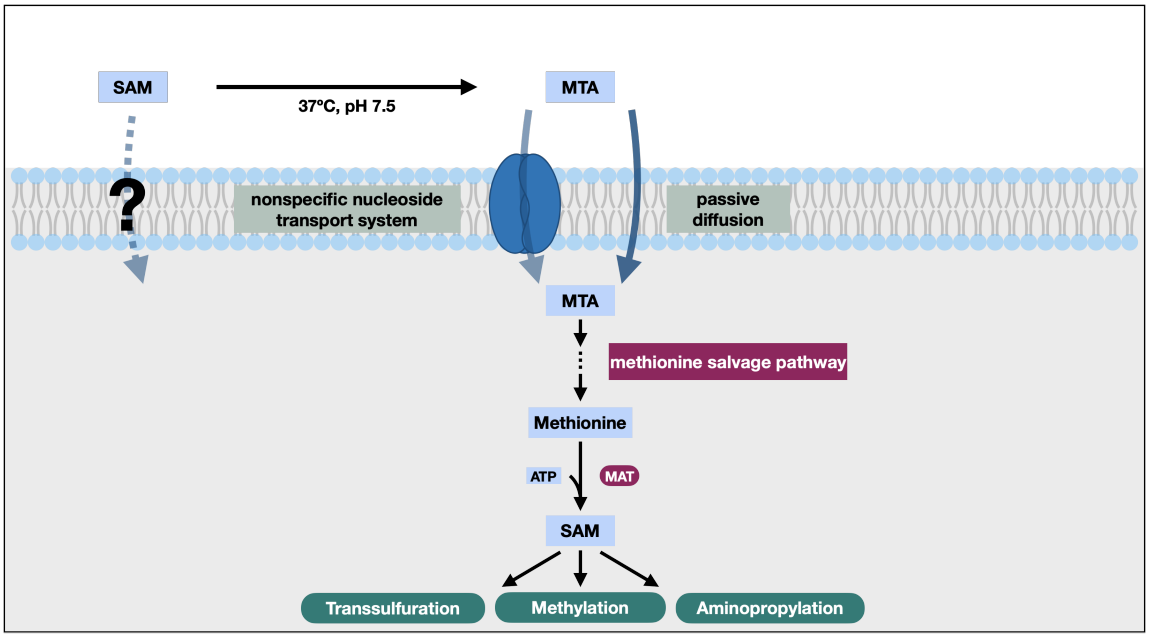

FIGURE 2.2: **The indirect SAM transport schematic.** The polar nature of SAM and the likely absence of SAM transporters in the plasma membrane presents challenges for the direct transport of SAM across the plasma membrane and limits its bioavailability. Under physiological conditions, however, SAM readily degrades into MTA. Unlike SAM, MTA can cross cell membrane through both nonspecific nucleoside transport system and passive diffusion. Once inside the cell, MTA can participate in the methionine salvage pathway to regenerate methionine, which can be utilized by the SAM synthase, methionine adenosyltransferase (MAT), to replenish intracellular SAM. When viewed as a whole, MTA effectively brings in the sulfur and activated methyl group of the extracellular SAM into the cell, overcomes the challenges of direct SAM transport across plasma membrane, and enables the utilization of those functional groups for reactions such as methylation and transsulfuration.

Considering SAM's inherent instability and its difficulty in permeating cell membranes, coupled with MTA's ability to both cross the cell membrane and

participate in methionine salvage, it's plausible that the effects observed from extracellular SAM supplementation in tissue culture experiments are primarily mediated through methionine and SAM derived from MTA. This is particularly relevant considering that SAM synthase MAT2A has been identified within the nucleus [57], suggesting an in situ capacity for SAM production inside the nucleus.

2.6 Implications of the indirect SAM transport schematic

When considering the possibility that SAM supplementation operates primarily through MTA, several implications come to the fore. Firstly, this mechanism, in addition to supplying methionine and SAM, could elevate MTA levels beyond those typical of regular SAM metabolism. MTA itself has a myriad of cellular impacts. Notably, it has been documented to inhibit histone methylation and impede the activity of S-adenosylhomocysteine (SAH) hydrolase [22]. The latter can cause SAH accumulation, a known inhibitor of many methyltransferases, which also plays a significant role in one-carbon metabolism via the methionine cycle [99]. Elevated MTA levels, surpassing 50 μM, have indeed shown toxicity in lymphoblasts [14].

Secondly, the intricate methionine salvage pathway, which underlies this indirect SAM transport mechanism, is composed of a series of delicate steps. With at least five enzymatic reactions bridging MTA and methionine [2], a defect in any single enzyme could derail the entire pathway. A prime example is the methylthioadenosine phosphorylase (MTAP) – essential for the initial step of converting MTA into methionine – which is often defective in numerous cancer cell lines [99]. Such anomalies could muddle the interpretation of experimental results stemming from SAM supplementation.

Lastly, due to the inherent step of methionine salvage, SAM supplementation could inadvertently increase intracellular methionine levels. This poses a conundrum when trying to distinguish methionine's broader roles, like protein synthesis and nutrient sensing, from its specific function in methyl group donation via SAM.

2.7 Conclusions

Given the complexities surrounding extracellular SAM supplementation and the potential nuances of indirect SAM transport, several considerations are pivotal for experiment design involving SAM supplementation or when enhancing SAM's therapeutic utility. Firstly, it's essential to scrutinize the genetic background of the experimental system, with particular attention to genes integral to the methionine salvage pathways. Secondly, conducting parallel MTA supplementation alongside SAM might bolster the causal relationship between SAM and the observed outcomes. Lastly, leveraging genetic manipulation or pharmacological interventions targeting SAM-utilizing enzymes could help differentiate the influences of SAM from those of methionine on a particular phenotype.

3

Methionine-dependent H3K36me3 and myogenic differentiation[1]

3.1 Summary

Histone modifications play a pivotal role in epigenetic regulation, influencing DNA accessibility and gene expression. It's known that metabolism, especially the metabolism of methionine, can affect histone methylation by modulating the availability of substrates for histone methyltransferases. However, the direct role of methionine availability in key histone modifications such as H3K36me3 and its cellular effects has been less explored. Here, we show that methionine, via its metabolic derivative, S-adenosylmethionine (SAM), dynamically regulates H3K36me3 levels and myogenic differentiation of C2C12 mouse myoblast cells. We also demonstrate that the influence of methionine on differentiation is partially acted through the methionine-SAM-Setd2 axis. Moreover, when applying methionine restriction in C2C12 cells, there's a preferential decrease in H3K36me3 lev-

[1] This chapter was adapted and modified from published work: Sun Y, Ramesh V, Wei F, Locasale JW "Methionine availability influences essential H3K36me3 dynamics during cell differentiation" *bioRxiv* (2023). [110]

els and chromatin accessibility at gene loci that are tied to myogenic differentiation. Interestingly, some effects of methionine restriction on differentiation and chromatin accessibility are mirrored by the knockout of methyltransferase Setd2. Collectively our findings reveal the dynamic interactions between methionine metabolism, histone methylation, and cell differentiation, enhancing our understanding of how metabolic changes might influence epigenetic regulations and cellular processes.

3.2 Introduction

Histone methylations are central to epigenetic regulatory mechanisms. It modulates DNA accessibility, adding an additional layer of control over gene expression and cell fate determination [60, 83, 54, 4, 98]. Intriguingly, the link between histone methylation and metabolism is increasingly evident [94, 26, 120]. For instance, metabolic derivatives like SAM from the methionine cycle are directly employed as substrates for histone methylation [81]. Moreover, products like α-ketoglutaric (2-OG), generated by isocitrate dehydrogenase (IDH) in the TCA cycle, function as cofactors for histone demethylases [78]. Another compound, 2-hydroxyglutarate (2-HG) — a byproduct of mutated IDH — has been shown to inhibit histone demethylase [21, 121].

Some investigations have probed the interplay between 2-HG/2-OG, histone methylation, and cellular processes such as cell differentiation [73, 17, 101]. Nevertheless, the opposing process of histone methylation by histone methyltransferase and SAM remains relatively less studied. Prior research indicates that methionine availability can modulate intracellular SAM concentrations, affecting key histone methylation markers such as H3K4me3 [81, 43]. However, the implication of methionine restriction on cellular processes and other histone methylation markers

remain underexplored.

To fill this gap in knowledge, we investigated how methionine restriction affects H3K36me3 dynamics and its subsequent ramifications during the myogenic differentiation of C2C12 cells. Our findings underscore that both H3K36me3 levels and C2C12 myogenic differentiation are dependent on methionine, exhibiting reversible characteristics. Further, the evidence suggests that the influence of methionine on differentiation partially stems from the methionine-SAM-Setd2 axis. In addition, we observed a preferential reduction in H3K36me3 levels and chromatin accessibility at gene loci that are tied to muscle differentiation, further bolstering the model of a methionine-epigenetic crosstalk in orchestrating cell differentiation.

3.3 Results

3.3.1 Myogenic differentiation and H3K36me3 are methionine-dependent processes

To investigate how methionine impacts cell differentiation, we utilized the widely-studied C2C12 mouse myoblast cell line. This cell line is known to initiate myogenic differentiation when switched from nutrient-rich growth media (GM) to the relatively nutrient-poor differentiation media (DM) [32]. Specifically, cells were cultured to confluence in GM supplemented with 200 μM of full methionine (MET). Subsequent transition to DM involved either limiting methionine (MR) to 20 μM or completely removing it (MD, 0 μM) (Figure 3.1). Over a five-day differentiation period, cells undergoing MR or MD treatment exhibited disrupted differentiation, evidenced by the absence of elongated myotube formation (Figure 3.3A). Additionally, we created a machine learning-based program to quantify differentiation from phase-contrast microscope images (Figure 3.2 and Methods) and observed reduced differentiation scores for cells on MR and MD conditions at

D3 and D5 relative to controls (Figure 3.3B). This impaired differentiation in MR and MD conditions was corroborated by reduced protein levels of myosin heavy chain (MyHC) observed through immunoblotting (Figure 3.3C). The analysis of methionine cycle intermediates revealed a significant reduction in their levels under MR or MD (Figures 3.4).

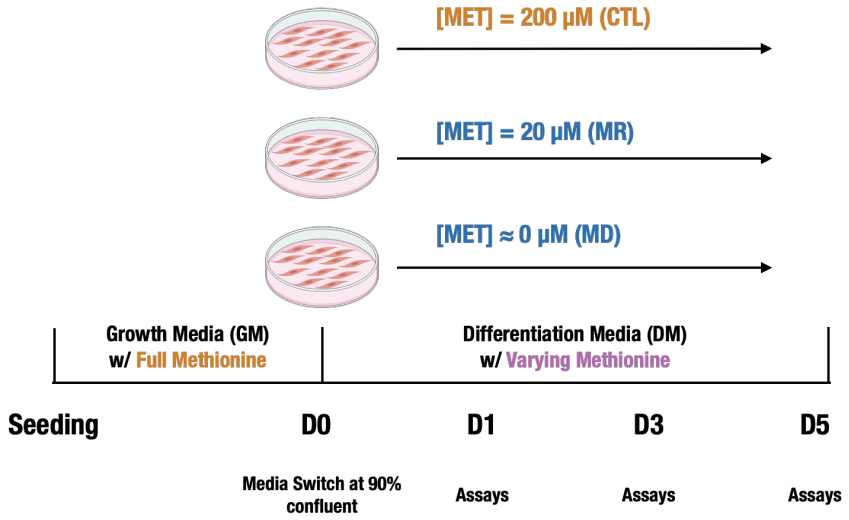

FIGURE 3.1: **Schematic representation of the experimental design for exploring dependency on methionine in myogenic differentiation.** C2C12 cells were transitioned from growth media (GM) with 200 μM methionine (MET) to differentiation media (DM) with methionine either stayed at 200 μM (CTL), restricted to 20 μM (MR) or completely depleted (MD, 0 μM). Imaging and assays were performed on D1, D3 and D5.

In examining the epigenetic consequences of methionine restriction, we evaluated several key histone methylation marks. Notably, H3K36me3 exhibited a substantial decrease in response to both MR and MD (Figure 3.5A). Chromatin Immunoprecipitation Sequencing (ChIP-Seq) analysis for H3K36me3 revealed that, although its abundance across all genes remained relatively unchanged during the differentiation period, MR notably reduced its levels (Figure 3.5B).

Importantly, our MR treatment did not exert severe cellular stress; evidenced

by minimal impact on cell proliferation at 24 and 48 hours and an unhindered progression to confluence (Figure 3.6), a prerequisite for differentiation.

To further elucidate the relationship between methionine availability, differentiation, and histone methylation, we exposed cells to varying methionine concentrations. Our findings indicated a dose-dependent relationship between methionine concentration, relative differentiation score, MyHC expression, and H3K36me3 levels (Figures 3.7), thus demonstrating a methionine dose-dependent effect on these phenotypes. In summary, our data highlight the dose-responsive nature of myogenic differentiation and H3K36me3 dynamics in relation to methionine availability.

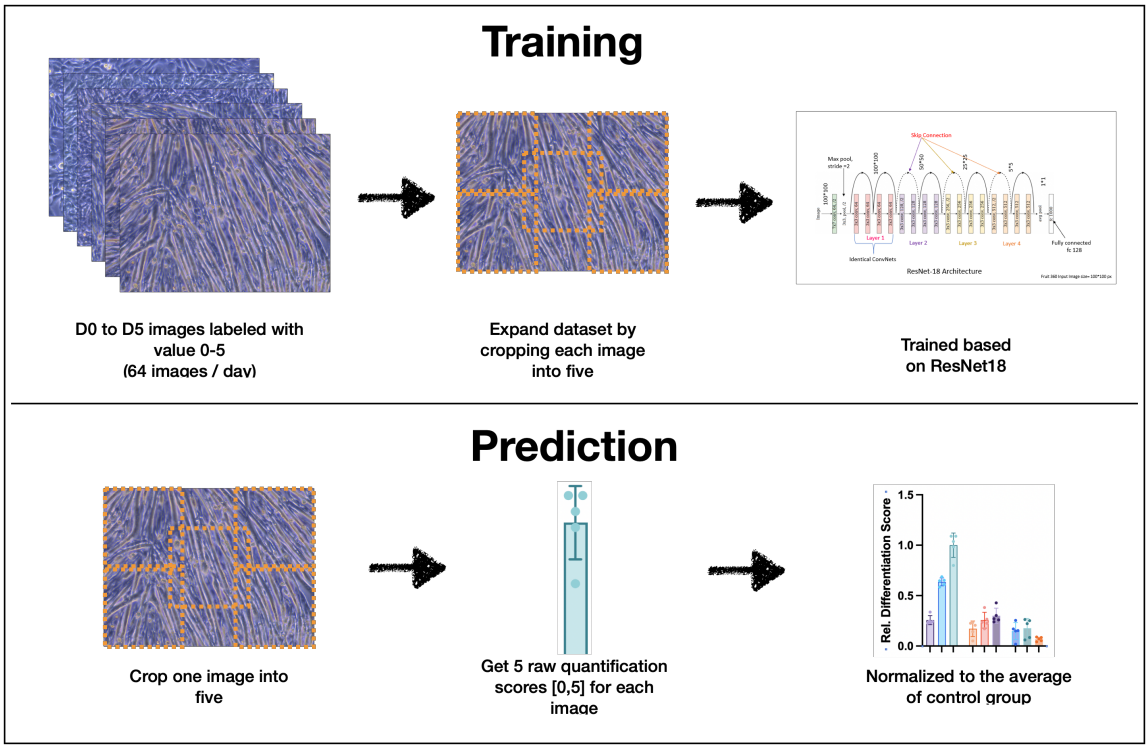

FIGURE 3.2: **Schematic of training and prediction process of DiffQuant** - a machine learning-based tool designed to quantify C2C12 cell differentiation from phase contrast microscope images.

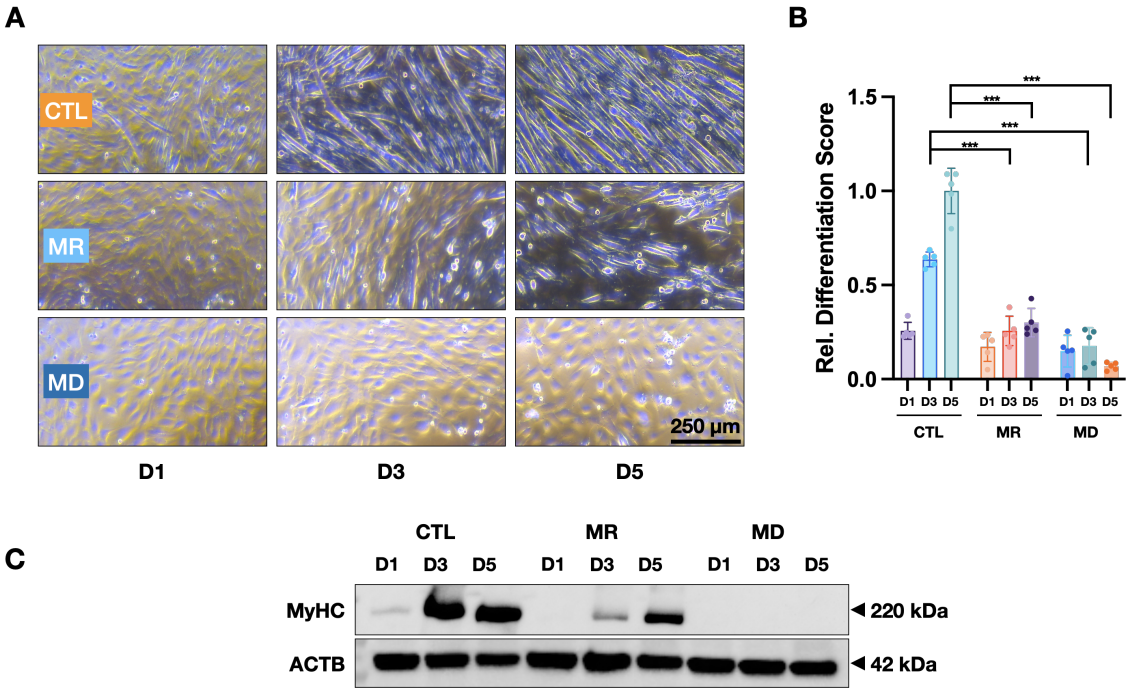

FIGURE 3.3: **Myogenic differentiation is methionine-dependent.** (A) Representative images of C2C12 cells on Day 1 (D1), Day 3 (D3) and Day 5 (D5) under MET, MR, and MD conditions. (B) Quantification results of C2C12 cell images during differentiation under different methionine conditions. (C) Immunoblot analysis of myosin heavy chain protein (MyHC) expression during differentiation under different methionine conditions.

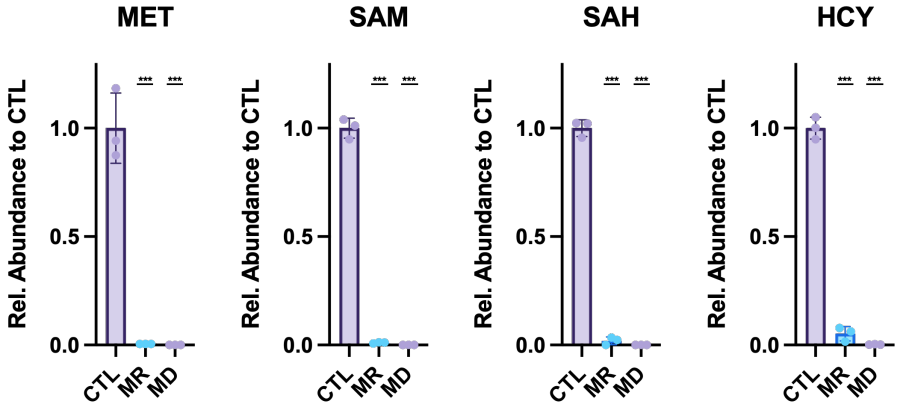

FIGURE 3.4: **Methionine cycle metabolites reduced in response to methionine restriction.**

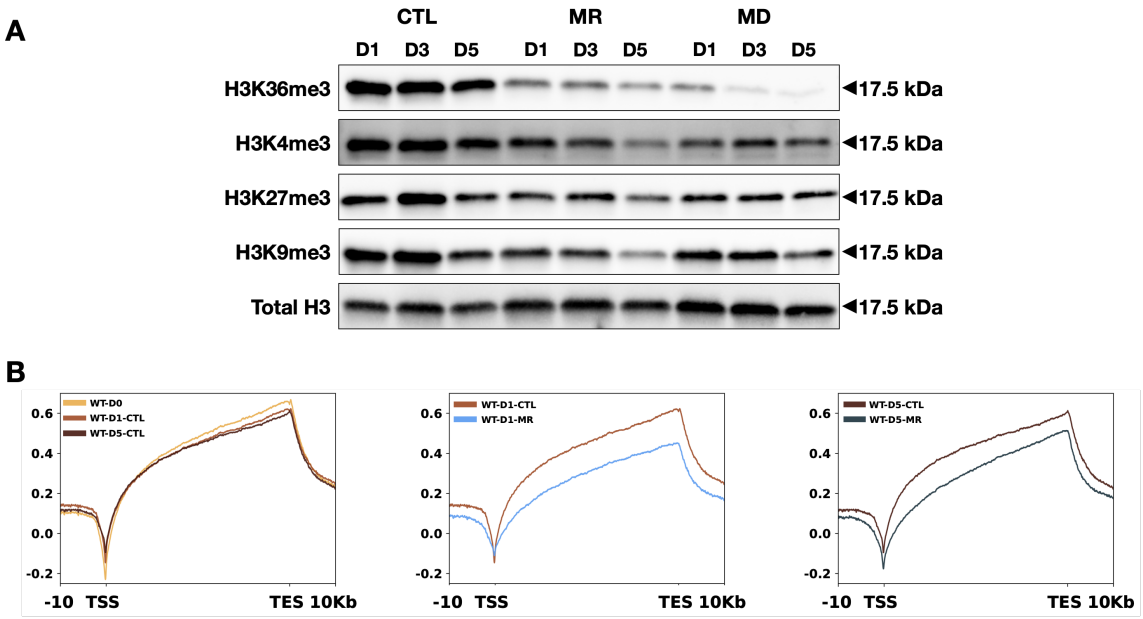

FIGURE 3.5: **H3K36me3 is methionine-dependent.** (A) Immunoblot analysis of common histone tri-methylation marks in response to MR and MD. (B) ChIP-Seq profile of H3K36me3 abundance across all genes during normal course of differentiation. TSS: Transcription Start Site, TES: Transcription End Site.

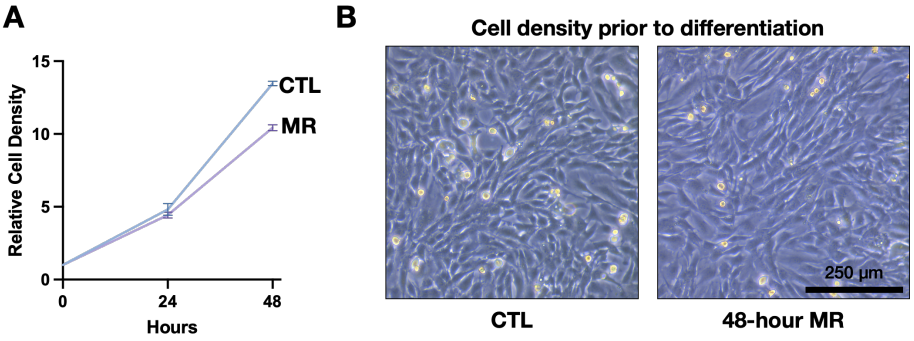

FIGURE 3.6: **Methionine restriction has minimal impact on C2C12 cell proliferation.** (A) Relative cell density at 24 hours and 48 hours post seeding. (B) Representative microscope images of C2C12 cells 48 hours post seeding.

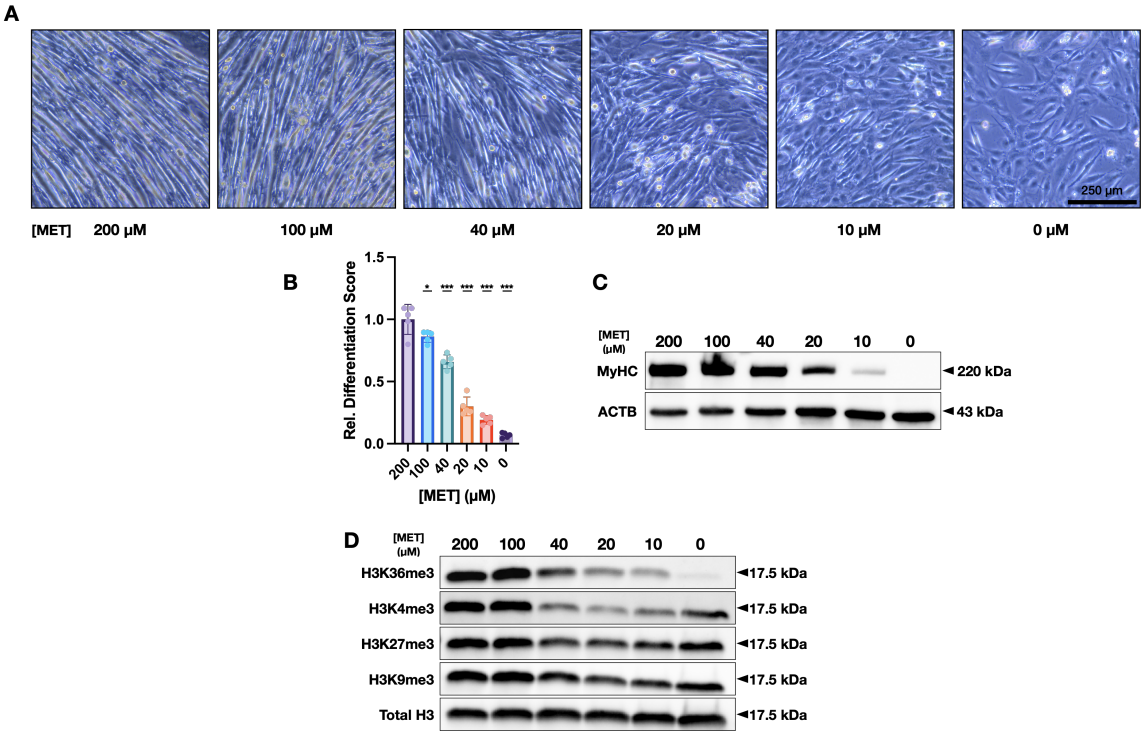

FIGURE 3.7: **Dose-dependent relationship between methionine concentration, relative differentiation score, MyHC expression, and H3K36me3.** (A) Representative images of C2C12 cells on Day 5 (D5) that were kept on differential media with a gradient of methionine concentration. (B) Quantification of differentiation on D5 cell images. (C) Immunoblot analysis of myosin heavy chain protein (MyHC) expression and (D) common histone tri-methylation marks on Day 5 (D5) in cells that were kept on differentiation media with a varying methionine concentration.

3.3.2 *Methionine dynamically controls H3K36me3 and myogenic differentiation*

Subsequently, we investigated whether the decrease in H3K36me3 levels and the hindrance in differentiation induced by MR were reversible. Cells were subjected to either MR or MD conditions during the five-day differentiation window, which resulted in the expected disruption in differentiation. Following this phase, methionine was reintroduced at the control concentration of 200 μM (Figure 3.8). Remarkably, this reinstatement led to a progressive recovery of the differentiation process in cells pre-treated with both MR and MD (Figure 3.9), along with a restoration of H3K36me3 levels (Figure 3.10).

Moreover, when cells previously exposed to MR or MD – both exhibiting pronounced differentiation defects – were granted an additional five-day differentiation window without methionine repletion, no substantial differentiation advancement was observed, based on relative differentiation scores (Figure 3.9). This suggests that MR doesn't merely decelerate differentiation but rather imposes a halt to the process.

These findings highlight the reversible nature of the effects of methionine on H3K36me3 modulation and differentiation dynamics. Importantly, the reversibility of these effects narrows down the possible underlying mechanisms. For instance, it suggests that processes inherently incompatible with such reversibility, like increased mutation rates due to compromised DNA damage repair systems or extensive chromatin instability caused by the loss of H3K36me3, are unlikely contributors. Our results are thus consistent with transient and reversible alterations in the epigenetic landscape mediated by methionine availability.

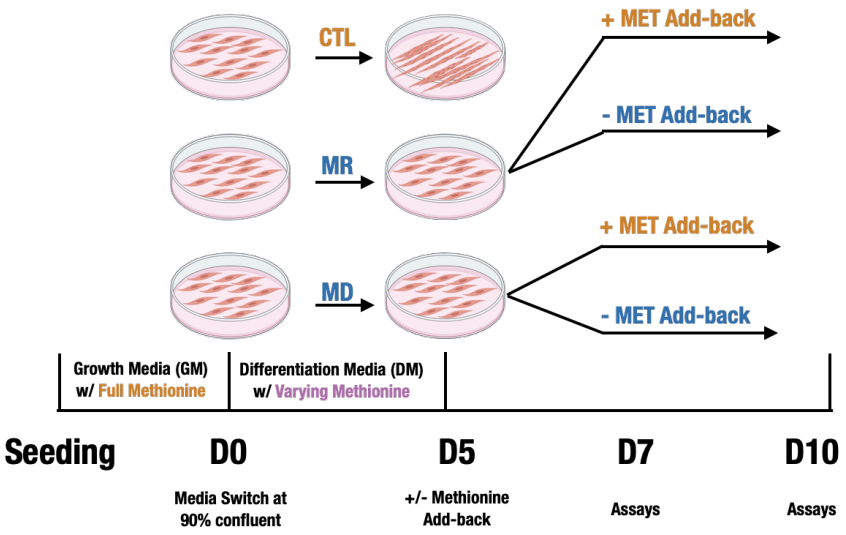

FIGURE 3.8: **Schematic representation of the experimental design for investigating the reversibility of the effects of methionine restriction on H3K36me3 and myogenic differentiation.** The normal 5-day differentiation period with methionine restriction (MR) or depletion (MD) is followed by additional 5-day differentiation period with or without reintroduction of methionine at control concentration (200 μM).

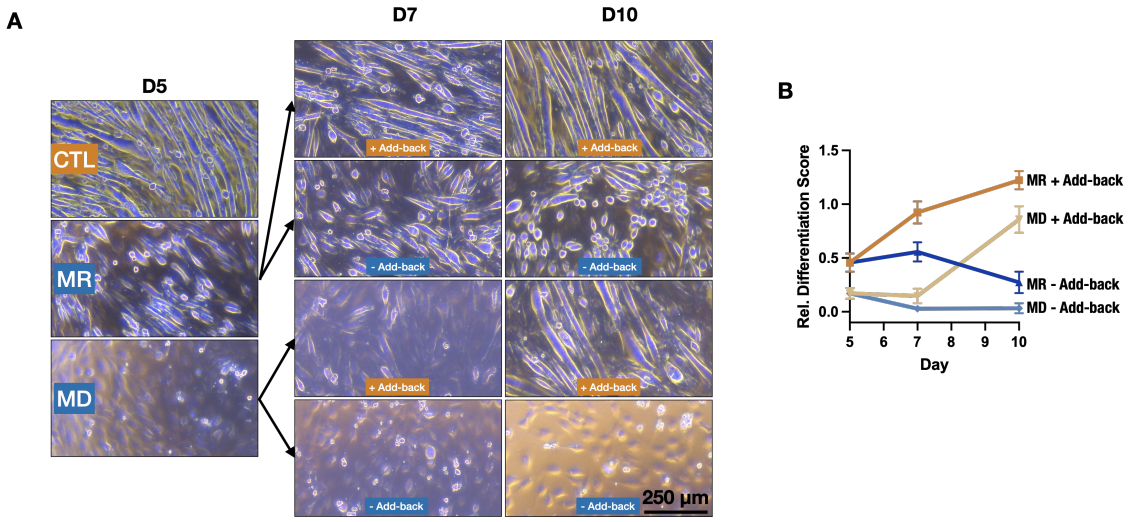

FIGURE 3.9: **Methionine-dependent myogenic differentiation is reversible.** (A) Representative images of C2C12 cells. (B) Differentiation score showcasing differentiation recovery in MR and MD pre-treated cells post-methionine add-back.

3.3.3 *H3K36me3 and methionine metabolism rapidly respond to methionine restriction*

To delve deeper into the kinetics of H3K36me3 and overall methionine metabolism in response to MR, we conducted time series experiments. These experiments measured the levels of H3K36me3 within the first 24 hours following the onset of methionine restriction. We observed that the levels of H3K36me3 begin to decline as early as 2 hours (our initial time point) after the initiation of restriction and continue to diminish across all subsequent time points up to 24 hours (Figure 3.11), a trend that continues to persist from D1 to D5 as indicated earlier (Figure 3.5A). This rapid response in H3K36me3 is mirrored by a swift reduction in cellular methionine and SAM levels, noticeable 1.5 hours after restriction starts, with levels continuing to fall thereafter (Figure 3.12). Intriguingly, the response of S-adenosylhomocysteine (SAH) and homocysteine (HCY) levels to methionine restriction is not immediately apparent at these early time points, only beginning to display around 12 hours post-restriction (Figure 3.12). Collectively, these findings demonstrate that methionine restriction elicits a rapid response in methionine

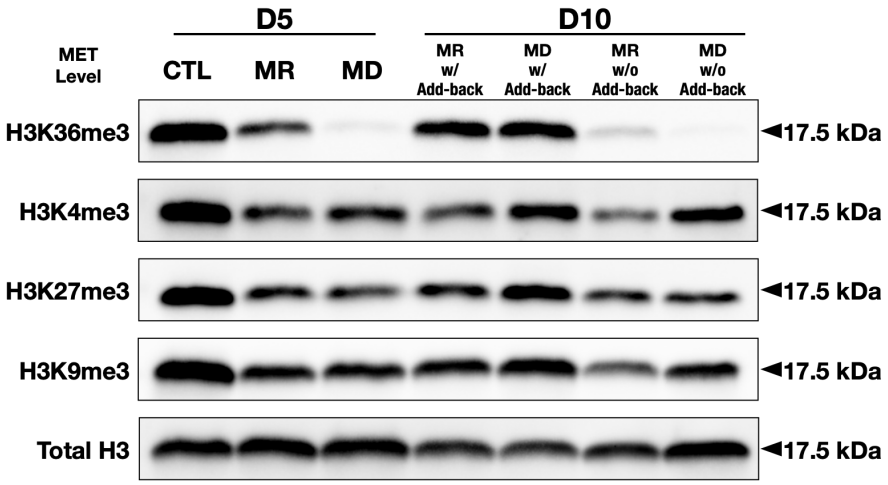

FIGURE 3.10: **Methionine-dependent H3K36me3 is reversible.** Immunoblot analysis of common histone tri-methylation marks showcasing restoration of H3K36me3 levels upon methionine add-back.

metabolism, which is sensed by epigenetic mechanisms.

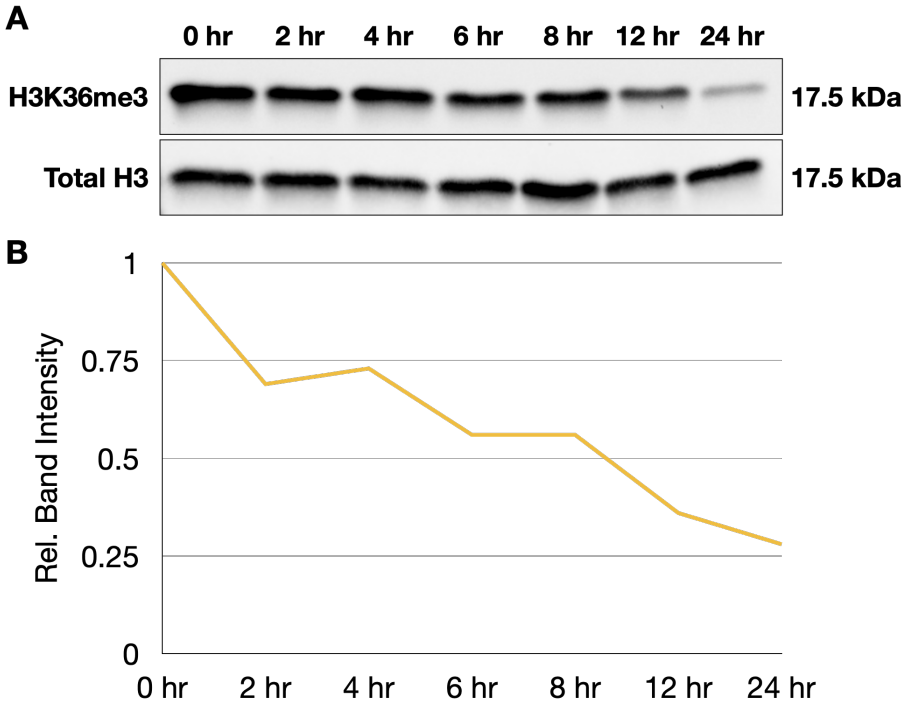

FIGURE 3.11: **H3K36me3 levels rapidly respond to methionine availability.** (A) Time series immunoblot analysis of H36K36me3 up to 24-hour post methionine restriction. (B) Relative band intensity of H3K36me3 over total H3.

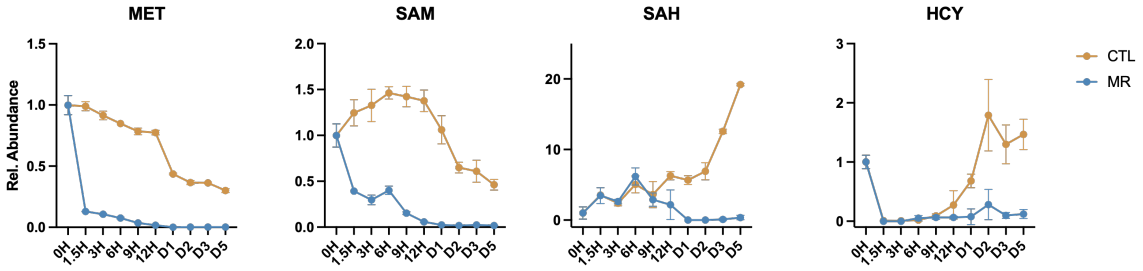

FIGURE 3.12: **Methionine cycle metabolites levels rapidly respond to methionine availability.** Time series analysis of methionine cycle metabolites during the 5-day differentiation window.

3.3.4 *Early stage methionine availability is critical for myogenic differentiation*

To delve deeper into the mechanism of MR-induced differentiation impediment and determine the critical stage at which methionine is essential for the differentiation process, we conducted a time-specific methionine restriction experiment. After reaching confluence, we introduced MR at various points during the differentiation window to ascertain the most crucial time frame for methionine's role (Figure 3.13). As anticipated, initiating MR from day 0 (D0) disrupted the differentiation process. However, surprisingly, introducing MR from day 2 (D2) onwards had a minimal effect on differentiation by the end of the five-day period, as reflected by the differentiation scores (Figure 3.14).

This finding has significant implications. By D2, cells typically have not yet exhibited the primary morphological changes characteristic of differentiation, such as the formation of elongated myotubes. If the role of methionine were solely to facilitate the synthesis of MyHC and other proteins related to myogenesis, then introducing MR from D2 should produce similar differentiation impairments as observed when MR is applied from D0. The observed disparity hints at the possibility that MR primarily impacts differentiation by hindering the cell's ability to orchestrate the essential gene expression profiles required for myogenic differentiation upon initiation.

3.3.5 *Myogenic differentiation and H3K36me3 are SAM-dependent*

To further elucidate the role of methionine in differentiation, we focus on its function as a methyl group donor, distinguishing it from its other biological roles. Our approach targeted the availability of S-adenosylmethionine (SAM), the primary metabolic product of methionine and the primary methyl group donor within cells. Owing to the challenges associated with SAM transport in mammalian cells

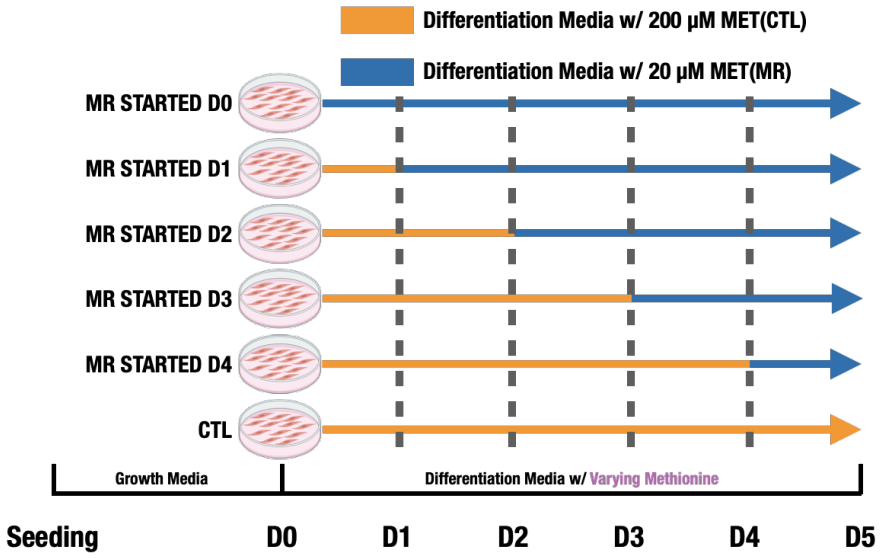

FIGURE 3.13: **Schematic outline of the experimental design for the methionine cut-off study for determining the critical stage for methionine in differentiation,** with methionine restriction (MR) introduced at various time points throughout the differentiation.

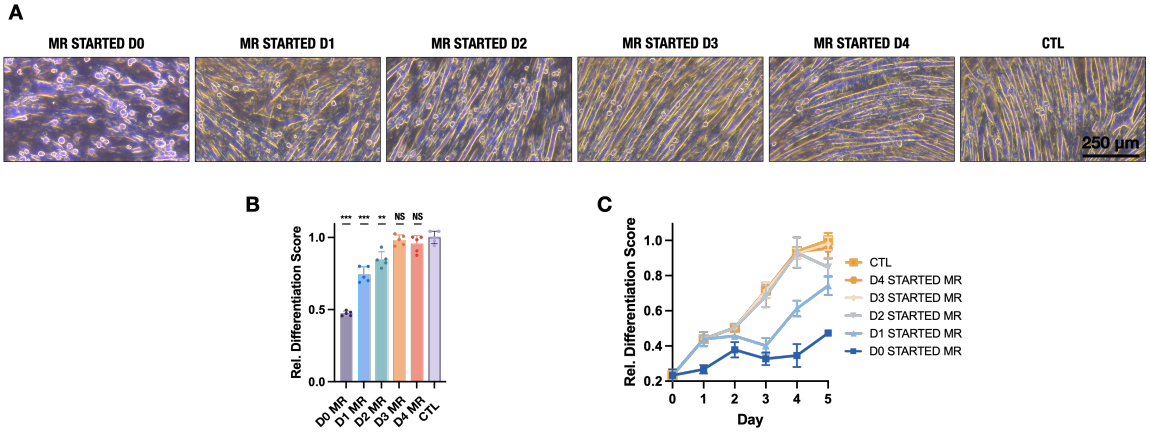

FIGURE 3.14: **Early stage methionine availability is critical for myogenic differentiation.** (A) Representative images of C2C12 cells images and (B) differentiation score at Day (D5) endpoint. (C) Time series plot of differentiation scores.

as alluded to the earlier chapter [109], we opted not for direct SAM supplementation under MR conditions. Instead, we choose to inhibit SAM synthesis while maintaining control levels of methionine. By inhibiting MAT2A, the SAM synthetase, using cycloleucine (cLEU) [71] (Figure 3.15), we observed a decline in the levels of methionine cycle metabolites (Figure 3.16), with the exception of methionine itself, which showed an increase in intracellular levels—likely a consequence of reduced MAT2A activity. Notably, even in the presence of sufficient methionine, we observed a disruption in differentiation that paralleled the effects seen under MR conditions (Figure 3.17A, B), accompanied by a reduction in H3K36me3 levels (Figure 3.17C). Consistent outcomes were also noted upon treating cells with AG-270, another MAT2A inhibitor [61] (Figure 3.18). These observations collectively highlight the pivotal role of methionine as a methyl group donor in dictating the differentiation outcomes noted under MR conditions.

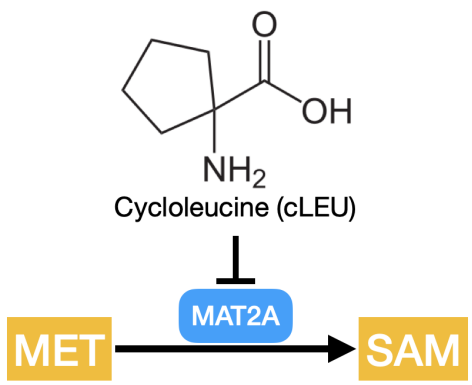

FIGURE 3.15: **Schematic representation of SAM synthesis highlighting the SAM synthetase, MAT2A, and its inhibition by cycloleucine (cLEU).**

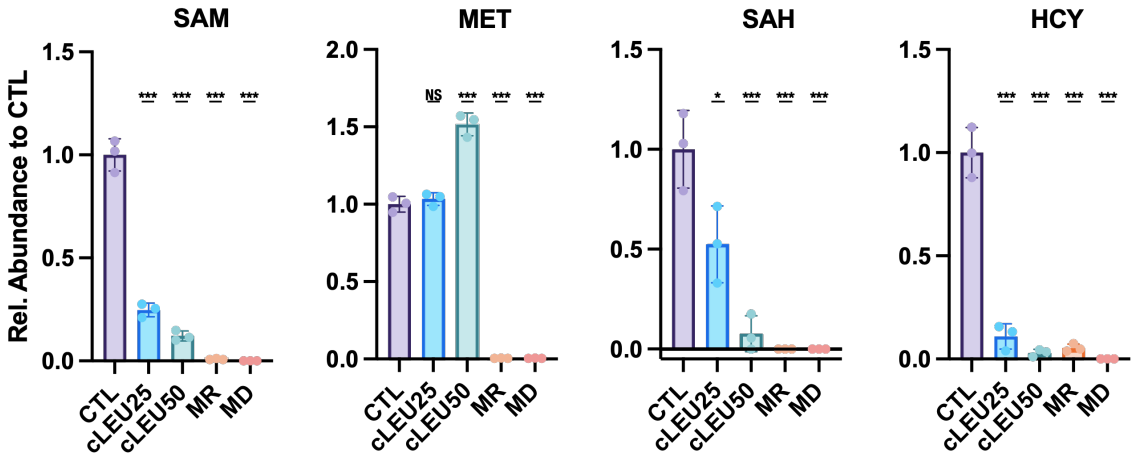

FIGURE 3.16: **cycloleucine (cLEU) reduces levels of SAM, SAH and HCY.**

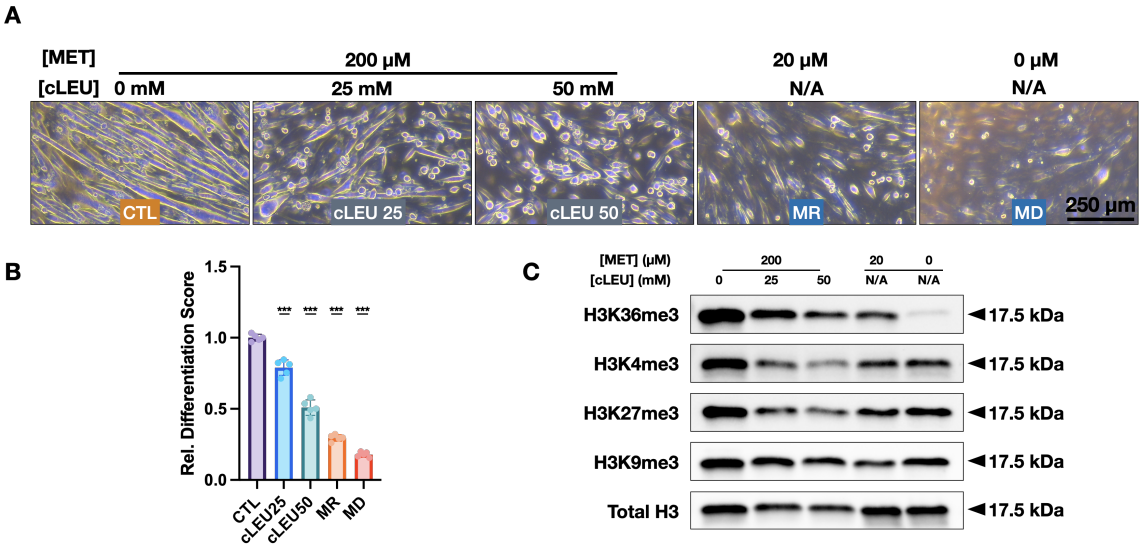

FIGURE 3.17: **Myogenic differentiation and H3K36me3 are SAM-dependent.** (A) Representative images of C2C12 cells images, (B) differentiation score and (C) levels of common histone tri-methylation marks at Day (D5) endpoint.

3.3.6 *SETD2 expression is linked to to methionine restriction*

In light of the rapid response of epigenetic mechanisms to methionine restriction, we explored whether SETD2, the histone methyltransferase implicated in this process, would react similarly. We assessed SETD2 protein levels in response to a methionine concentration gradient at the end of the 5-day differentiation period. Intriguingly, we found an inverse correlation: SETD2 levels increased as methionine concentration decreased (Figure 3.19A). However, this correlation is complicated by concurrent changes in MyHC levels, making it hard to discern whether SETD2 alterations are attributable to differentiation progression, as indicated by MyHC, or methionine restriction.

To unravel this complexity, we first addressed whether SETD2 levels change during cell differentiation. Our data revealed a decline in SETD2 levels as cells advanced through the differentiation process (Figure 3.19B), adding a layer of complexity to our investigation of methionine restriction's impact on SETD2 ex-

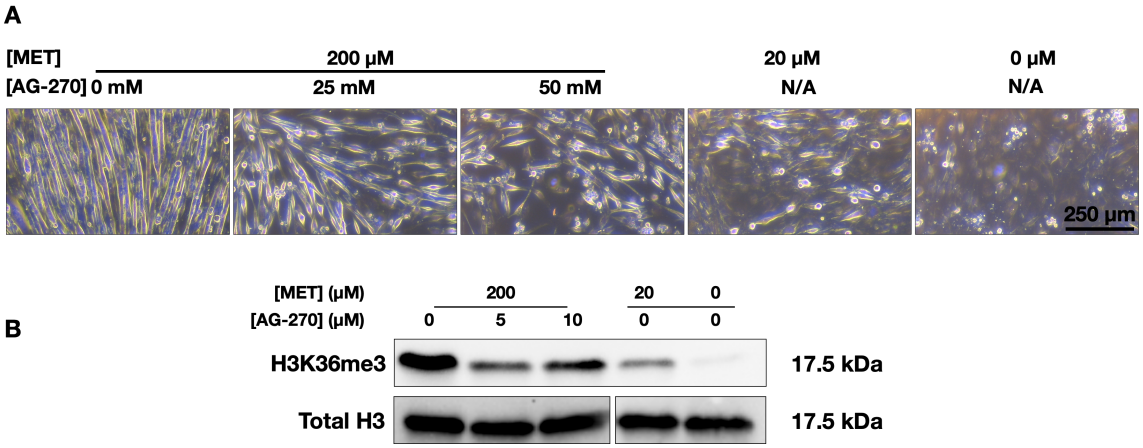

FIGURE 3.18: **Inhibition of MAT2A through AG-270 results in a disruption of differentiation comparable to that observed with cLEU.** (A) Representative images of C2C12 cells images and (B) levels of H3K36me3 mark at Day (D5) endpoint.

pression. To circumvent this, we devised an experimental setup where a 24-hour methionine restriction was introduced at either D2 or D4, stages at which cells just began to express MyHC or nearly completely differentiated (Figure 3.20). Our findings were revealing: a 24-hour methionine restriction initiated at both D2 and D4 elicited an increase in SETD2 expression, observable at both transcriptional and translational levels (Figure 3.21). These results hint at a potential sensing and compensatory mechanism aiming to maintain H3K36me3 levels under methionine-restricted conditions. This is intriguing, especially considering similar observations have been made with the SAM synthase MAT2A [76, 105]. However, the intricate mechanisms underpinning this response remain to be elucidated beyond the scope of this thesis.

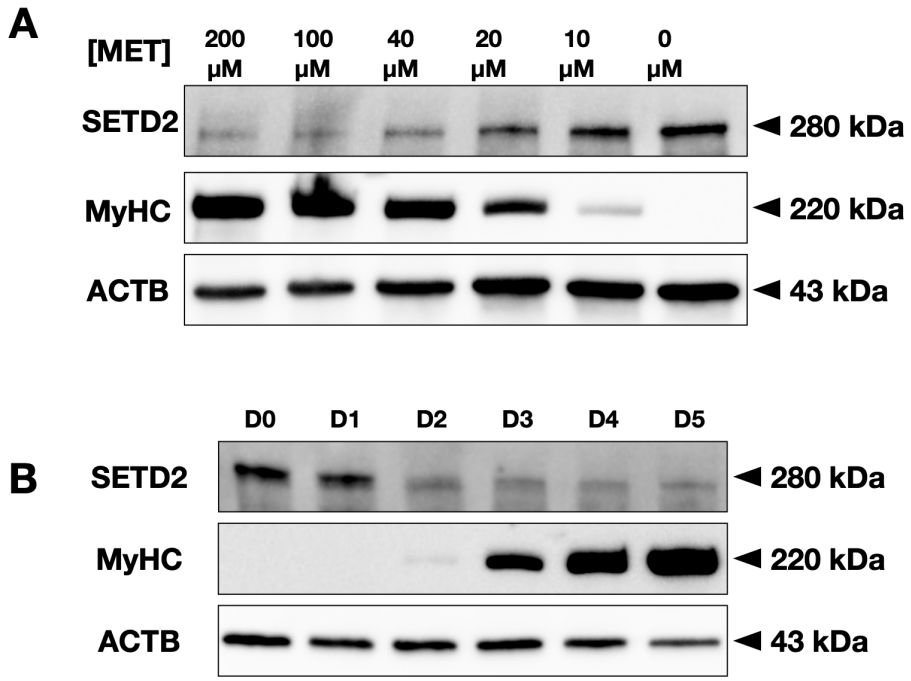

FIGURE 3.19: **SETD2 levels are potentially responsive to methionine availability.** (A) Immunoblot analysis of SETD2 and MyHC levels in response to MR treatment. (B) Immunoblot analysis of SETD2 and MyHC levels as differentiation progresses.

3.3.7 *Methionine-dependent differentiation acts through SETD2*

Recognizing the crucial role of SAM in myogenic differentiation, we aimed to identify its downstream mediators. The observed reduction in H3K36me3 levels in response to SAM, coupled with a peak in the expression of the corresponding methyltransferase, SETD2, at the early stages of differentiation led us to speculate whether the influence of methionine on differentiation might operate, at least partly, through SAM and SETD2.

To test this hypothesis, we used a lentiviral system to ectopically express a truncated variant of SETD2 (tSETD2) [7] (Figure 3.22A). Remarkably, the expression of tSETD2 not only increased H3K36me3 levels under MR conditions (Figure 3.22B) but also mitigated the differentiation impairments induced by MR, as evidenced by improvements in cell morphology, differentiation scores, and MyHC expression (Figure 3.23)

In contrast, Setd2 knockout via CRISPR-Cas9 (Figure 3.24A, Methods) led to a substantial reduction in H3K36me3 levels Figure 3.24B, C) and severely disrupted

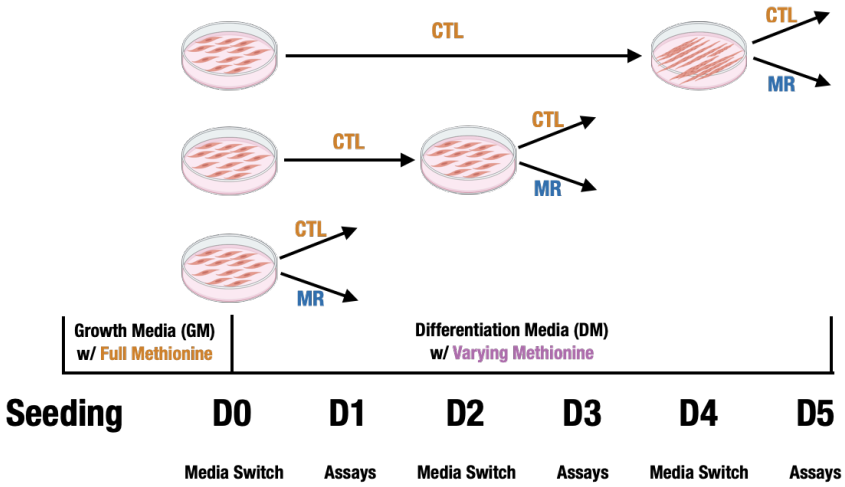

FIGURE 3.20: **Schematic of the experimental design to evaluate the response of SETD2 to MR.**

the differentiation process, even under control level methionine concentrations (Figure 3.25). Moreover, Setd2-knockout cells displayed an indifference to variations in methionine levels, remaining unresponsive even when methionine was supplied at double the control or MR levels (Figure 3.24B, Figure 3.25). Taken together, these insights affirm the role of SETD2 as a mediator in methionine-influenced differentiation processes.

3.3.8 *Methionine restriction preferentially reduces H3K36me3 levels at differentiation related genes*

Upon establishing the connection between methionine and differentiation through SETD2, we turned our attention to its product, H3K36me3, to decipher its role in methionine-dependent myogenic differentiation. We analyzed the H3K36me3 ChIP-Seq data of myogenic-related genes that are the targets of key myogenic transcription factors. Unlike the relatively stable H3K36me3 levels aggregated across all genes during the 5-day differentiation period observed earlier (Figure 3.26A), myogenic-related genes exhibited a progressive increase in H3K36me3, culminating on D5 (Figure 3.40). As anticipated, methionine restriction (MR) led

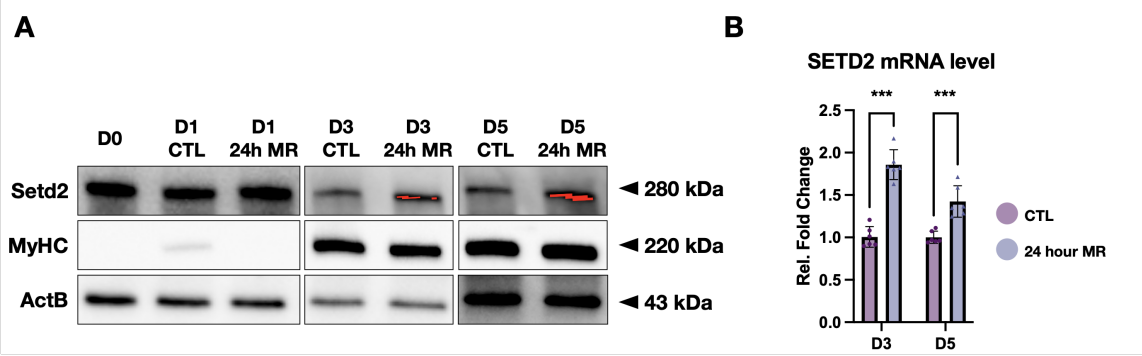

FIGURE 3.21: **Methionine restriction leads to increased level of SETD2 expression.** (A) Immunoblot analysis and (B) qPCR analysis of SETD2/Setd2 levels in response to 24-hour MR initiated on D2 or D4

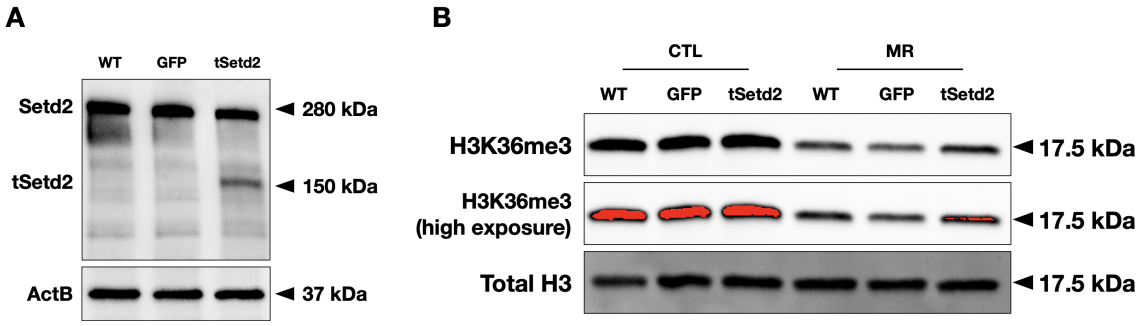

FIGURE 3.22: **Ectopic expression of Setd2 increases H3K36me3 levels under MR.** (A) Immunoblot analysis of SETD2 and truncated SETD2 (tSETD2) levels in WT, WT-GFP and WT-tSetd2 cells. (B) Immunoblot analysis of H36K36me3 in WT, WT-GFP and WT-tSetd2 cells under CTL and MR conditions.

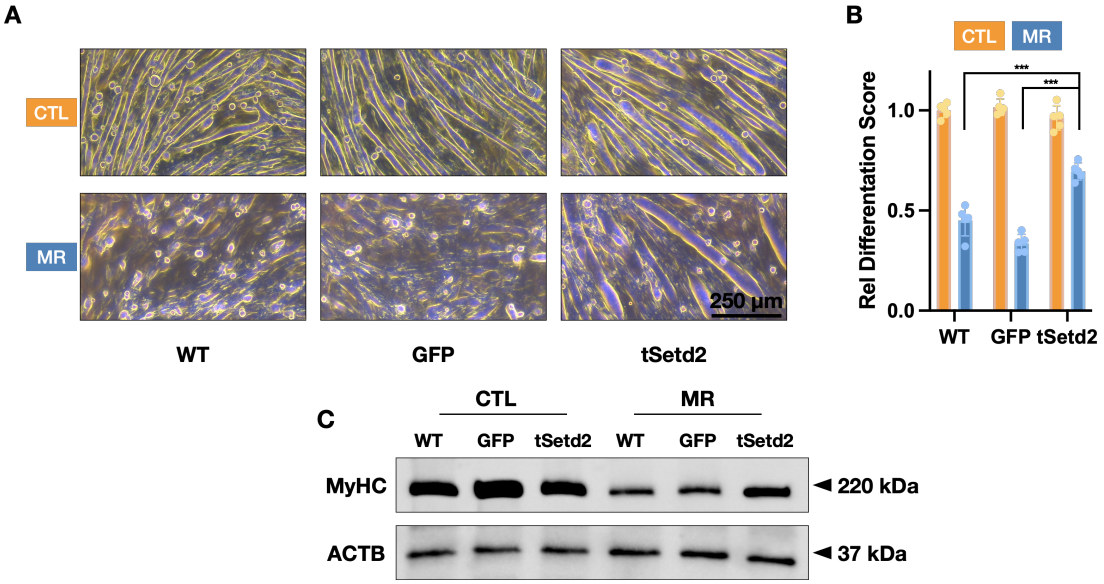

FIGURE 3.23: **Ectopic expression of Setd2 improves differentiation under MR.** (A) Representative images of C2C12 cells and (B) differentiation score at Day (D5) endpoint. (C) Immunoblot analysis of myosin heavy chain protein (MyHC) expression.

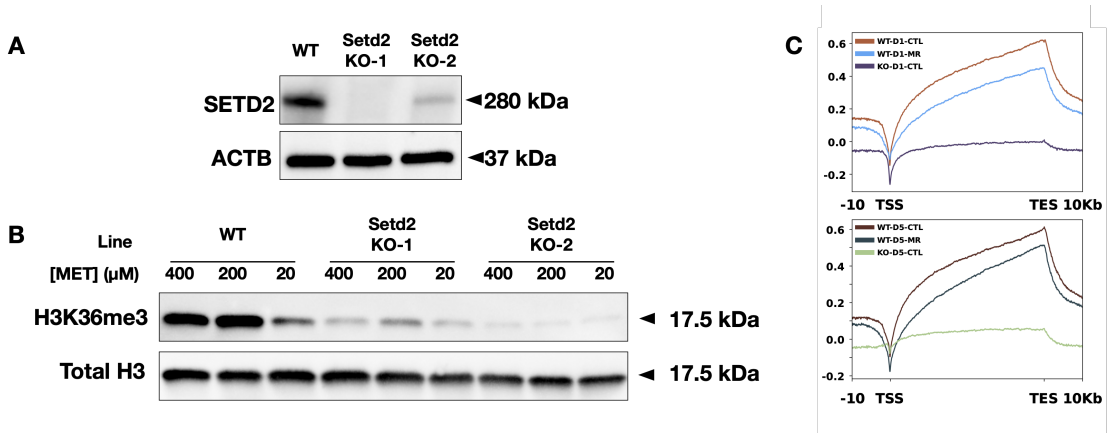

FIGURE 3.24: **Setd2 knockout leads to the loss of H3K36me3.** (A) Immunoblot analysis of SETD2 levels in WT, Setd2 knockout cell lines. (B) Immunoblot analysis of H36K36me3 in WT and Setd2 knockout cell lines under 2X, CTL and MR conditions. (C) ChIP-Seq profile of H3K36me3 abundance across all genes in response to MR and Setd2 knockout compared to CTL.

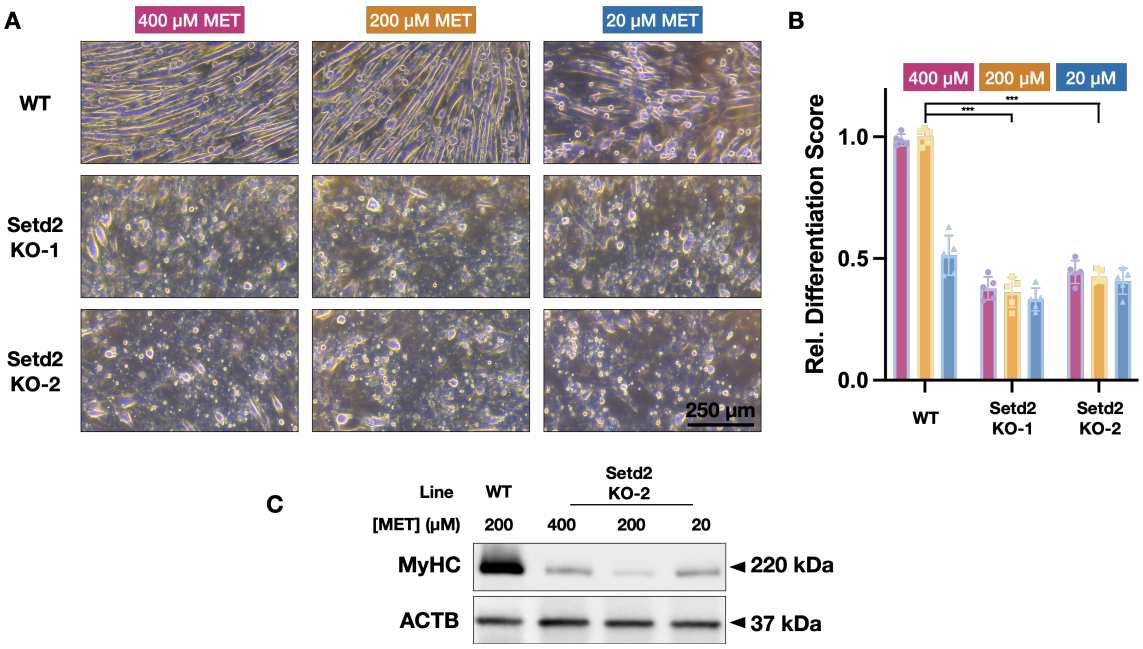

FIGURE 3.25: **Setd2 knockout leads to disruptions in differentiation.** (A) Representative images of C2C12 cells and (B) differentiation score at Day (D5) endpoint. (C) Immunoblot analysis of myosin heavy chain protein (MyHC) expression.

to diminished H3K36me3 levels at these specific genes (Figure 3.26B, C).

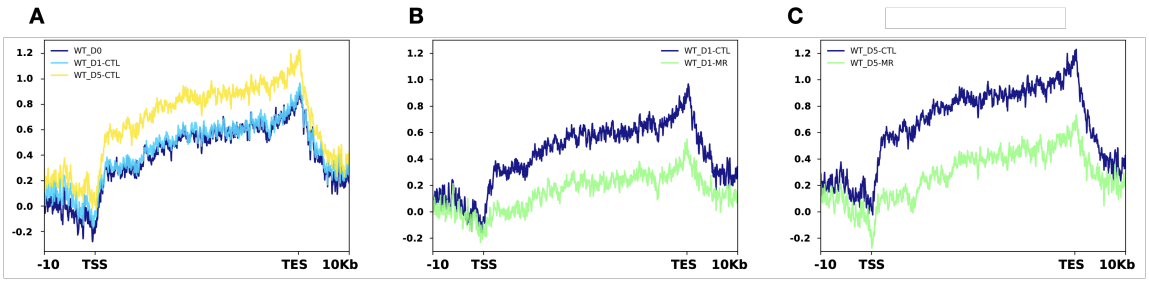

FIGURE 3.26: **H3K36me3 abundance increases at differentiation-related genes during normal course of differentiation.** (A) ChIP-Seq profile of H3K36me3 abundance across myogenic differentiation-related genes during normal course of differentiation. (B, C) ChIP-Seq profile of H3K36me3 abundance across myogenic differentiation-related genes in response to MR compared to CTL.

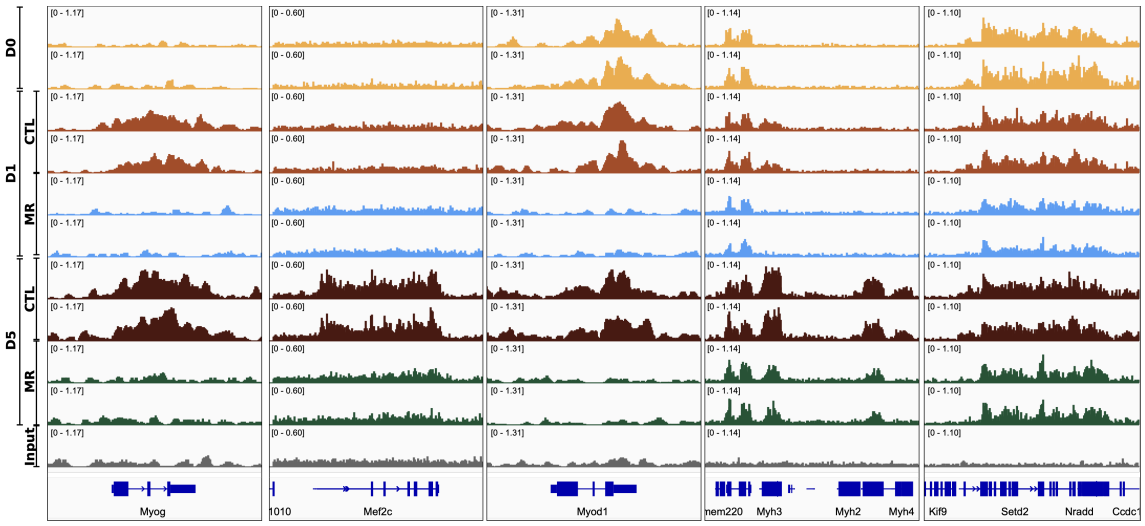

FIGURE 3.27: **Gene-specific H3K36me3 profiles under CTL and MR conditions at representative genes.**

Intriguingly, MR's impact on H3K36me3 varied across different genes. For instance, MR hindered the rising trend of H3K36me3 levels at Myog and Mef2c and disrupted the previously stable levels at Myod1. Conversely, the Myh genes manifested more subtle change in response to MR. Moreover, certain non-myogenic

genes, such as Setd2, showed no significant H3K36me3 fluctuations in response to MR (Figure 3.27), suggesting a targeted effect of MR on genes imperative for differentiation.

To probe deeper, we scrutinized the differential ChIP peaks of H3K36me3 under various conditions and conducted gene set enrichment analysis (Figure 3.28). A comparison between D5 and D1 under full methionine conditions highlighted the enrichment of muscle differentiation-related GO terms in genes with increased H3K36me3 levels (Figure 3.29A). On the flip side, peaks diminished by MR at either D1 or D5 also showed an enrichment in muscle differentiation-related GO terms, with D5 exhibiting a stronger association with myogenic differentiation than D1 (Figure 3.29B, C). These observations collectively suggest that MR preferentially reduces H3K36me3 levels at genes crucial for myogenic differentiation.

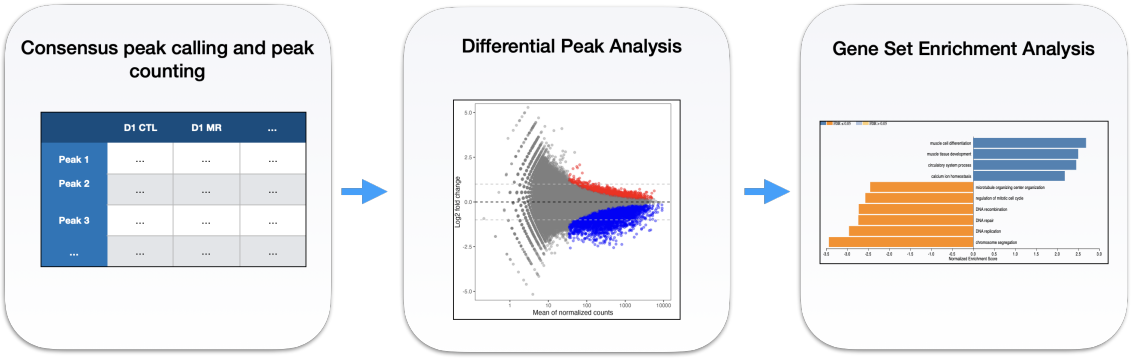

FIGURE 3.28: **Schematic representation of the workflow for differential ChIP peak analysis of H3K36me3 under different methionine conditions.**

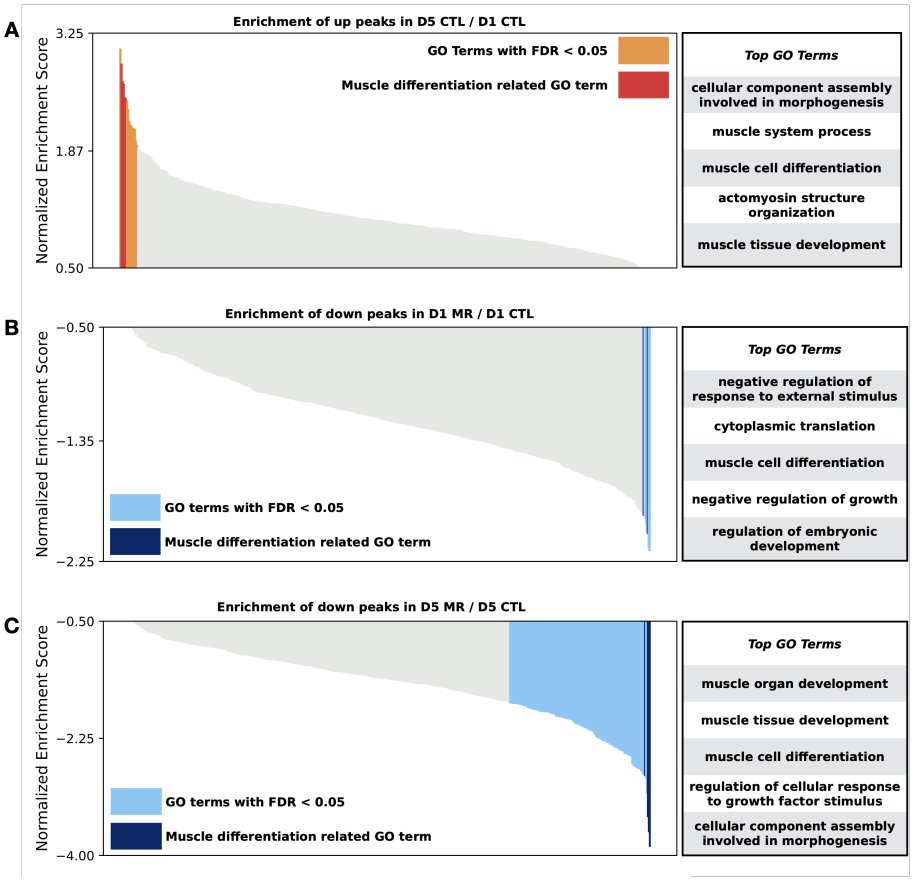

FIGURE 3.29: **Methionine restriction preferentially diminishes H3K36me3 levels at differentiation-related genes.** (A) Gene Set Enrichment Analysis (GSEA) of genes displaying increased H3K36me3 levels in a D5 vs. D1 comparison at control methionine levels, with muscle differentiation related Gene Ontology (GO) terms dominate the top of the list. (B, C) GSEA of genes with diminished H3K36me3 peaks under MR: (B) D1 comparison and (C) D5 comparison, with muscle differentiation-related GO terms dominate the top of the lists.

3.3.9 *Methionine restriction and Setd2 knockout preferentially reduce chromatin accessibility at differentiation related genes*

To delve deeper into the broader epigenetic ramifications of methionine restriction and to draw comparisons with the effects of Setd2 knockout, we conducted Assay for Transposase-Accessible Chromatin using sequencing (ATAC-Seq) on both wild-type (WT) and knockout (KO) cells under control (CTL) and methionine restriction (MR) conditions. When then performed differential peak analysis and a subsequent Genomic Regions Enrichment of Annotations (GREAT) analysis [79] (Figure 3.30). Notably, in WT cells, ATAC-Seq peaks with increased intensity from D0 to D1 exhibited enrichment in GO terms associated with muscle differentiation (Figure 3.30A). When contrasting D1 MR to D1 CTL, peaks displaying decreased intensity similarly showcased enrichment in muscle differentiation-related GO terms (Figure 3.30B). Likewise, comparing D1 KO CTL with D1 WT CTL revealed peaks of diminished intensity, once again enriched in muscle differentiation-related GO terms (Figure 3.30C).

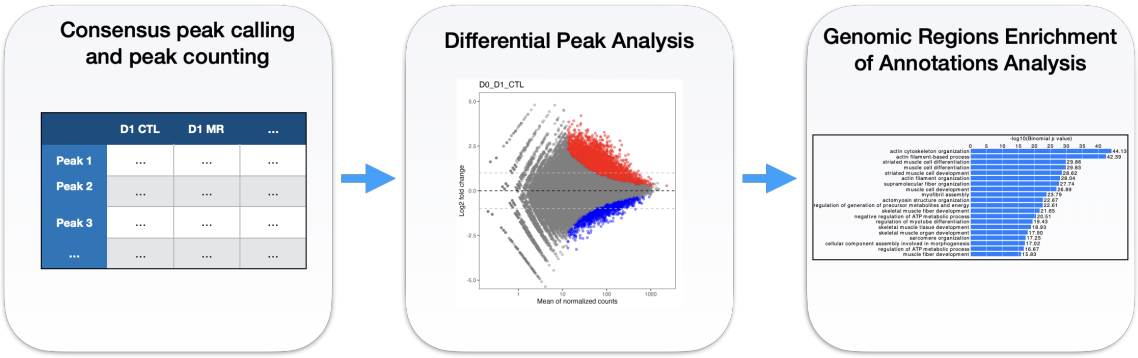

FIGURE 3.30: **Schematic representation of the workflow for differential ChIP peak analysis of H3K36me3 under different methionine conditions.**

Moreover, ATAC-Seq peaks that decreased in response to MR were found to also decrease in KO cells under CTL conditions. Exposing KO cells to MR did

not induce further reductions in these peak intensities (Figure 3.32). Overall, our data suggested that the epigenetic shifts caused by MR, as indicated by chromatin accessibility, are mediated at least partially by Setd2.

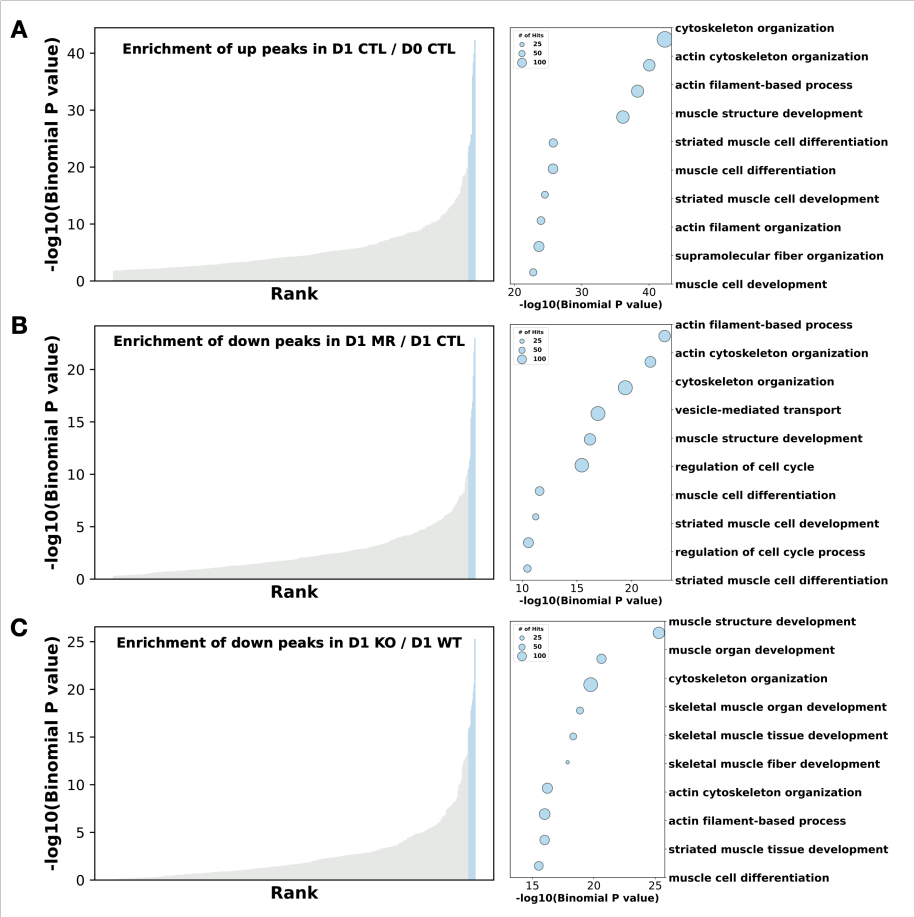

FIGURE 3.31: **Methionine restriction and Setd2 knockout preferentially reduce chromatin accessibility at differential related genes.** (A) Genomic Regions Enrichment of Annotations (GREAT) analysis of ATAC-seq peaks that increased in intensity from Day 0 (D0) to Day 1 (D1) in WT cells. Muscle differentiation-related GO terms are predominantly enriched. (B) GREAT analysis of ATAC-seq peaks with diminished intensity comparing Day 1 under MR conditions to Day 1 under CTL conditions in WT cells. Muscle differentiation-related GO terms are predominantly enriched. (C) GREAT analysis of ATAC-seq peaks with diminished intensity between KO cells under CTL conditions and WT cells under CTL conditions on Day 1. Muscle differentiation-related GO terms are predominantly enriched.

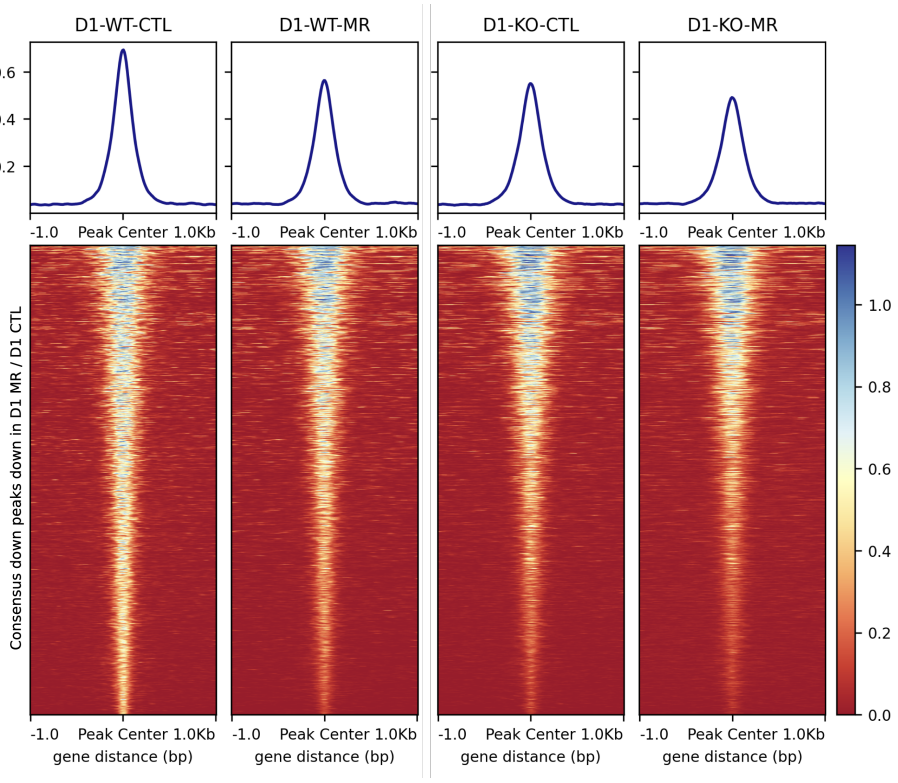

FIGURE 3.32: **ATAC-seq profiles and heatmaps of peaks that are diminished in response to MR compared to CTL in WT, and Setd2 knockout lines under CTL and MR conditions.** Notably, applying MR to KO cells did not lead to a further reduction in profile peak intensities.

3.4 Discussions

The relationship between metabolism and epigenetics has garnered significant interest in recent years.This heightened attention stems from the understanding that metabolic products, crucial for a range of epigenetic processes, act as links between these two previously distinct areas.From histone acetylation to RNA methylation, metabolic intermediates play pivotal roles. While the connection between metabolism and epigenetics is established, the nuanced details of how specific metabolic processes and metabolites fine-tune the epigenetic landscape are yet to be thoroughly elucidated.

Historically, the study of epigenetic processes primarily rested upon genetic manipulations, including inducing mutations in epigenetic modifiers and readers. However, the kinetic properties of certain modifiers, notably methyltransferases, offer avenues for regulation through changes in substrate concentration, achievable by dietary means, such as restricting methionine intake. Leveraging this, our research delves into methionine's role in determining H3K36me3 levels and its implications in crucial cellular processes, such as differentiation.

Our research uncovered how H3K36me3 levels and C2C12 cell differentiation are dependent on methionine, shedding light on the dynamics and reversibility of this dependency. Further, we explored the mechanism behind this methionine dependency by establishing the role of SAM and Setd2 as instrumental links in the causal chain connecting methionine to differentiation. Complementing this, our H3K36me3 ChIP-seq and ATAC-seq data provide additional insights on how methionine and Setd2 ultimately contribute to myogenic differentiation, laying a foundation for future investigations.

Tracing a direct causal pathway from methionine to SAM, then to Setd2, H3K36me3, and ultimately to differentiation, presents a challenge due to various confounding

factors. Each element in this sequence plays multiple roles. For example, methionine has functions beyond methyl group donation, including roles in protein synthesis and redox balance [99]. Similarly, SAM is utilized by numerous methyltransferases, and Setd2 has a range of functions, such as interacting with RNA Pol II [59].

In addition, the reason why methylation restriction might differentially affect different methylation marks remains an open question. Mechanistically, at the enzyme level, this disparity could stem from the unique kinetic properties of various methyltransferases, some of which may bind more effectively to the substrate SAM under conditions of limited SAM availability. When examining this from a broader regulatory perspective, it could also be a consequence of feedback regulation that controls the expression and degradation of methyltransferase in response to fluctuations in substrate levels. Furthermore, the counteracting process of demethylation, along with the kinetics and regulatory mechanisms of demethylases, might also play a significant role in this complex scenario [83]. Deciphering the exact contributions of these interconnected elements is a challenging task.

A pressing question is why certain genes experience more pronounced changes in H3K36me3 levels compared to others. Despite stable H3K36me3 levels across the genome during differentiation, as shown in Figure 3.5, differential analysis followed by over-representation analysis (ORA) indicates that genes involved in muscle differentiation see significant increases in H3K36me3 (Figure 3.33). This pattern, observed under control conditions with adequate methionine levels, suggests that these phenomena are inherently linked to myogenesis.

To further elucidate the specificity of H3K36me3 deposition, we distinguish between two phases: the initial establishment and the subsequent maintenance and amplification of this specificity. Our focus is on the role of SETD2, while also recognizing that lysine demethylases (KDMs) play a significant role in the broader

context of methylation dynamics.

We propose that key events in the differentiation cascade, preceding notable H3K36me3 changes, create a conducive environment for differential H3K36me3 deposition. For example, the co-occurrence of elevated H3K4me3 levels at Pax7 and high expression of Pax7 likely predates the differentiation stage modeled by C2C12 cells [25]. These early events, characterized by increased transcriptional activity at a specific set of genes, could be the driving force behind the initial preferential deposition of H3K36me3. This may be aided by SETD2's interaction with RNA polymerase II (Pol II), enhancing H3K36me3 deposition along transcribed regions [66].

Other effectors might also guide SETD2 to specific gene loci. Evidence indicates that transcription factors (TFs) may directly interact with histone methyltransferases, exemplified by the interaction between MyoD and SET7/9 [112]. However, specificity based on direct interactions with TF seem less probable for SETD2, considering H3K36me's preferential distribution within the gene body, as opposed to the promoter regions near transcription start sites (TSS) where transcription factors typically bind [50].

The maintenance and amplification of H3K36me3 at myogenic differentiation-

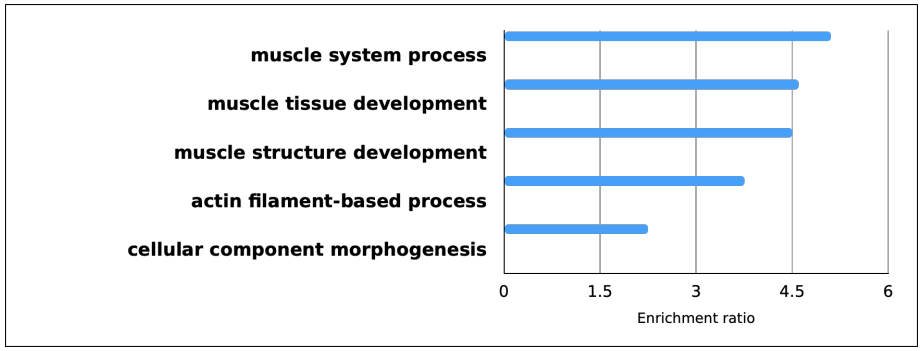

FIGURE 3.33: **Top results from Over-Representation Analysis (ORA) reveal enrichment of myogenic genes among those experiencing increased H3K36me levels.**

related loci may involve positive feedback loops between H3K36me3 and transcription. It is well-documented that the SET2 SRI domain interacts with the C-terminal domain (CTD) of Pol II, potentially facilitating its recruitment to chromatin. Concurrently, the H3K36me3 mark supports processes such as alternative splicing [74] and the prevention of cryptic transcription initiation [45], both of which promote further transcriptional activities.

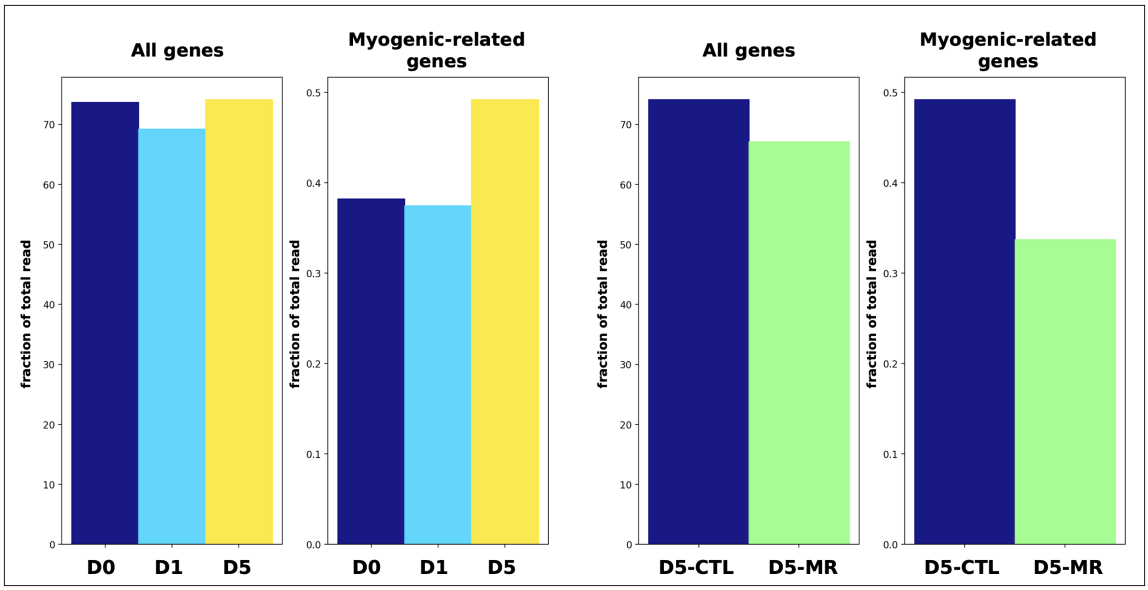

FIGURE 3.34: **Aggregated levels of H3K36me3 at all genes or at myogenic-related genes during differentiation under CTL or MR conditions.**

We also observed that genes with the most increased H3K36me3 during differentiation are more sensitive to methionine restriction (Figure 3.34). To explain this observation, we draw analogies with phenomena in other biological contexts, such as the vulnerability of cancer cells, which, due to their high reliance on cell proliferation, are especially susceptible to cell cycle disruptions. Similarly, we hypothesize that genes showing the greatest increase in H3K36me3 during differentiation may be more dependent on a sufficient supply of methionine, making them particularly vulnerable under methionine-restricted conditions.

To understand the variations in methylation levels, we consider local environmental factors at the gene loci. These factors may encompass the affinity of SETD2 to these loci, potentially influenced by feedback loops between transcription and H3K36me3 deposition or the targeted recruitment of SETD2 by other transcription factors or chromatin remodelers.

Quantitatively, this can be modeled using an effective affinity constant (K_{eff}), encapsulating the overall affinities resulting from the mechanisms mentioned above. A smaller K_{eff} indicates a stronger affinity, leading to increased methylation levels. This framework allows us to simplify the system to one with a single substrate, SAM, and enables us to model this process with Michaelis-Menten kinetics. The reaction rate is defined by the Michaelis-Menten equation:

$$v = \frac{V_{\text{max}} \cdot [\text{SAM}]}{K_{\text{eff}} + [\text{SAM}]}$$

Upon plotting this relationship, it becomes evident that a smaller K_{eff} results in a more pronounced decrease in reaction rate when [SAM] is reduced, particularly when [SAM] approaches or falls below K_{eff} (Figure 3.35). This aligns with our observation that gene locations with greater increases in methylation also experience more significant impacts under conditions of reduced SAM availability (Figure 3.34).

For a more detailed analysis, we compute the derivative of the reaction rate with respect to [SAM], which yields:

$$\frac{dv}{d[\text{SAM}]} = \frac{d}{d[\text{SAM}]}\left(\frac{V_{\text{max}} \cdot [\text{SAM}]}{K_{\text{eff}} + [\text{SAM}]}\right) = \frac{K_{\text{eff}} \cdot V_{\text{max}}}{(K_{\text{eff}} + [\text{SAM}])^2}$$

From here, we consider two scenarios:

1. When the substrate concentration roughly matches the K_{eff} of the enzymes,

a common observation with many methyltransferases [94], the expression can be approximated as:

$$\frac{1}{K_{\text{eff}}} \cdot \frac{V_{\text{max}}}{4}$$

2. Under conditions of methionine restriction, the concentration of SAM might fall below the K_{eff}. In this scenario, the expression simplifies to:

$$\frac{1}{K_{\text{eff}}} \cdot V_{\text{max}}$$

In both scenarios, the inverse correlation with K_{eff} supports our observation that genes with more substantial H3K36me3 increases during normal conditions are more affected under methionine restriction.

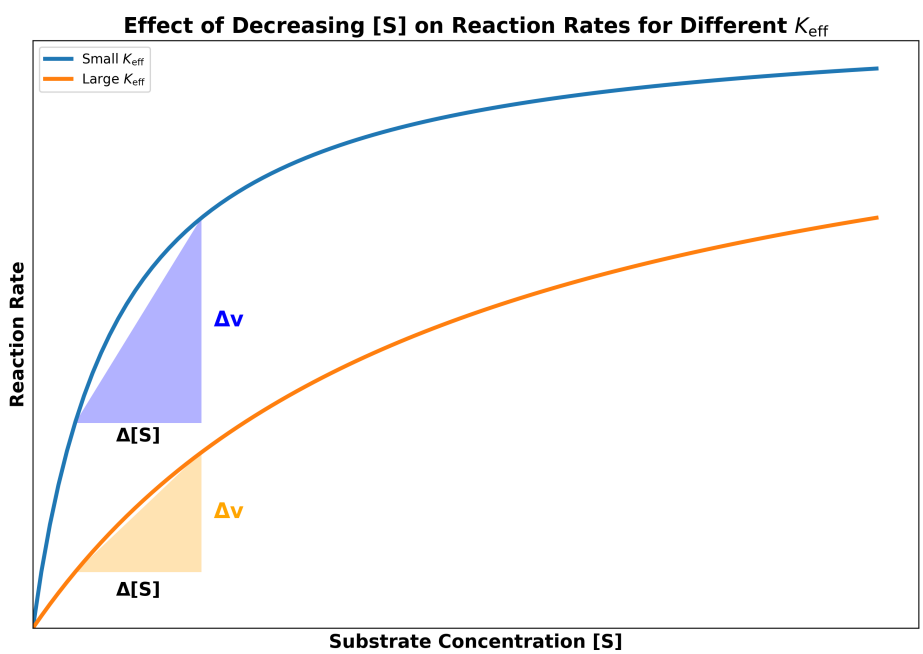

FIGURE 3.35: **Effect of K_{eff} on reaction rate based on Michaelis-Menten Kinetics.**

Thermodynamics, in addition to kinetics, may also dictate the differential H3K36me3 levels. The process is described by the following equation:

$$K_{eq} = \frac{[\text{H3K36me3}][\text{SAH}]}{[\text{SAM}][\text{Histone substrates}]}$$

The discussed mechanisms could alter the Gibbs free energy (ΔG) of the methylation reaction, influencing the equilibrium constant K_{eq}. We propose that methylation reactions at genes with significant H3K36me3 increases during differentiation would have a higher K_{eq}. Consequently, the H3K36me3 equilibrium concentration, described by the following equation, would become more sensitive to changes in [SAM] for methylation reactions with larger K_{eq}.

$$[\text{H3K36me3}] = K_{eq} \cdot \frac{[\text{SAM}][\text{Histone substrates}]}{[\text{SAH}]}$$

Taken together, these kinetics and thermodynamics analyses suggest that gene loci with significant increases in H3K36me3 levels are also more sensitive to the availability of SAM, and by extension, methionine, aligning with our empirical observations.

Our research underscores the significance of the methionine-SAM-Setd2 pathway in cellular differentiation. We also demonstrated that cellular and genomic outcomes typically achieved through genetic interventions, like Setd2 knockout, can be partially replicated by modifying the nutrient environment of the cells. This revelation paves the way for new avenues of research.

In summary, our study underscores the direct response of chromatin to methionine in the context of myogenic differentiation, particularly through components like Setd2 and H3K36me3, both of which play crucial roles in crucial processes such as development and cancer. This contributes significantly to our un-

derstanding of the regulation of the epigenetic landscape.

3.5 Methods

3.5.1 Cell culture

C2C12 cells were procured from the Duke Cell Culture Facility. They were maintained at 37°C and 5% CO2 on growth media (GM) for C2C12 comprised of DMEM (Gibco 11965092), 10% heat-inactivated fetal bovine serum (Sigma-Aldrich F2442), and 1X penicillin-streptomycin (Gibco 15140163). For differentiation induction, cells were seeded at a density of 1.25E5 cells/well in a 6-well plate and allowed to proliferate for 48 hours in GM to reach confluence.

Post confluence, the culture medium was switched to differentiation media (DM), which consisted of DMEM without methionine, cystine-2HCl, and glutamine (Gibco 21013024), supplemented with 2% heat-inactivated horse serum (Hyclone SH30074.03), 1X pen/strep (Gibco 15140163), and 1 μM insulin (Sigma-Aldrich I6634). Both cystine-2HCl (Sigma C6727) and glutamine (Alfa Aesar A12919) were reintroduced to levels found in standard DMEM. Depending on the experimental conditions, methionine (Amresco E801) was either added to a concentration of 200 μM (for control) or to other specified concentrations. The differentiation process was allowed to proceed for 5 days, with media changes occurring every 48 hours. MAT2A inhibitors used in the study were Cycloleucine (Sigma A48105) and AG-270 (MedChemExpress HY-138630).

3.5.2 Microscopy

Images of C2C12 cells were acquired using a Leica DM IL LED microscope, which was outfitted with a Leica MC170HD camera. Imaging was performed using 20x, 10x, and 4x objectives, and images were captured and processed using the LAS EZ software.

3.5.3 *Differentiation Quantification*

A convolutional neural network (CNN) was trained using the ResNet-18 architecture with PyTorch [48][89]. We modified ResNet-18 by replacing its final fully connected layer to yield a single continuous output value. 64 images, captured using the 10x objective, were obtained each day from Day 0 (D0) to Day 5 (D5) for cells exposed to differentiation media (DM) containing full methionine. To augment our dataset, each of these images was subdivided into five sub-images. For labeling, each image was assigned a numeric value corresponding to the day; e.g., an image of a Day 3 (D3) cell received a label of 3.0. Out of the 320 augmented images obtained each day, 270 of them were used for training while the remaining 50 of them served as the test set. The CNN was trained for 15 epochs using a learning rate of 1e-4, utilizing the Mean Squared Error Loss (nn.MSELoss) as the criterion, and Adam as the optimizer. To ascertain the differentiation score of a given image relative to image of cells on a control condition—in which cells differentiated over an identical duration—each image was partitioned into five sub-images and assessed five times. Subsequent results were normalized to the average score of the control group.

3.5.4 *Histone extraction*

Cells were washed twice with room-temperature PBS before being scraped into ice-cold Triton extraction buffer (TEB) containing 0.5% Triton X-100, 0.2% NaN3, and 2 mM PMSF in PBS. The suspension was transferred to a 1.5 ml centrifuge tube and briefly vortexed, followed by a 10-minute incubation on ice. The cells were then centrifuged at 12,000 g at 4°C for 10 minutes. After discarding the supernatant, the cell pellet was resuspended in 500 μl of TEB and centrifuged again using the same parameters. The supernatant was removed, and the cell

pellet was resuspended in 500 μl of 0.2N HCl, which was then incubated at 4°C overnight. The next day, the samples were centrifuged at 12,000 g at 4°C for 10 minutes. The supernatant was collected, neutralized with 2M NaOH, and their concentrations were determined using a BCA assay.

3.5.5 Total protein extraction

Cells were rinsed twice with room-temperature PBS and subsequently scraped into ice-cold RIPA buffer (Sigma-Aldrich R0278) supplemented with a 1x Protease Inhibitor Cocktail (Roche 11836170001). After transferring the cell suspension to a 1.5 ml centrifuge tube, it was briefly vortexed and then incubated on a nutator at 4°C for 25 minutes. Following incubation, the cells were centrifuged at 12,000 g at 4°C for 25 minutes. The supernatant was carefully collected, and protein concentrations were quantified using a BCA assay.

3.5.6 Immunoblot

Samples were diluted to the desired concentrations (4 mg/well for histone and 15 mg/well for total protein extracts) using water and combined with Laemmli sample buffer containing 10% 2-Mercaptoethanol. This mixture was heated at 95°C for 5 minutes. The samples were subsequently subjected to electrophoresis on 12% SDS-PAGE gels for histone samples and 4-15% SDS-PAGE gels for total protein extracts, after which they were transferred onto PVDF membranes (Bio-Rad 1704156).The membranes were blocked using 5% BSA (Rockland BSA-50) in TBS-T buffer for an hour, then probed overnight at 4ºC with primary antibodies, all diluted 1:1000: Myosin Heavy Chain (R&D System mAB4470), ActB (CST 8457T), Histone H3 (CST 96C10), H3K36me3 (Active Motif 61102), H3K27me3 (Active Motif 61018), H3K9me3 (Abcam ab8898), H3K4me3 (Active Motif 39060), and Setd2 (CST E4WQ8). After overnight incubation, membranes were washed three times

with TBS-T, each for 5 minutes. This was followed by a one-hour incubation at room temperature with peroxidase-conjugated Rabbit or Mouse secondary antibodies (Rockland 610-1302 and 611-7302) at a dilution of 1:10000. Post-incubation, membranes underwent another set of three washes with TBS-T, each lasting 5 minutes. Membranes were then exposed to the ECL substrate kit (Pierce 34850 and 34095) for 3 minutes before imaging with the ChemiDoc Touch Imaging System (Bio-Rad).

3.5.7 Metabolites extraction

Cell culture medium was quickly removed before adding 1 ml of an 80% methanol/water solvent (Fisher Scientific A456 and W6), cooled to -80°C, to each well of the six-well plates. These plates were then chilled at -80°C for 15 minutes. After this, the cells were scraped into the solvent while on dry ice, and the extracts were centrifuged at 20,000g at 4°C for 10 minutes. The solvent was then evaporated using a speed vacuum and the dried metabolites pallets were stored at -80ºC.

3.5.8 Liquid chromatography

Dried metabolites pallets were reconstituted in 15 μl of H2O, followed by the addition of 15 μl of a 1:1 v/v methanol/acetonitrile mix (Fisher Scientific A456 and A955). The samples were then centrifuged at 20,000g at 4°C for 10 minutes, after which the supernatants were moved to LC vials, preparing them for a 3 μl HPLC injection. The compounds were separated at room temperature using an XBridge amide column (Waters 100 × 2.1 mm i.d., 3.5 μm;) on a Thermo Scientific UltiMate 3000 UHPLC system. Mobile phases and flow rate was configured as described in previous study [69].

3.5.9 *Mass spectrometry*

The Q Exactive Plus mass spectrometer (Thermo Fisher Scientific) was equipped with a heated electrospray ionization probe and configured with the following settings: heater temperature at 120°C; sheath gas flow rate at 30; auxiliary gas at 10; and sweep gas at 3. The spray voltage was set to 3.6 kV in positive mode and 2.5 kV in negative mode. The capillary temperature and S-lens were maintained at 320°C and 55, respectively. Scans were conducted across a range of 60 to 900 m/z at a resolution of 70,000. The automated gain control (AGC) was targeted at 3E6 ions.

3.5.10 *Peak extraction and metabolomics data analysis*

The acquired raw LC-MS data were analyzed using Thermo Scientific Sieve 2.0 software, with peak alignment and detection executed as per the manufacturer's guidelines. For targeted metabolite analysis in positive mode, a frame seed encompassing 194 metabolites was utilized, whereas a frame seed comprising 262 metabolites was adopted for the negative mode. The m/z width was set at 10 ppm for both modes. Subsequently, peak integration values were exported. Sample values were normalized based on the mean value of the control group.

3.5.11 *Quantitative PCR*

RNA was extracted using the Qiagen RNeasy Micro Kit in accordance with the manufacturer's instructions. The quality and quantity of the RNA were determined using NanoDrop (Thermo Scientific). Subsequently, 1 μg of RNA was reverse transcribed into single-stranded complementary DNA utilizing the SuperScript III First-Strand Synthesis SuperMix for qRT-PCR from Invitrogen. Quantitative analysis was carried out on a CFX384 system (Bio-Rad) using the iQ SYBR Green Supermix (Bio-Rad) as directed by the manufacturer.

The following primers were used:

- Myh4: Forward: GGCTGAGGAGGCTGAGGA
  Reverse: CTCCTGTCACCTCTCAACAGAAA
- Setd2: Forward: ACCTCGCCCGAAAGCTGAC
  Reverse: ACTCTGGCCTGAGGTCACTCTA
- Hprt: Forward: ATGGACTGATTATGGACAGGACTG
  Reverse: TCCAGCAGGTCAGCAAAGAAC

3.5.12 Lentiviral transduction

Lentivirus containing GFP or truncated Setd2, obtained from Vectorbuilder, was used to transduce C2C12 cells. Cells were seeded in a 12-well plate at a density of 0.45E5 cells per well and allowed to proliferate for 24 hours, reaching approximately 1E5 cells per well. For the transduction, 100 μl of lentivirus (1E8 TU) was combined with 300 μl of fresh growth media containing polybrene at 5 μg/ml. After removing the existing cell culture medium, cells were cultured with the 400 μl of lentivirus-containing media for 24 hours. The following day, cells were transferred to a 10 cm culture dish. Subsequently, puromycin was added at a concentration of 3 μg/ml to initiate the selection process. After 24 hours, surviving cells were relocated to a 12-well plate without puromycin. These cells were then incrementally transferred first to a 6-well plate and later to a 10 cm plate. A final round of selection was done by reintroducing puromycin. The expression levels of tSetd2 and GFP were then confirmed using a fluorescent microscope and immunoblotting.

3.5.13 CRISPR Knockout of Setd2

CRISPR Cas-9 mediated Setd2 knockout in C2C12 cells was performed by the Duke Functional Genomics Core. Three sgRNAs targeting Setd2 were designed using ChopChop and ordered as modified synthetic sgRNAs from Synthego [64]. 5 x 10e4 C2C12 cells were electroporated with 7.5 pmol TrueCut Cas9 protein v2 (ThermoFisher Scientific) complexed with 22.5 pmol sgRNA using the Neon system (ThermoFisher Scientific) with the following settings: 1650 V, 10 ms, 3 pulses. Cells were recovered and expanded, followed by PCR sequencing and immunoblotting analysis to determine KO efficiencies. Based on this analysis, knockout clones were subsequently isolated from the pools generated with sgRNA #1 (GTCGGTCCGAAAGAGATCGA) and sgRNA #3 (GCATTCGCTTAATATCC-CGG) by plating at limited dilution in 96 well plates. Clones were expanded for approximately 10-14 days before screening by PCR-sequencing to confirm out-of-frame insertions or deletions.

3.5.14 ChIP-Seq and data analysis

Samples were sent to Active Motif (Carlsbad, CA) for ChIP-Seq. Active Motif prepared chromatin, performed ChIP reactions, generated libraries, and sequenced the libraries. In brief, C2C12 cells were fixed in formaldehyde. Chromatin was isolated by adding lysis buffer, followed by disruption with a Dounce homogenizer. Lysates were sonicated and the DNA sheared with Active Motif's EpiShear probe sonicator (cat# 53051). Genomic DNA (Input) was prepared by treating aliquots of chromatin with RNase, proteinase K and heat for de-crosslinking, followed by SPRI beads clean up (Beckman Coulter) and quantitation by Clariostar (BMG Labtech). Extrapolation to the original chromatin volume allowed determination of the total chromatin yield.

An aliquot of chromatin, 30 ug chromatin (750 ng of Drosophila chromatin for spike-in for H3K36me3 [35]) was precleared with protein G agarose beads (Invitrogen). Genomic DNA regions of interest were isolated using 4ul of H3K36me3 (Active Motif cat# 61101, lot# 22264149) and 0.4ug of antibody against H2Av (Active Motif cat# 61686). Complexes were washed, eluted from the beads with SDS buffer, and subjected to RNase and proteinase K treatment. Crosslinks were reversed by incubation overnight at 65°C, and ChIP DNA was purified by phenol-chloroform extraction and ethanol precipitation.

Quantitative PCR (qPCR) reactions were carried out in triplicate on specific genomic regions using SYBR Green Supermix (Bio-Rad). The resulting signals were normalized for primer efficiency by carrying out qPCR for each primer pair using Input DNA.

Illumina sequencing libraries (a custom type, using the same paired read adapter oligonucleotides [5]) were prepared from the ChIP and Input DNAs on an automated system (Apollo 342, Wafergen Biosystems/Takara). After a final PCR amplification step, the resulting DNA libraries were quantified and sequenced on Illumina's NovaSeq 6000 (75 nt reads, single end).

The resulting sequence data were processed using the nf-core/chipseq pipeline [38]. Targets of key myogenic transcription factors were queried from TRRUST v2 [47]. deepTools2 [92] were used for generating profile plots, while the Integrative Genomics Viewer was used for track visualization [96]. For the analysis of differential peaks, DESeq2 [72] was used. Gene Set Enrichment Analysis was subsequently performed using WebGestalt [68].

3.5.15 ATAC-Seq and data analysis

Cryopreserved C2C12 cells were sent to Active Motif to perform the ATAC-Seq assay. The cells were then thawed in a 37°C water bath, pelleted, washed with

cold PBS, and tagmented as previously described [12], with additional modifications [24]. Briefly, cell pellets were resuspended in lysis buffer, pelleted, and tagmented using the enzyme and buffer provided in the ATAC-Seq Kit (Active Motif). Tagmented DNA was then purified using the MinElute PCR purification kit (Qiagen), amplified with 10 cycles of PCR, and purified using Agencourt AMPure SPRI beads (Beckman Coulter). Resulting material was quantified using Qubit (Invitrogen) and TapeStation (Agilent), then sequenced with PE42 sequencing on the NovaSeq 6000 sequencer (Illumina).

The resulting sequencing data were processed using the nf-core/atacseq pipeline [38]. deepTools2 [92] were used for generating profile plots and heatmaps. For the analysis of differential peaks, DESeq2 [72] was used. Genomic Regions Enrichment of Annotations (GREAT) analysis was subsequently performed using GREAT online server [79] [111].

3.5.16 Statistical analysis

Independent sample T-tests and ANOVA were conducted using the ttest_ind and f_oneway functions from the SciPy stats package [113]. Post-hoc analyses were conducted using the pairwise_turkeyhsd function from the statsmodels package [102].Significance levels are denoted as follows: * for p ¡ 0.05, ** for p ¡ 0.01 and *** for p¡0.001. Bar graphs depict the mean, with the error bars representing the standard deviation.

3.5.17 Generative AI

During the preparation of this manuscript, the author employed Bard and ChatGPT for language refinement to improve clarity and readability, as well as for assistance with specific aspects of code implementation and debugging. After using these tools, the authors thoroughly reviewed and revised the content as necessary.

We take full responsibility for the final content of this publication.

4

Conclusions

4.1 Summary

In this dissertation, I explore how methionine metabolism, through SAM and Setd2, influences H3K36me3 modification and cell differentiation. While the connection between metabolic products, histone modifications and gene expression is partially established, the extent to which dietary nutrients can influence this link, and how changes in cellular nutrient environment can affect histone methylation and gene expression, leading to cellular decisions, remains to be fully understood.

The study begins with the discovery that both H3K36me3 and myogenic differentiation are dependent on methionine. To aid further investigations, we developed a neural network-based method to quantify differentiation using only phase-contrast microscope images as input. Built on this foundation, we probe the mechanisms underlying this dependency further.

Our detailed examination of the kinetics and reversibility of these dependencies revealed the rapid response of cellular methionine metabolism and subsequently histone methylation to methionine restriction, highlighting the timescale

at which these responses happen and the importance of sufficient methionine in the early stages of differentiation.

To address potential confounding factors, we focused on methionine's role as a methyl group donor via SAM. During this phase, we explored the often overlooked aspects of SAM transport properties and chemical stability. We reasoned that the likely absence of a dedicated SAM transporter in mammalian cell membranes, combined with its low permeability and instability under standard culture conditions, would limit its uptake from the extracellular space. Consequently, we chose to impose SAM restriction in the presence of full methionine, rather than supplementing SAM to methionine-restricted conditions, to specifically examine the role of SAM in mediating methionine-dependent myogenic differentiation. Using pharmacological agents to inhibit SAM synthesis, we observed similar impairments in myogenic differentiation, affirming the importance of methionine as a methyl donor in this process.

Next, we examine a downstream effector of SAM, the histone methyltransferase SETD2. Our findings show that Setd2 levels are responsive to both the progression of differentiation and methionine availability, suggesting its crucial role in methionine-dependent myogenic differentiation. By conducting experiments involving both the ectopic expression and knockout of Setd2, we confirm SETD2's role in mediating methionine-dependent myogenic differentiation.

To further link our findings to gene expression, we complement our study with ChIP-Seq and ATAC-Seq experiments. These studies revealed that methionine restriction selectively impacts H3K36me3 levels and chromatin accessibility at gene sites critical for muscle differentiation. Additionally, we observed that the effects of methionine restriction on chromatin accessibility could be partially replicated by a Setd2 knockout. These results provide deeper insights into the interplay between methionine and Setd2 in driving myogenic differentiation.

In conclusion, this collective body of work offers new insights into the complex interplay of metabolism and epigenetics, laying the groundwork for a deeper understanding of how these processes converge to dictate cellular fate decisions.

4.2 Future directions

My research has unveiled the relationship between methionine availability, H3K36me3, and myogenic differentiation, establishing a foundation for many promising future studies. Broadly, these can be categorized into three two directions:

Firstly, the multifaceted nature of Setd2 poses several intriguing questions. As highlighted earlier, Setd2 not only methylates H3K36 and other non-histone substrates but also interacts with RNA polymerase II. Employing point mutations in specific enzyme domains to disrupt these functions could yield significant insights into which aspects of Setd2 are crucial for its role in methionine-dependent myogenesis.

Additionally, the regulatory network involving Setd2 also warrants further investigation. While I have shown that Setd2 levels respond to methionine availability, suggesting its role as a methionine sensor, the precise mechanisms and feedback loops governing this response remain an exciting avenue for discovery.

Secondly, while we've observed that H3K36me3 levels change preferentially around muscle differentiation-related genes in response to methionine restriction (MR), this correlation doesn't necessarily imply causation. To address this, directly manipulating H3K36, perhaps through mutations like H3K36M, could provide more definitive insights into the specific role of H3K36 in mediating methionine-dependent myogenic differentiation.

Lastly, exploring systems of muscle differentiation closer to human physiology, such as the recent advances in inducing skeletal myogenesis from pluripotent

stem cells, offers an exciting opportunity. Similarly, examining additional models of cell differentiation would help reinforce the universality of our findings and extend their application to a broader range of biological contexts.

Bibliography

[1] Agrimi, G., Di Noia, M. A., Marobbio, C. M., Fiermonte, G., Lasorsa, F. M., and Palmieri, F. (2004), "Identification of the human mitochondrial S-adenosylmethionine transporter: Bacterial expression, reconstitution, functional characterization and tissue distribution," *Biochemical Journal*, 379, 183–190.

[2] Albers, E. (2009), "Metabolic characteristics and importance of the universal methionine salvage pathway recycling methionine from 5-methylthioadenosine," *IUBMB Life*, 61, 1132–1142.

[3] An, S., Yeo, K. J., Jeon, Y. H., and Song, J. J. (2011), "Crystal structure of the human histone methyltransferase ASH1L catalytic domain and its implications for the regulatory mechanism," *Journal of Biological Chemistry*, 286, 8369–8374.

[4] Barth, T. K. and Imhof, A. (2010), "Fast signals and slow marks: the dynamics of histone modifications," *Trends in Biochemical Sciences*, 35, 618–626.

[5] Bentley, D. R., Balasubramanian, S., Swerdlow, H. P., Smith, G. P., Milton, J., Brown, C. G., Hall, K. P., Evers, D. J., Barnes, C. L., Bignell, H. R., Boutell, J. M., Bryant, J., Carter, R. J., Keira Cheetham, R., Cox, A. J., Ellis, D. J., Flatbush, M. R., Gormley, N. A., Humphray, S. J., Irving, L. J., Karbelashvili, M. S., Kirk, S. M., Li, H., Liu, X., Maisinger, K. S., Murray, L. J., Obradovic, B., Ost, T., Parkinson, M. L., Pratt, M. R., Rasolonjatovo, I. M., Reed, M. T., Rigatti, R., Rodighiero, C., Ross, M. T., Sabot, A., Sankar, S. V., Scally, A., Schroth, G. P., Smith, M. E., Smith, V. P., Spiridou, A., Torrance, P. E., Tzonev, S. S., Vermaas, E. H., Walter, K., Wu, X., Zhang, L., Alam, M. D., Anastasi, C., Aniebo, I. C., Bailey, D. M., Bancarz, I. R., Banerjee, S., Barbour, S. G., Baybayan, P. A., Benoit, V. A., Benson, K. F., Bevis, C., Black, P. J., Boodhun, A., Brennan, J. S., Bridgham, J. A., Brown, R. C., Brown, A. A., Buermann, D. H., Bundu, A. A., Burrows, J. C., Carter, N. P., Castillo, N., Catenazzi, M. C. E., Chang, S., Neil Cooley, R., Crake, N. R., Dada, O. O., Diakoumakos, K. D., Dominguez-Fernandez, B., Earnshaw, D. J., Egbujor, U. C., Elmore, D. W., Etchin, S. S., Ewan, M. R., Fedurco, M., Fraser, L. J., Fuentes Fajardo, K. V., Scott Furey, W., George, D., Gietzen, K. J., Goddard, C. P., Golda, G. S., Granieri, P. A., Green, D. E., Gustafson, D. L., Hansen, N. F., Harnish, K., Haudenschild, C. D., Heyer, N. I., Hims, M. M., Ho, J. T.,

Horgan, A. M., Hoschler, K., Hurwitz, S., Ivanov, D. V., Johnson, M. Q., James, T., Huw Jones, T. A., Kang, G. D., Kerelska, T. H., Kersey, A. D., Khrebtukova, I., Kindwall, A. P., Kingsbury, Z., Kokko-Gonzales, P. I., Kumar, A., Laurent, M. A., Lawley, C. T., Lee, S. E., Lee, X., Liao, A. K., Loch, J. A., Lok, M., Luo, S., Mammen, R. M., Martin, J. W., McCauley, P. G., McNitt, P., Mehta, P., Moon, K. W., Mullens, J. W., Newington, T., Ning, Z., Ling Ng, B., Novo, S. M., O'Neill, M. J., Osborne, M. A., Osnowski, A., Ostadan, O., Paraschos, L. L., Pickering, L., Pike, A. C., Pike, A. C., Chris Pinkard, D., Pliskin, D. P., Podhasky, J., Quijano, V. J., Raczy, C., Rae, V. H., Rawlings, S. R., Chiva Rodriguez, A., Roe, P. M., Rogers, J., Rogert Bacigalupo, M. C., Romanov, N., Romieu, A., Roth, R. K., Rourke, N. J., Ruediger, S. T., Rusman, E., Sanches-Kuiper, R. M., Schenker, M. R., Seoane, J. M., Shaw, R. J., Shiver, M. K., Short, S. W., Sizto, N. L., Sluis, J. P., Smith, M. A., Ernest Sohna Sohna, J., Spence, E. J., Stevens, K., Sutton, N., Szajkowski, L., Tregidgo, C. L., Turcatti, G., Vandevondele, S., Verhovsky, Y., Virk, S. M., Wakelin, S., Walcott, G. C., Wang, J., Worsley, G. J., Yan, J., Yau, L., Zuerlein, M., Rogers, J., Mullikin, J. C., Hurles, M. E., McCooke, N. J., West, J. S., Oaks, F. L., Lundberg, P. L., Klenerman, D., Durbin, R., and Smith, A. J. (2008), "Accurate whole human genome sequencing using reversible terminator chemistry," *Nature*, 456, 53–59.

[6] Berger, S. L., Kouzarides, T., Shiekhattar, R., and Shilatifard, A. (2009), "An operational definition of epigenetics," *Genes and Development*, 23, 781–783.

[7] Bhattacharya, S. and Workman, J. L. (2020), "Regulation of SETD2 stability is important for the fidelity of H3K36me3 deposition," *Epigenetics and Chromatin*, 13, 1–14.

[8] Bhattacharya, S., Lange, J. J., Levy, M., Florens, L., Washburn, M. P., and Workman, J. L. (2021), "The disordered regions of the methyltransferase SETD2 govern its function by regulating its proteolysis and phase separation," *Journal of Biological Chemistry*, 297, 101075.

[9] Biggar, K. K. and Li, S. S. (2015), "Non-histone protein methylation as a regulator of cellular signalling and function," *Nature Reviews Molecular Cell Biology*, 16, 5–17.

[10] Black, J. C., Van Rechem, C., and Whetstine, J. R. (2012), "Histone Lysine Methylation Dynamics: Establishment, Regulation, and Biological Impact," *Molecular Cell*, 48, 491–507.

[11] Brunk, C. F. and Martin, W. F. (2019), "Archaeal Histone Contributions to the Origin of Eukaryotes," *Trends in Microbiology*, 27, 703–714.

[12] Buenrostro, J. D., Giresi, P. G., Zaba, L. C., Chang, H. Y., and Greenleaf, W. J. (2013), "Transposition of native chromatin for fast and sensitive epigenomic

profiling of open chromatin, DNA-binding proteins and nucleosome position," *Nature Methods*, 10, 1213–1218.

[13] Campagna-Slater, V., Mok, M. W., Nguyen, K. T., Feher, M., Najmanovich, R., and Schapira, M. (2011), "Structural chemistry of the histone methyltransferases cofactor binding site," *Journal of Chemical Information and Modeling*, 51, 612–623.

[14] Carson, D. A., Willis, E. H., and Kamatani, N. (1983), "Metabolism to methionine and growth stimulation by 5′-methylthioadenosine and 5′-methylthioinosine in mammalian cells." *Biochemical and biophysical research communications*, 112, 391–7.

[15] Cartenì-Farina, M., della Ragione, F., Cacciapuoti, G., Porcelli, M., and Zappia, V. (1983), "Transport and metabolism of 5′-methylthioadenosine in human erythrocytes." *Biochimica et biophysica acta*, 727, 221–9.

[16] Cavalli, G. and Heard, E. (2019), "Advances in epigenetics link genetics to the environment and disease," *Nature*, 571, 489–499.

[17] Chakraborty, A. A., Laukka, T., Myllykoski, M., Ringel, A. E., Booker, M. A., Tolstorukov, M. Y., Meng, Y. J., Meier, S. R., Jennings, R. B., Creech, A. L., Herbert, Z. T., McBrayer, S. K., Olenchock, B. A., Jaffe, J. D., Haigis, M. C., Beroukhim, R., Signoretti, S., Koivunen, P., and Kaelin, W. G. (2019), "Histone demethylase KDM6A directly senses oxygen to control chromatin and cell fate," *Science*, 363, 1217–1222.

[18] Chan, J. C. and Maze, I. (2020), "Nothing Is Yet Set in (Hi)stone: Novel Post-Translational Modifications Regulating Chromatin Function," *Trends in Biochemical Sciences*, 45, 829–844.

[19] Chandel, N. S. (2015), *Navigating metabolism*, Cold Spring Harbor Laboratory Press Cold Spring Harbor, New York.

[20] Chen, K., Liu, J., Liu, S., Xia, M., Zhang, X., Han, D., Jiang, Y., Wang, C., and Cao, X. (2017), "Methyltransferase SETD2-Mediated Methylation of STAT1 Is Critical for Interferon Antiviral Activity," *Cell*, 170, 492–506.

[21] Chowdhury, R., Yeoh, K. K., Tian, Y. M., Hillringhaus, L., Bagg, E. A., Rose, N. R., Leung, I. K., Li, X. S., Woon, E. C., Yang, M., McDonough, M. A., King, O. N., Clifton, I. J., Klose, R. J., Claridge, T. D., Ratcliffe, P. J., Schofield, C. J., and Kawamura, A. (2011), "The oncometabolite 2-hydroxyglutarate inhibits histone lysine demethylases," *EMBO Reports*, 12, 463–469.

[22] Clarke, S. G. (2006), "Inhibition of mammalian protein methyltransferases by 5′-methylthioadenosine (MTA): A mechanism of action of dietary SAMe?" *The Enzymes*, 24, 467–93.

[23] Cluntun, A. A., Huang, H., Dai, L., Liu, X., Zhao, Y., and Locasale, J. W. (2015), "The rate of glycolysis quantitatively mediates specific histone acetylation sites," *Cancer & Metabolism*, 3, 1–12.

[24] Corces, M. R., Trevino, A. E., Hamilton, E. G., Greenside, P. G., Sinnott-Armstrong, N. A., Vesuna, S., Satpathy, A. T., Rubin, A. J., Montine, K. S., Wu, B., Kathiria, A., Cho, S. W., Mumbach, M. R., Carter, A. C., Kasowski, M., Orloff, L. A., Risca, V. I., Kundaje, A., Khavari, P. A., Montine, T. J., Greenleaf, W. J., and Chang, H. Y. (2017), "An improved ATAC-seq protocol reduces background and enables interrogation of frozen tissues," *Nature Methods*, 14, 959–962.

[25] Cordeiro-Spinetti, E. and Rothbart, S. B. (2023), "Lysine methylation signaling in skeletal muscle biology: from myogenesis to clinical insights," *The Biochemical journal*, 480, 1969–1986.

[26] Dai, Z., Ramesh, V., and Locasale, J. W. (2020), "The evolving metabolic landscape of chromatin biology and epigenetics," *Nature Reviews Genetics*, 21, 737–753.

[27] Dai, Z., Zheng, W., and Locasale, J. W. (2022), "Amino acid variability, tradeoffs and optimality in human diet," *Nature Communications*, 13.

[28] Daugaard, M., Baude, A., Fugger, K., Povlsen, L. K., Beck, H., Sørensen, C. S., Petersen, N. H., Sorensen, P. H., Lukas, C., Bartek, J., Lukas, J., Rohde, M., and Jäättelä, M. (2012), "LEDGF (p75) promotes DNA-end resection and homologous recombination," *Nature Structural and Molecular Biology*, 19, 803–810.

[29] Davey, C. A., Sargent, D. F., Luger, K., Maeder, A. W., and Richmond, T. J. (2002), "Solvent mediated interactions in the structure of the nucleosome core particle at 1.9 Å resolution," *Journal of Molecular Biology*, 319, 1097–1113.

[30] de Mendoza, A. and Sebé-Pedrós, A. (2019), "Origin and evolution of eukaryotic transcription factors," *Current Opinion in Genetics and Development*, 58-59, 25–32.

[31] Dillon, S. C., Zhang, X., Trievel, R. C., and Cheng, X. (2005), "The SET-domain protein superfamily: Protein lysine methyltransferases," *Genome Biology*, 6.

[32] Diokmetzidou, A., Tsikitis, M., Nikouli, S., Kloukina, I., Tsoupri, E., Papathanasiou, S., Psarras, S., Mavroidis, M., and Capetanaki, Y. (2016), *Strategies to Study Desmin in Cardiac Muscle and Culture Systems*, vol. 568, Elsevier Inc., 1 edn.

[33] Du, J., Johnson, L. M., Jacobsen, S. E., and Patel, D. J. (2015), "DNA methylation pathways and their crosstalk with histone methylation," *Nature Reviews Molecular Cell Biology*, 16, 519–532.

[34] Edmunds, J. W., Mahadevan, L. C., and Clayton, A. L. (2008), "Dynamic histone H3 methylation during gene induction: HYPB/Setd2 mediates all H3K36 trimethylation," *EMBO Journal*, 27, 406–420.

[35] Egan, B., Yuan, C. C., Craske, M. L., Labhart, P., Guler, G. D., Arnott, D., Maile, T. M., Busby, J., Henry, C., Kelly, T. K., Tindell, C. A., Jhunjhunwala, S., Zhao, F., Hatton, C., Bryant, B. M., Classon, M., and Trojer, P. (2016), "An alternative approach to ChIP-Seq normalization enables detection of genome-wide changes in histone H3 lysine 27 trimethylation upon EZH2 inhibition," *PLoS ONE*, 11, 1–20.

[36] El-Sayed, A. S. (2010), "Microbial l-methioninase: Production, molecular characterization, and therapeutic applications," *Applied Microbiology and Biotechnology*, 86, 445–467.

[37] Eram, M. S., Kuznetsova, E., Li, F., Lima-Fernandes, E., Kennedy, S., Chau, I., Arrowsmith, C. H., Schapira, M., and Vedadi, M. (2015), "Kinetic characterization of human histone H3 lysine 36 methyltransferases, ASH1L and SETD2," *Biochimica et Biophysica Acta - General Subjects*, 1850, 1842–1848.

[38] Ewels, P. A., Peltzer, A., Fillinger, S., Patel, H., Alneberg, J., Wilm, A., Garcia, M. U., Di Tommaso, P., and Nahnsen, S. (2020), "The nf-core framework for community-curated bioinformatics pipelines," *Nature Biotechnology*, 38, 276–278.

[39] Feinberg, A. P. and Daniele Fallin, M. (2015), "Epigenetics at the crossroads of genes and the environment," *JAMA - Journal of the American Medical Association*, 314, 1129–1130.

[40] Fiechhi, A. (1974), "Double salts of S-adenosil-L-methionine," .

[41] Finogenova, K., Bonnet, J., Poepsel, S., Schäfer, I. B., Finkl, K., Schmid, K., Litz, C., Strauss, M., Benda, C., and Müller, J. (2020), "Structural basis for prc2 decoding of active histone methylation marks h3k36me2/3," *eLife*, 9, 1–30.

[42] Gao, X., Sanderson, S. M., Dai, Z., Reid, M. A., Cooper, D. E., Lu, M., Richie, J. P., Ciccarella, A., Calcagnotto, A., Mikhael, P. G., Mentch, S. J., Liu, J., Ables, G., Kirsch, D. G., Hsu, D. S., Nichenametla, S. N., and Locasale, J. W. (2019), "Dietary methionine influences therapy in mouse cancer models and alters human metabolism," *Nature*, 572, 397–401.

[43] Godbole, A. A., Gopalan, S., Nguyen, T. K., Munden, A. L., Lui, D. S., Fanelli, M. J., Vo, P., Lewis, C. A., Spinelli, J. B., Fazzio, T. G., and Walker, A. K. (2023), "S-adenosylmethionine synthases specify distinct H3K4me3 populations and gene expression patterns during heat stress," *eLife*, 12, 1–26.

[44] Greer, E. L. and Shi, Y. (2012), "Histone methylation: A dynamic mark in health, disease and inheritance," *Nature Reviews Genetics*, 13, 343–357.

[45] Guan, H., Wang, P., Zhang, P., Ruan, C., Ou, Y., Peng, B., Zheng, X., Lei, J., Li, B., Yan, C., and Li, H. (2023), "Diverse modes of H3K36me3-guided nucleosomal deacetylation by Rpd3S," *Nature*, 620, 669–675.

[46] Hacker, K. E., Fahey, C. C., Shinsky, S. A., Chiang, Y. C. J., DiFiore, J. V., Jha, D. K., Vo, A. H., Shavit, J. A., Davis, I. J., Strahl, B. D., and Rathmell, W. K. (2016), "Structure/function analysis of recurrent mutations in SETD2 protein reveals a critical and conserved role for a SET domain residue in maintaining protein stability and histone H3 Lys-36 trimethylation," *Journal of Biological Chemistry*, 291, 21283–21295.

[47] Han, H., Cho, J. W., Lee, S., Yun, A., Kim, H., Bae, D., Yang, S., Kim, C. Y., Lee, M., Kim, E., Lee, S., Kang, B., Jeong, D., Kim, Y., Jeon, H. N., Jung, H., Nam, S., Chung, M., Kim, J. H., and Lee, I. (2018), "TRRUST v2: An expanded reference database of human and mouse transcriptional regulatory interactions," *Nucleic Acids Research*, 46, D380–D386.

[48] He, K., Zhang, X., Ren, S., and Sun, J. (2016), "Deep residual learning for image recognition," *Proceedings of the IEEE Computer Society Conference on Computer Vision and Pattern Recognition*, 2016-Decem, 770–778.

[49] Hirata, F. and Axelrod, J. (1980), "Phospholipid Methylation and Biological Signal Transmission," *Science*, 209, 1082–1090.

[50] Ho, J. W., Jung, Y. L., Liu, T., Alver, B. H., Lee, S., Ikegami, K., Sohn, K. A., Minoda, A., Tolstorukov, M. Y., Appert, A., Parker, S. C., Gu, T., Kundaje, A., Riddle, N. C., Bishop, E., Egelhofer, T. A., Hu, S. S., Alekseyenko, A. A., Rechtsteiner, A., Asker, D., Belsky, J. A., Bowman, S. K., Chen, Q. B., Chen, R. A., Day, D. S., Dong, Y., Dose, A. C., Duan, X., Epstein, C. B., Ercan, S., Feingold, E. A., Ferrari, F., Garrigues, J. M., Gehlenborg, N., Good, P. J., Haseley, P., He, D., Herrmann, M., Hoffman, M. M., Jeffers, T. E., Kharchenko, P. V., Kolasinska-Zwierz, P., Kotwaliwale, C. V., Kumar, N., Langley, S. A., Larschan, E. N., Latorre, I., Libbrecht, M. W., Lin, X., Park, R., Pazin, M. J., Pham, H. N., Plachetka, A., Qin, B., Schwartz, Y. B., Shoresh, N., Stempor, P., Vielle, A., Wang, C., Whittle, C. M., Xue, H., Kingston, R. E., Kim, J. H., Bernstein, B. E., Dernburg, A. F., Pirrotta, V., Kuroda, M. I., Noble, W. S., Tullius, T. D., Kellis, M., MacAlpine, D. M., Strome, S., Elgin, S. C., Liu, X. S., Lieb, J. D., Ahringer, J., Karpen, G. H., and Park, P. J. (2014), "Comparative analysis of metazoan chromatin organization," *Nature*, 512, 449–452.

[51] Huang, H., Weng, H., Zhou, K., Wu, T., Zhao, B. S., Sun, M., Chen, Z., Deng, X., Xiao, G., Auer, F., Klemm, L., Wu, H., Zuo, Z., Qin, X., Dong, Y., Zhou, Y.,

Qin, H., Tao, S., Du, J., Liu, J., Lu, Z., Yin, H., Mesquita, A., Yuan, C. L., Hu, Y. C., Sun, W., Su, R., Dong, L., Shen, C., Li, C., Qing, Y., Jiang, X., Wu, X., Sun, M., Guan, J. L., Qu, L., Wei, M., Müschen, M., Huang, G., He, C., Yang, J., and Chen, J. (2019), "Histone H3 trimethylation at lysine 36 guides m6A RNA modification co-transcriptionally," *Nature*, 567, 414–419.

[52] Huang, Z., Cai, L., and Tu, B. P. (2015), "Dietary control of chromatin," *Current Opinion in Cell Biology*, 34, 69–74.

[53] Jaenisch, R. and Bird, A. (2003), "Epigenetic regulation of gene expression: How the genome integrates intrinsic and environmental signals," *Nature Genetics*, 33, 245–254.

[54] Jambhekar, A., Dhall, A., and Shi, Y. (2019), "Roles and regulation of histone methylation in animal development," *Nature Reviews Molecular Cell Biology*, 20, 625–641.

[55] Jenuwein, T. and Allis, C. D. (2001), "Translating the histone code," *Science*, 293, 1074–1080.

[56] Kaelin, W. G. and McKnight, S. L. (2013), "Influence of metabolism on epigenetics and disease," *Cell*, 153, 56–69.

[57] Katoh, Y., Ikura, T., Hoshikawa, Y., Tashiro, S., Ito, T., Ohta, M., Kera, Y., Noda, T., and Igarashi, K. (2011), "Methionine Adenosyltransferase II Serves as a Transcriptional Corepressor of Maf Oncoprotein," *Molecular Cell*, 41, 554–566.

[58] Kearns, S., Mason, F. M., Rathmell, W. K., Park, I. Y., Walker, C., Verhey, K. J., and Cianfrocco, M. A. (2021), "Molecular determinants for α-tubulin methylation by SETD2," *Journal of Biological Chemistry*, 297.

[59] Kizer, K. O., Phatnani, H. P., Shibata, Y., Hall, H., Greenleaf, A. L., Strahl, B. D., and Iol, M. O. L. C. E. L. L. B. (2005), "A Novel Domain in Set2 Mediates RNA Polymerase II Interaction and Couples Histone H3 K36 Methylation with Transcript Elongation," 25, 3305–3316.

[60] Klose, R. J. and Zhang, Y. (2007), "Regulation of histone methylation by demethylimination and demethylation," *Nature Reviews Molecular Cell Biology*, 8, 307–318.

[61] Konteatis, Z., Travins, J., Gross, S., Marjon, K., Barnett, A., Mandley, E., Nicolay, B., Nagaraja, R., Chen, Y., Sun, Y., Liu, Z., Yu, J., Ye, Z., Jiang, F., Wei, W., Fang, C., Gao, Y., Kalev, P., Hyer, M. L., Delabarre, B., Jin, L., Padyana, A. K., Dang, L., Murtie, J., Biller, S. A., Sui, Z., and Marks, K. M. (2021), "Discovery of AG-270, a First-in-Class Oral MAT2A Inhibitor for the Treatment of Tumors with Homozygous MTAP Deletion," *Journal of Medicinal Chemistry*, 64, 4430–4449.

[62] Kouzarides, T. (2007), "Chromatin Modifications and Their Function," *Cell*, 128, 693–705.

[63] Krautkramer, K. A., Dhillon, R. S., Denu, J. M., and Carey, H. V. (2017), "Metabolic programming of the epigenome: host and gut microbial metabolite interactions with host chromatin," *Translational Research*, 189, 30–50.

[64] Labun, K., Montague, T. G., Krause, M., Torres Cleuren, Y. N., Tjeldnes, H., and Valen, E. (2019), "CHOPCHOP v3: Expanding the CRISPR web toolbox beyond genome editing," *Nucleic Acids Research*, 47, W171–W174.

[65] Li, F., Mao, G., Tong, D., Huang, J., Gu, L., Yang, W., and Li, G. M. (2013), "The histone mark H3K36me3 regulates human DNA mismatch repair through its interaction with MutSα," *Cell*, 153, 590–600.

[66] Li, J., Moazed, D., and Gygi, S. P. (2002), "Association of the histone methyltransferase Set2 with RNA polymerase II plays a role in transcription elongation," *Journal of Biological Chemistry*, 277, 49383–49388.

[67] Li, X., Egervari, G., Wang, Y., Berger, S. L., and Lu, Z. (2018), "Regulation of chromatin and gene expression by metabolic enzymes and metabolites," *Nature Reviews Molecular Cell Biology*, 19, 563–578.

[68] Liao, Y., Wang, J., Jaehnig, E. J., Shi, Z., and Zhang, B. (2019), "WebGestalt 2019: gene set analysis toolkit with revamped UIs and APIs," *Nucleic Acids Research*, 47, W199–W205.

[69] Liu, X., Ser, Z., and Locasale, J. W. (2014), "Development and quantitative evaluation of a high-resolution metabolomics technology," *Analytical Chemistry*, 86, 2175–2184.

[70] Locasale, J. W. (2013), "Serine, glycine and one-carbon units: Cancer metabolism in full circle," *Nature Reviews Cancer*, 13, 572–583.

[71] Lombardini, J. B. and Sufrin, J. R. (1983), "Chemotherapeutic potential of methionine analogue inhibitors of tumor-derived methionine adenosyltransferases," *Biochemical Pharmacology*, 32, 489–495.

[72] Love, M. I., Huber, W., and Anders, S. (2014), "Moderated estimation of fold change and dispersion for RNA-seq data with DESeq2," *Genome Biology*, 15, 1–21.

[73] Lu, C., Ward, P. S., Kapoor, G. S., Rohle, D., Turcan, S., Abdel-Wahab, O., Edwards, C. R., Khanin, R., Figueroa, M. E., Melnick, A., Wellen, K. E., Oĝrourke, D. M., Berger, S. L., Chan, T. A., Levine, R. L., Mellinghoff, I. K., and Thompson, C. B. (2012), "IDH mutation impairs histone demethylation and results in a block to cell differentiation," *Nature*, 483, 474–478.

[74] Luco, R. F., Pan, Q., Tominaga, K., Blencowe, B. J., Pereira-Smith, O. M., and Misteli, T. (2010), "Regulation of alternative splicing by histone modifications," *Science*, 327, 996–1000.

[75] Martin, C. and Zhang, Y. (2007), "Mechanisms of epigenetic inheritance," *Current Opinion in Cell Biology*, 19, 266–272.

[76] Martínez-Chantar, M. L., Latasa, M. U., Varela-Rey, M., Lu, S. C., García-Trevijano, E. R., Mato, J. M., and Avila, M. A. (2003), "L-methionine availability regulates expression of the methionine adenosyltransferase 2A gene in human hepatocarcinoma cells. Role of S-adenosylmethionine," *Journal of Biological Chemistry*, 278, 19885–19890.

[77] McDaniel, S. L. and Strahl, B. D. (2017), "Shaping the cellular landscape with Set2/SETD2 methylation," *Cellular and Molecular Life Sciences*, 74, 3317–3334.

[78] McDonough, M. A., Loenarz, C., Chowdhury, R., Clifton, I. J., and Schofield, C. J. (2010), "Structural studies on human 2-oxoglutarate dependent oxygenases," *Current Opinion in Structural Biology*, 20, 659–672.

[79] McLean, C. Y., Bristor, D., Hiller, M., Clarke, S. L., Schaar, B. T., Lowe, C. B., Wenger, A. M., and Bejerano, G. (2010), "GREAT improves functional interpretation of cis-regulatory regions," *Nature Biotechnology*, 28, 495–501.

[80] McMillan, J. M., Walle, U. K., and Walle, T. (2010), "S-adenosyl-l-methionine: transcellular transport and uptake by Caco-2 cells and hepatocytes," *Journal of Pharmacy and Pharmacology*, 57, 599–605.

[81] Mentch, S. J., Mehrmohamadi, M., Huang, L., Liu, X., Gupta, D., Mattocks, D., Gómez Padilla, P., Ables, G., Bamman, M. M., Thalacker-Mercer, A. E., Nichenametla, S. N., and Locasale, J. W. (2015), "Histone Methylation Dynamics and Gene Regulation Occur through the Sensing of One-Carbon Metabolism," *Cell Metabolism*, 22, 861–873.

[82] Morselli, M., Pastor, W. A., Montanini, B., Nee, K., Ferrari, R., Fu, K., Bonora, G., Rubbi, L., Clark, A. T., Ottonello, S., Jacobsen, S. E., and Pellegrini, M. (2015), "In vivo targeting of de novo DNA methylation by histone modifications in yeast and mouse," *eLife*, 2015, 1–21.

[83] Mosammaparast, N. and Shi, Y. (2010), "Reversal of histone methylation: Biochemical and molecular mechanisms of histone demethylases," *Annual Review of Biochemistry*, 79, 155–179.

[84] Moussaieff, A., Rouleau, M., Kitsberg, D., Cohen, M., Levy, G., Barasch, D., Nemirovski, A., Shen-Orr, S., Laevsky, I., Amit, M., Bomze, D., Elena-Herrmann, B., Scherf, T., Nissim-Rafinia, M., Kempa, S., Itskovitz-Eldor, J.,

Meshorer, E., Aberdam, D., and Nahmias, Y. (2015), "Glycolysis-mediated changes in acetyl-CoA and histone acetylation control the early differentiation of embryonic stem cells," *Cell Metabolism*, 21, 392–402.

[85] Musselman, C. A., Lalonde, M. E., Côté, J., and Kutateladze, T. G. (2012), "Perceiving the epigenetic landscape through histone readers," *Nature Structural and Molecular Biology*, 19, 1218–1227.

[86] Neri, F., Rapelli, S., Krepelova, A., Incarnato, D., Parlato, C., Basile, G., Maldotti, M., Anselmi, F., and Oliviero, S. (2017), "Intragenic DNA methylation prevents spurious transcription initiation," *Nature*, 543, 72–77.

[87] Nestorov, P., Tardat, M., and Peters, A. H. (2013), *H3K9/HP1 and Polycomb. Two Key Epigenetic Silencing Pathways for Gene Regulation and Embryo Development.*, vol. 104, Copyright © 2013 Elsevier Inc. All rights reserved., 1 edn.

[88] Park, I. Y., Powell, R. T., Tripathi, D. N., Dere, R., Ho, T. H., Blasius, T. L., Chiang, Y. C., Davis, I. J., Fahey, C. C., Hacker, K. E., Verhey, K. J., Bedford, M. T., Jonasch, E., Rathmell, W. K., and Walker, C. L. (2016), "Dual Chromatin and Cytoskeletal Remodeling by SETD2," *Cell*, 166, 950–962.

[89] Paszke, A., Gross, S., Massa, F., Lerer, A., Bradbury, J., Chanan, G., Killeen, T., Lin, Z., Gimelshein, N., Antiga, L., Desmaison, A., Köpf, A., Yang, E., DeVito, Z., Raison, M., Tejani, A., Chilamkurthy, S., Steiner, B., Fang, L., Bai, J., and Chintala, S. (2019), "PyTorch: An imperative style, high-performance deep learning library," *Advances in Neural Information Processing Systems*, 32.

[90] Patel, A., Vought, V. E., Swatkoski, S., Viggiano, S., Howard, B., Dharmarajan, V., Monteith, K. E., Kupakuwana, G., Namitz, K. E., Shinsky, S. A., Cotter, R. J., and Cosgrove, M. S. (2014), "Automethylation activities within the mixed lineage leukemia-1 (MLL1) core complex reveal evidence supporting a "two-active site" model for multiple histone H3 lysine 4 methylation," *Journal of Biological Chemistry*, 289, 868–884.

[91] Piovesan, A., Pelleri, M. C., Antonaros, F., Strippoli, P., Caracausi, M., and Vitale, L. (2019), "On the length, weight and GC content of the human genome," *BMC Research Notes*, 12, 1–7.

[92] Ramírez, F., Ryan, D. P., Grüning, B., Bhardwaj, V., Kilpert, F., Richter, A. S., Heyne, S., Dündar, F., and Manke, T. (2016), "deepTools2: a next generation web server for deep-sequencing data analysis," *Nucleic Acids Research*, 44, W160–W165.

[93] Rathert, P., Zhang, X., Freund, C., Cheng, X., and Jeltsch, A. (2008), "Analysis of the Substrate Specificity of the Dim-5 Histone Lysine Methyltransferase Using Peptide Arrays," *Chemistry and Biology*, 15, 5–11.

[94] Reid, M. A., Dai, Z., and Locasale, J. W. (2017), "The impact of cellular metabolism on chromatin dynamics and epigenetics," *Nature Cell Biology*, 19, 1298–1306.

[95] Richmond, T. J. and Davey, C. A. (2003), "The structure of DNA in the nucleosome core," *Nature*, 423, 145–150.

[96] Robinson, J. T., Thorvaldsdóttir, H., Winckler, W., Guttman, M., Lander, E. S., Getz, G., and Mesirov, J. P. (2011), "Integrative genomics viewer," *Nature Biotechnology*, 29, 24–26.

[97] Rouillon, A., Surdin-Kerjan, Y., and Thomas, D. (1999), "Transport of sulfonium compounds. Characterization of the S- adenosylmethionine and S-methylmethionine permeases from the yeast Saccharomyces cerevisiae," *Journal of Biological Chemistry*, 274, 28096–28105.

[98] Ryall, J. G., Cliff, T., Dalton, S., and Sartorelli, V. (2015), "Metabolic Reprogramming of Stem Cell Epigenetics," *Cell Stem Cell*, 17, 651–662.

[99] Sanderson, S. M., Gao, X., Dai, Z., and Locasale, J. W. (2019), "Methionine metabolism in health and cancer: a nexus of diet and precision medicine," *Nature Reviews Cancer*.

[100] Schapira, M. (2011), "Structural chemistry of human SET domain protein methyltransferases," *Current Chemical Genomics*, 5, 85–94.

[101] Schvartzman, J. M., Reuter, V. P., Koche, R. P., and Thompson, C. B. (2019), "2-hydroxyglutarate inhibits MyoD-mediated differentiation by preventing H3K9 demethylation," *Proceedings of the National Academy of Sciences of the United States of America*, 116, 12851–12856.

[102] Seabold, S. and Perktold, J. (2010), "statsmodels: Econometric and statistical modeling with python," in *9th Python in Science Conference*.

[103] Seervai, R. N., Jangid, R. K., Karki, M., Tripathi, D. N., Jung, S. Y., Kearns, S. E., Verhey, K. J., Cianfrocco, M. A., Millis, B. A., Tyska, M. J., Mason, F. M., Kimryn Rathmell, W., Park, I. Y., Dere, R., and Walker, C. L. (2020), "The Huntingtin-interacting protein SETD2/HYPB is an actin lysine methyltransferase," *Science Advances*, 6, 1–16.

[104] Separovich, R. J. and Wilkins, M. R. (2021), "Ready, SET, Go: Post-translational regulation of the histone lysine methylation network in budding yeast," *Journal of Biological Chemistry*, 297, 1–29.

[105] Shima, H., Matsumoto, M., Ishigami, Y., Ebina, M., Muto, A., Sato, Y., Kumagai, S., Ochiai, K., Suzuki, T., and Igarashi, K. (2017), "S-Adenosylmethionine Synthesis Is Regulated by Selective N6-Adenosine

Methylation and mRNA Degradation Involving METTL16 and YTHDC1," *Cell Reports*, 21, 3354–3363.

[106] Shyh-Chang, N., Locasale, J. W., Lyssiotis, C. A., Zheng, Y., Teo, R. Y., Ratanasirintrawoot, S., Zhang, J., Onder, T., Unternaehrer, J. J., Zhu, H., Asara, J. M., Daley, G. Q., and Cantley, L. C. (2013), "Influence of Threonine Metabolism on S -Adenosylmethionine and Histone Methylation," *Science*, 339, 222–226.

[107] Stoeckler, J. D. and Shih-Ying Li (1987), "Influx of 5′-deoxy-5′-methylthioadenosine into HL-60 human leukemia cells and erythrocytes," *Journal of Biological Chemistry*, 262, 9542–9546.

[108] Strahl, B. D. and Allis, C. D. (2000), "The language of covalent histone modifications," *Nature*, 403, 41–45.

[109] Sun, Y. and Locasale, J. W. (2021), "Rethinking the bioavailability and cellular transport properties of S-adenosylmethionine," *Cell Stress*, 6, 1–5.

[110] Sun, Y., Ramesh, V., Wei, F., and Locasale, J. W. (2023), "Methionine availability influences essential H3K36me3 dynamics during cell differentiation," *bioRxiv*, p. 2023.11.22.568331.

[111] Tanigawa, Y., Dyer, E. S., and Bejerano, G. (2022), "WhichTF is functionally important in your open chromatin data?" *PLoS Computational Biology*, 18, 1–29.

[112] Tao, Y., Neppl, R. L., Huang, Z. P., Chen, J., Tang, R. H., Cao, R., Zhang, Y., Jin, S. W., and Wang, D. Z. (2011), "The histone methyltransferase Set7/9 promotes myoblast differentiation and myofibril assembly," *Journal of Cell Biology*, 194, 551–565.

[113] Virtanen, P., Gommers, R., Oliphant, T. E., Haberland, M., Reddy, T., Cournapeau, D., Burovski, E., Peterson, P., Weckesser, W., Bright, J., van der Walt, S. J., Brett, M., Wilson, J., Millman, K. J., Mayorov, N., Nelson, A. R., Jones, E., Kern, R., Larson, E., Carey, C. J., Polat, , Feng, Y., Moore, E. W., VanderPlas, J., Laxalde, D., Perktold, J., Cimrman, R., Henriksen, I., Quintero, E. A., Harris, C. R., Archibald, A. M., Ribeiro, A. H., Pedregosa, F., van Mulbregt, P., Vijaykumar, A., Bardelli, A. P., Rothberg, A., Hilboll, A., Kloeckner, A., Scopatz, A., Lee, A., Rokem, A., Woods, C. N., Fulton, C., Masson, C., Häggström, C., Fitzgerald, C., Nicholson, D. A., Hagen, D. R., Pasechnik, D. V., Olivetti, E., Martin, E., Wieser, E., Silva, F., Lenders, F., Wilhelm, F., Young, G., Price, G. A., Ingold, G. L., Allen, G. E., Lee, G. R., Audren, H., Probst, I., Dietrich, J. P., Silterra, J., Webber, J. T., Slavič, J., Nothman, J., Buchner, J., Kulick, J., Schönberger, J. L., de Miranda Cardoso, J. V., Reimer, J., Harrington, J., Rodríguez, J. L. C., Nunez-Iglesias, J., Kuczynski, J., Tritz, K., Thoma, M., Newville, M., Kümmerer, M.,

Bolingbroke, M., Tartre, M., Pak, M., Smith, N. J., Nowaczyk, N., Shebanov, N., Pavlyk, O., Brodtkorb, P. A., Lee, P., McGibbon, R. T., Feldbauer, R., Lewis, S., Tygier, S., Sievert, S., Vigna, S., Peterson, S., More, S., Pudlik, T., Oshima, T., Pingel, T. J., Robitaille, T. P., Spura, T., Jones, T. R., Cera, T., Leslie, T., Zito, T., Krauss, T., Upadhyay, U., Halchenko, Y. O., and Vázquez-Baeza, Y. (2020), "SciPy 1.0: fundamental algorithms for scientific computing in Python," *Nature Methods*, 17, 261–272.

[114] Waterland, R. A. (2006), "Assessing the effects of high methionine intake on DNA methylation," *Journal of Nutrition*, 136, 1706S–1710S.

[115] Wellen, K. E., Hatzivassiliou, G., Sachdeva, U. M., Bui, T. V., Cross, J. R., and Thompson, C. B. (2009), "ATP-citrate lyase links cellular metabolism to histone acetylation," *Science*, 324, 1076–1080.

[116] Wu, S. E., Huskey, W. P., Borchardt, R. T., and Schowen, R. L. (1983), "Chiral Instability at Sulfur of S-Adenosylmethionine," *Biochemistry*, 22, 2828–2832.

[117] Wu, T. P., Wang, T., Seetin, M. G., Lai, Y., Zhu, S., Lin, K., Liu, Y., Byrum, S. D., Mackintosh, S. G., Zhong, M., Tackett, A., Wang, G., Hon, L. S., Fang, G., Swenberg, J. A., and Xiao, A. Z. (2016), "DNA methylation on N6-adenine in mammalian embryonic stem cells," *Nature*, 532, 329–333.

[118] Wysocka, J., Swigut, T., Xiao, H., Milne, T. A., Kwon, S. Y., Landry, J., Kauer, M., Tackett, A. J., Chait, B. T., Badenhorst, P., Wu, C., and Allis, C. D. (2006), "A PHD finger of NURF couples histone H3 lysine 4 trimethylation with chromatin remodelling," *Nature*, 442, 86–90.

[119] Xiao, C. L., Zhu, S., He, M., Chen, D., Zhang, Q., Chen, Y., Yu, G., Liu, J., Xie, S. Q., Luo, F., Liang, Z., Wang, D. P., Bo, X. C., Gu, X. F., Wang, K., and Yan, G. R. (2018), "N 6 -Methyladenine DNA Modification in the Human Genome," *Molecular Cell*, 71, 306–318.

[120] Xiao, Z. and Locasale, J. W. (2021), "Epigenomic links from metabolism—methionine and chromatin architecture," *Current Opinion in Chemical Biology*, 63, 11–18.

[121] Xu, W., Yang, H., Liu, Y., Yang, Y., Wang, P., Kim, S. H., Ito, S., Yang, C., Wang, P., Xiao, M. T., Liu, L. X., Jiang, W. Q., Liu, J., Zhang, J. Y., Wang, B., Frye, S., Zhang, Y., Xu, Y. H., Lei, Q. Y., Guan, K. L., Zhao, S. M., and Xiong, Y. (2011), "Oncometabolite 2-hydroxyglutarate is a competitive inhibitor of α-ketoglutarate-dependent dioxygenases," *Cancer Cell*, 19, 17–30.

[122] Yaffe, D. and Ora, S. (1977), "Serial passaging of myogenic cells isolated from dystrophic mouse muscle," *Nature*, 270, 725–727.

[123] Yang, S., Zheng, X., Lu, C., Li, G. M., Allis, C. D., and Li, H. (2016), "Molecular basis for oncohistone H3 recognition by SETD2 methyltransferase," *Genes and Development*, 30, 1611–1616.

[124] Youdell, M. L., Kizer, K. O., Kisseleva-Romanova, E., Fuchs, S. M., Duro, E., Strahl, B. D., and Mellor, J. (2008), "Roles for Ctk1 and Spt6 in Regulating the Different Methylation States of Histone H3 Lysine 36," *Molecular and Cellular Biology*, 28, 4915–4926.

[125] Zaccara, S., Ries, R. J., and Jaffrey, S. R. (2019), "Reading, writing and erasing mRNA methylation," *Nature Reviews Molecular Cell Biology*, 20, 608–624.

[126] Zee, B. M., Levin, R. S., Xu, B., LeRoy, G., Wingreen, N. S., and Garcia, B. A. (2010), "In vivo residue-specific histone methylation dynamics," *Journal of Biological Chemistry*, 285, 3341–3350.

[127] Zhang, N. (2018), "Role of methionine on epigenetic modification of DNA methylation and gene expression in animals," *Animal Nutrition*, 4, 11–16.

[128] Zhang, S., Zhang, Y., Chen, C., Hu, Q., Fu, Y., Xu, L., Wang, C., and Liu, Y. (2022), "Identification of Robust and Key Differentially Expressed Genes during C2C12 Cell Myogenesis Based on Multiomics Data," *International Journal of Molecular Sciences*, 23, 1–18.

[129] Zhang, X., Tamaru, H., Khan, S. I., Horton, J. R., Keefe, L. J., Selker, E. U., and Cheng, X. (2002), "Structure of the Neurospora SET domain protein DIM-5, a histone H3 lysine methyltransferase," *Cell*, 111, 117–127.

Biography

Yudong Sun received his Bachelor of Science degree in Computer Sciences and Molecular Biology from the University of Wisconsin-Madison in 2017. Initially poised for a career in software development, his trajectory took a dramatic turn during an introductory biology course. A pivotal moment occurred when Dr. Seth Blair and Dr. Antony Stretton presented "The Inner Life of a Cell" video in the class, captivating him with the complex beauty of cellular mechanisms. This led him to pursue research under the guidance of Dr. Alessandro Senes, focusing on the prediction of protein structures through co-evolutionary information.

In 2017, Yudong started graduate school in the Department of Biochemistry at Duke University. He joined Dr. Jason Locasale's laboratory. There he has studied the connection between metabolism and epigenetics. During his time in the lab, Yudong contributed to several scientific papers, including *Methionine availability influences essential H3K36me3 dynamics during cell differentiation*, *Nucleotide metabolism is linked to cysteine availability*, and *Uncoupling of longevity and reproductive tradeoffs by dietary methionine and one-carbon metabolism*. He also authored a commentary titled *Rethinking the Bioavailability and Cellular Transport Properties of S-adenosylmethionine*, in which he proposed a model for the indirect cellular entry of SAM.